Universidade de Aveiro Departamento de Química
Ano 2016

Magda Alexandra Carvalho Henriques

Curcumin and a new Rutheno(II)curcumin Complex: characterisation and evaluation of the biological potential

Curcumina e um novo complexo Ruteno(II)curcumina: caracterização e avaliação das suas potencialidades biológicas

Universidade de Aveiro Departamento de Química
Ano 2016

Magda Alexandra Carvalho Henriques

Curcumin and a new Rutheno(II)curcumin Complex: characterisation and evaluation of the biological potential

Curcumina e um novo complexo Ruteno(II)curcumina: caracterização e avaliação das suas potencialidades biológicas

Tese apresentada à Universidade de Aveiro para cumprimento dos requisitos necessários à obtenção do grau de Mestre em Bioquímica, ramo Métodos Biomoleculares, realizada sob a orientação científica da Doutora Susana Isabel Fonseca de Almeida Santos Braga, Equiparada a Investigadora Principal do Departamento de Química da Universidade de Aveiro e da Doutora Maria do Amparo Ferreira Faustino, Professora Auxiliar do Departamento de Química da Universidade de Aveiro.

o júri

presidente

Doutora Maria do Rosário Gonçalves dos Reis Marques Domingues
Professora Associada com Agregação do Departamento de Química da Universidade de Aveiro

Doutora Teresa Margarida dos Santos
Professora Auxiliar do Departamento de Química da Universidade de Aveiro

Doutora Susana Isabel Fonseca de Almeida Santos Braga
Equiparada a Investigadora Principal do Departamento de Química da Universidade de Aveiro

agradecimentos

Às minhas orientadoras, Doutora Susana Braga e Doutora Maria do Amparo Faustino, pela ajuda que me deram ao longo deste ano e principalmente por toda a paciência que tiveram. Muito obrigada por terem estado sempre disponíveis para mim e por me terem sempre acompanhado não só a nível "profissional" como pessoal, por me terem feito sentir em casa mesmo estando no laboratório. O vosso apoio foi a chave para o êxito deste trabalho.

À Doutora Margarida Fardilha e à Juliana Felgueiras pela ajuda no desenvolvimento do desenho experimental dos ensaios de citotoxicidade e por todos os ensinamentos na cultura de células. Obrigada pela forma carinhosa como me acolheram e me integraram no vosso grupo de trabalho. Foi uma ótima ajuda para que tudo corresse pelo melhor.

Ao Professor Doutor Artur Silva pela disponibilidade para ajudar na análise dos espectros de RMN e em tudo o que foi preciso.

Ao Doutor Flávio Figueira pela ajuda nas purificações e cristalizações. Foi uma mais-valia numa questão tão importante do meu trabalho.

A todas as pessoas do Departamento de Química e do iBiMED da Universidade de Aveiro que tornaram possível a realização deste trabalho.

Aos meus pais, aos meus irmãos e ao Rui o maior agradecimento. Para vos agradecer tudo o que já fizeram por mim eu precisava de uma tese inteira e não apenas de uma secção nos agradecimentos, vocês foram o meu pilar ao longo destes anos. Obrigada por terem sempre acreditado em mim e por me ajudarem para conseguir fazer sempre mais e melhor. Obrigada por me mostrarem que não interessam as notas ou os graus que eu consiga, que aquilo que interessa é eu seguir o meu sonho e ser feliz. Obrigada por todos os sacrifícios que já fizeram por mim. Obrigada por não me deixarem sentir mal mesmo quando as coisas correm menos bem. Obrigada por estarem sempre presentes. Muito, muito obrigada, sem vocês isto nunca teria sido possível.

A todos os meus amigos e à minha segunda família, por toda a disponibilidade para me apoiarem nas minhas derrotas e por festejarem comigo as minhas vitórias.

palavras-chave

Curcumina, ruténio(II), cancro da próstata, avaliação da citotoxicidade, terapia fotodinâmica, intercalação com o ADN, caracterização espectroscópica

resumo

A curcumina é um pigmento de cor amarela, da família dos polifenóis, obtido a partir dos rizomas da planta *Curcuma longa*. É dotada de diversas propriedades biológicas que se relacionam com a vasta gama de alvos moleculares que possui, sendo de destacar a sua atividade anticancerígena já provada em diversas linhas celulares cancerígenas. No entanto, a atividade biológica da curcumina é limitada pela sua baixa biodisponibilidade que se deve principalmente à sua fraca solubilidade e rápida degradação em condições fisiológicas. Uma estratégia para contornar as limitações terapêuticas da curcumina é a sua complexação com iões metálicos, nomeadamente com complexos de ruténio(II).

Neste trabalho foi preparado um novo complexo de curcumina com ruténio(II) e tritiaciclononano [9anoS$_3$] com o objetivo de aumentar a solubilidade da curcumina em meio fisiológico. A curcumina foi extraída e purificada a partir de rizomas secos e pulverizados de *Curcuma longa* sendo depois desprotonada e coordenada com o precursor [Ru(II)(9anoS$_3$)(DMSO)Cl$_2$] (DMSO=dimetilsulfóxido). A estrutura e pureza do complexo formado, [Ru(II)(9aneS$_3$)(curcumina)(*S*-DMSO)]Cl foi avaliada por Ressonância Magnética Nuclear de ^{1}H e ^{13}C, espectrometria de massa e análise elementar. A afinidade do novo complexo para ligação ao ácido desoxirribonucleico (ADN) foi estudada por ensaios de titulação e por determinação da variação na temperatura de desnaturação do ADN de esperma de salmão. Este estudo permitiu determinar que o complexo tem a capacidade de intercalar com o ADN com uma constante de ligação comparável aos intercaladores de ADN já conhecidos (4.00×10^5 M^{-1}). A atividade citotóxica deste complexo contra o cancro de próstata foi estudada *in vitro*, usando como controlo positivo a curcumina. Mais ainda, aproveitando o potencial fotossensibilizador da curcumina, os ensaios foram feitos na presença e na ausência de luz. Para isso, usaram-se culturas celulares humanas isoladas de carcinoma de próstata (PC-3) e a toxicidade foi avaliada em linhas celulares prostáticas não tumorais (PNT-2). Com estes ensaios verificou-se que o complexo preparado não tem efeito citotóxico nem fototóxico nas concentrações usadas para as linhas celulares estudas. Mais, observou-se que a curcumina apresenta, no escuro, efeito citotóxico nas concentrações usadas e ainda, que este efeito é fortemente potenciado na presença de luz, sendo um potencial agente para terapia fotodinâmica em cancro de próstata.

keywords

Curcumin, ruthenium(II), prostate cancer, cytotoxicity evaluation, photodynamic therapy, DNA intercalation, spectroscopic characterisation

abstract

Curcumin is a yellow pigment, of the family of polyphenols, obtained from the rhizomes of the *Curcuma longa.* It is provided with several biological properties which relate with the wide range of molecular targets that possesses, especially the anticancer activity already proven in various cell lines. However, the biological activity of curcumin is limited by their low bioavailability which is mainly because their poor solubility and rapid degradation in physiological conditions. One promising strategy to circumvent the therapeutic limitations of curcumin is the binding with metal ions, namely with ruthenium(II) complexes.

In this work, was prepared a new complex of curcumin with ruthenium(II) and trithiacyclononane ($9aneS_3$) with the aim of increasing the solubility of curcumin in physiological medium. The curcumina was extracted and purified from the powder rhizomes of *Curcuma longa* being after deprotonated and coordinated with the precursor $[Ru(II)(9aneS_3)(DMSO)Cl_2]$ (DMSO=dimethylsulfoxide). The structure and purity of the prepared complex, $[Ru(II)(9aneS_3)(curcumina)(S\text{-}DMSO)]Cl$ was evaluated by ^{1}H and ^{13}C Nuclear Magnetic Resonance spectroscopies, mass spectrometry and elemental analysis. The affinity of the new complex to bind to deoxyribonucleic acid (DNA) was studied by titration assays and determination of the variation on sperm salmon DNA melting temperature. This study allowed to determine that the complex has ability to intercalate with DNA with a binding constant comparable with classical intercalators. The cytotoxic activity of this complex against prostate cancer was studied *in vitro*, using curcumin as a positive control. Moreover, taking advantage of the photosensitizer potential of curcumin, the assays were made under dark and light conditions. For this, human cell cultures were used isolated from prostate carcinoma (PC-3) and the toxicity was evaluated in non-tumour prostate cells (PNT-2). With these tests, it was found that the new complex do not have any cytotoxic or phototoxic effect in the same concentrations range tested for cell lines studied. Further, was observed that the curcumin presents, in dark, cytotoxic effect and, that this effect is strongly potentiated by light presence, with a potential for photodynamic therapy in prostate cancer.

Contents

List of figures

List of tables

List of Abbreviations, symbols and acronyms

δ	chemical shift (ppm)
Φ_F	fluorescence quantum yields
Φ_Δ	singlet oxygen quantum yields
^{13}C NMR	carbon **N**uclear **M**agnetic **R**esonance
^{1}H NMR	proton **N**uclear **M**agnetic **R**esonance
J	coupling constant
^{1}J	coupling constant over one bonds
^{2}J	coupling constant over two bonds
^{3}J	coupling constant over three bonds
$^{1}O_2$	singlet state of oxygen
$^{3}O_2$	triplet state of oxygen
A2780	human ovarian cancer cell line
A2780cisR	human ovarian platinum-resistant cancer cell line
A431	human epidermoid carcinoma cell line
A549	human lung adenocarcinoma cell line
AB	**a**lamar**b**lue
A	**abs**orbance
ADT	**a**ndrogen-**d**eprivation **t**herapy
AMC-HN3	human head and neck cancer cell line
AP-1	**a**ctivator **p**rotein 1
AR	**a**ndrogen **r**eceptor
AUC	integrated **a**rea **u**nder the fluorescence **c**urves
Bax	**b**-cell lymphoma 2-**a**ssociated **X** protein
Bcl-2	**b**-**c**ell **l**ymphoma 2
Bcl-XL	**b**-**c**ell **l**ymphoma-e**x**tra **l**arge
CC	**c**olumn **c**hromatography
$CDCl_3$	deuterated chloroform
Cyclin-CDK	**c**yclin **d**ependent **k**inase **c**omplex
CNE1	human nasopharyngeal carcinoma cell line
CNE2	human nasopharyngeal carcinoma drug-resistant cell line

COSY	homonuclear **co**rrelation **s**pectroscop**y** ($^{1}H/^{1}H$)
COX-2	**c**yclo**ox**ygenase-2
d	doublet
dd	doublet of doublets
DMA	9,10-dimethylanthracene
DMF	*N,N*-dimethylformamide
DMSO	dimethylsulfoxide
DNA	**d**eoxyribo**n**ucleic **a**cid
DRE	**d**igital **r**ectal **e**xamination
EGF	**e**pidermal **g**rowth **f**actor
EGFR	**e**pidermal **g**rowth **f**actor **r**eceptor
ESI-MS	**e**lectro**s**pray **i**onization **m**ass **s**pectrometry
FBS	**f**etal **b**ovine **s**erum
FDA	**f**ood and **d**rug **a**dministration
FGF	**f**ibroblast **g**rowth **f**actor
FGFR	**f**ibroblast **g**rowth **f**actor **r**eceptor
GFR	**g**rowth **f**actor **r**eceptor
HaCaT	aneuploid immortal keratinocyte cell line
HCT116	human colon cancer cell line
HEK293	human embryonic kidney cell line
HMBC	**h**eteronuclear **m**ultiple **b**ond **c**orrelation ($^{13}C/^{1}H$)
HPLC	**h**igh **p**erformance **l**iquid **c**hromatography
HSQC	**h**eteronuclear **s**ingle **q**uantum **c**orrelation ($^{13}C/^{1}H$)
Hz	hertz
IC_{50}	drug concentration needed to reduce cell viability by 50%
IL	Interleukin
iNOS	**i**nducible **n**itric **o**xide **s**ynthase
JNK	c-**j**un ***N***-terminal **k**inase
K_b	binding constant
K_{obs}	observed rate constant
KP1019	trans-[tetrachlorobis(1H-indazole)ruthenate(III)]
LNCaP	**l**ymph **n**ode **ca**rcinoma of the **p**rostate

m	multiplet
MAPK	**m**itogen **a**ctivated **p**rotein **k**inase
MCF7	breast cancer cell line
MeOH	methanol
MMP	**m**atrix **m**etallo**p**roteinase
MS	**m**ass **s**pectrometry
NAMI-A	**n**ew **a**ntitumour **m**etastasis **i**nhibitor **A**
$NaOCH_3$	sodium methoxide
NF-kB	**n**uclear **f**actor **k**appa **B**
Nfr-2	**n**uclear **f**actor erythroid 2-**r**elated factor 2
NMR	**n**uclear magnetic resonance
OD	**o**ptical **d**ensity
OMe	methoxyl group
PBS	**p**hosphate **b**uffered **s**aline
PC-3	prostate cancer cell line
PCa	**p**rostate **ca**ncer
PDGF	**p**latelet-**d**erived **g**rowth **f**actor
PDGFR	**p**latelet-**d**erived **g**rowth **f**actor **r**eceptor
PDT	**p**hoto**d**ynamic **t**herapy
PKA	**p**rotein **k**inase **A**
PNT-2	prostatic epithelial cell line
PPAR-γ	**p**eroxisome **p**roliferator-**a**ctivated **r**eceptor gamma
ppm	parts per million
PS	photosensitizer
PSA	**p**rostate-**s**pecific **a**ntigen
PTA	1,3,5-triaza-7-phosphoadamantane
R_f	retardation factor
ROS	**r**eactive **o**xygen **s**pecies
RPMI	**r**oswell **p**ark **m**emorial **i**nstitute
Ru(II)	ruthenium(II)
Ru-curc	[ru([9]$anes_3$)(curcumin)(*S*-dmso)]Cl complex
s	singlet

S-DMSO	dimethylsulfoxide coordinated by the sulphur atom
sp-DNA	deoxyribonucleic acid of salmon sperm
STAT-3	**s**ignal **t**ransducer and **a**ctivator of **t**ranscription 3
TB	**t**rypan **b**lue
TLC	**t**hin-**l**ayer **c**hromatography
Tm	melting temperature
TMS	tetramethylsilane
TNF	**t**umour **n**ecrosis **f**actor
TPP	5,10,15,20-tetraphenylporphyrin
tPSA	**t**otal **p**rostate-**s**pecific **a**ntigen
TRUS	transrectal ultrasonography
U87	human primary glioblastoma cell line
USA	**U**nited **S**tates of **A**merica
UV-Vis	ultraviolet-visible spectroscopy
VEGF	**v**ascular **e**ndothelial **g**rowth **f**actor

1. Introduction

1.1. *Curcuma longa Linn*

Curcuma longa L., commonly known as turmeric or saffron-of-India, is a perennial plant of the Zingiberaceae family.[1,2] This plant is widely grown in South and Southeast Asia, especially in China and India. The part of the plant that is usually used is the rhizome, which can be eaten fresh or dried.[3] The use of *Curcuma longa L.* rhizomes is referred in Ayurvedic medicine (the characteristic medicinal system of Ancient India) as a home remedy for various diseases.[4] Currently, turmeric is considered as a functional food because of the therapeutic properties of their active components, namely anti-inflammatory, antioxidant and anticancer activity. This plant is also effective in the treatment of circulatory, liver and dermatological diseases (e.g., psoriasis).[5,6]

The powder extracted from the dried rhizome of turmeric has a yellow colour and its chemical composition is influenced by various factors, such as the geographical origin of the plant, the climate of farming, the environment and soil composition. It contains mainly starch and, in a lesser extent, proteins, lipids, fibres, curcuminoids, and essential oils, such as the α-phellandrene (1%), the sabinene (0.6%), the cineole (1%), the borneol (0.5%), the zingiberene (25%), and the sesquiterpenes (53%).[7,8] The essential oils have been isolated from *Curcuma longa* by distillation by steam entrainment. The curcuminoids, in amounts varying between 2% and 9% of the turmeric powder, are the active substances of the plant and comprise three structurally related phenolic compounds: [(1*E*,6*E*)-1,7-bis(4-hydroxy-3-methoxyphenyl)-hepta-1,6-diene-3,5-dione)], known under the designation of curcumin, desmethoxycurcumin [(1*E*,6*E*)-1-(4-hydroxy-3-methoxyphenyl)-7-(4-hydroxyphenyl)-hepta-1,6-diene-3,5-dione)] and bisdesmethoxycurcumin [(1*E*,6*E*)-1,7-bis(4-hydroxyphenyl)-hepta-1,6-diene-3,5-dione] (Figure 1).[9] The commercially available curcumin is a mixture of these three curcuminoids, in which the most abundant constituent is the curcumin (~77%), followed by desmethoxycurcumin (~18%) and the less abundant bisdesmethoxycurcumin (~5%).[10,11]

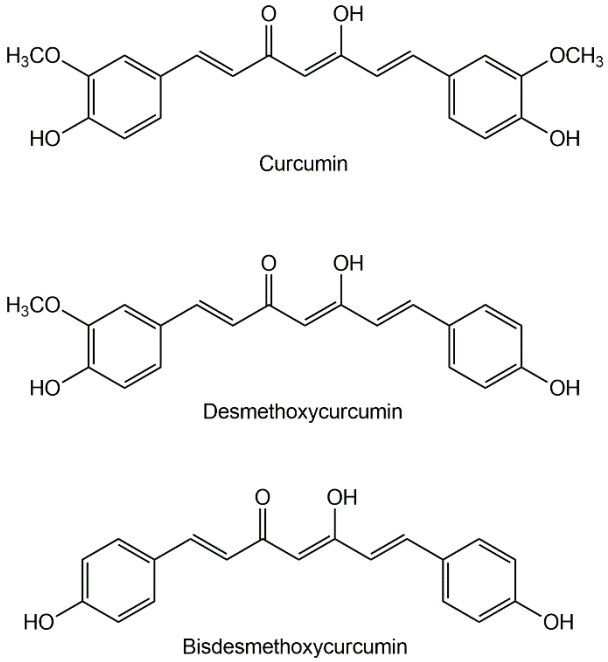

Figure 1 - Chemical structures of the three curcuminoids present in the plant *Curcuma longa L.*

Curcuminoids have an intense yellow colour and are poorly soluble in water at physiological and acidic pH, but easily soluble in alkaline solutions.[12] They are quite soluble in dimethylsulfoxide (DMSO), acetone, dichloromethane, methanol and ethanol. These pigments are sensitive to light, high temperature and oxidative conditions, decomposing easily.[13]

1.1.1. Extraction, purification and identification of curcuminoids

The biological relevance of curcuminoids pigments led to the development of several methods for their extraction, separation and identification. The conventional extraction methods are based on the combined maceration with ultrasound, heat, pressure or enzymatic treatment.[14–18] Another way to obtain the compounds is to use a Soxhlet apparatus, allowing extraction and filtration to be done in the same step.[19] However, all methods require long extraction times, high energy consumption and high volume of organic solvent. In addition, they exhibit low extraction efficiency and losses with heat because curcuminoids are heat-sensitive substances. New extraction methods more adapted to this reality, such as microwave-assisted extraction, are under development.[20]

Once extracted, the pigments can be separated by thin-layer chromatography (TLC),[7,10,21] column chromatography (CC)[10,22] and high performance liquid chromatography (HPLC).[10,23] CC has been the most commonly employed method for separating curcumin from turmeric. In CC, the mixture of curcuminoids adsorbed in silica gel is eluted using mixtures of organic solvents, such as dichloromethane/ethyl acetate or methanol/chloroform. The evaluation of the purity of the separated compounds can be made by ultraviolet-visible (UV-Vis) spectrophotometry but the HPLC is the most used technique.[24,25] Typically, reverse phase columns with 18 carbons are used, as well as acetonitrile/water or chloroform/methanol solvent mixtures as the mobile phase.

1.2. Curcumin

Curcumin has a scientific history of nearly two centuries that began in 1815, date of the first report of its isolation from the rhizome of *Curcuma longa,* being described simply as "a matter of yellow color".[26] Later, it was found that this extract was in fact a mixture of various curcuminoids with oils and resins derived from curcuma rhizomes. In 1870, Daube[27] found a method to isolate curcumin in the pure and crystalline form and described the crystals he observed under the optical microscope. Its chemical structure only was determined in 1910 by Milobedzka and Lampe.[28] In 1913, it was reported a well succeeded preparation of curcumin in laboratory for the first time.[29] The curcumin research then slowed and the resurgence of curcumin interest emerged in the year 1987 when Kuttan and his colleagues[30] reported that this polyphenolic compound had anticancer activity. Since then, the research for characterization and isolation of this compound has increased rapidly.[31]

The structure of curcumin consists of two methoxyl groups linked to each other, at the *orto* position of the phenolic rings, which are linked together by a hepta-unsaturated bridge.[32] In fact, it is an α,β-unsaturated β-diketo bridge that exhibits keto-enol tautomerism and can exist in different types of conformers depending on the nature of the solvent where it is dissolved (Figure 2).[32,33] Yellow curcumin changes to dark red colour at alkaline pH and under physiological conditions the $\lambda_{máx}$ for curcumin is observed at 420 nm.[34]

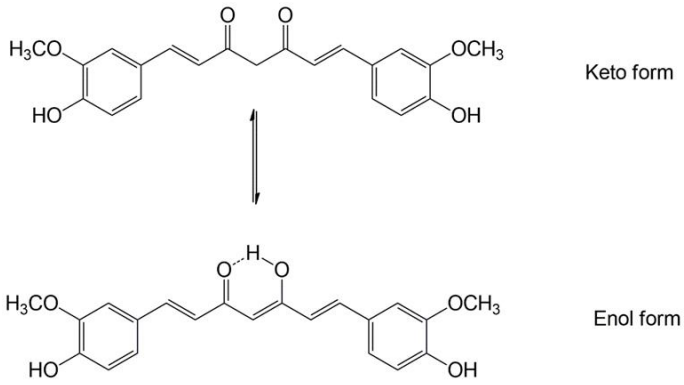

Figure 2 - Keto-enol tautomeric equilibrium of curcumin.

The degradation kinetics of curcumin under various pH conditions and its stability in physiological matrices are already reported.[35] When curcumin was incubated in 0.1 M phosphate buffer (PBS), pH 7.2, approximately 90% decomposed within 30 min. Moreover, on exposure to light curcumin degrades into several products, namely *trans*-6-(4'-hydroxy-3'-methoxyphenyl)-2,4-dioxo-5-hexanal, ferulic acid, feruloyl methane and vanillin (Figure 3).[35,36] Under acidic conditions, the degradation of curcumin is much slower, with less than 20% of total curcuminoids decomposed after 1 h. Degradation of curcumin has also been demonstrated upon addition to cultured cells.[35] Further, it is known that the degradation products resulting from the photodegradation of curcumin are the same as occur during chemical degradation of the polyphenol. However, the degradation is significantly decreased when curcumin is attached to lipids, liposomes, albumins, cyclodextrin, surfactants, polymers and many other systems.

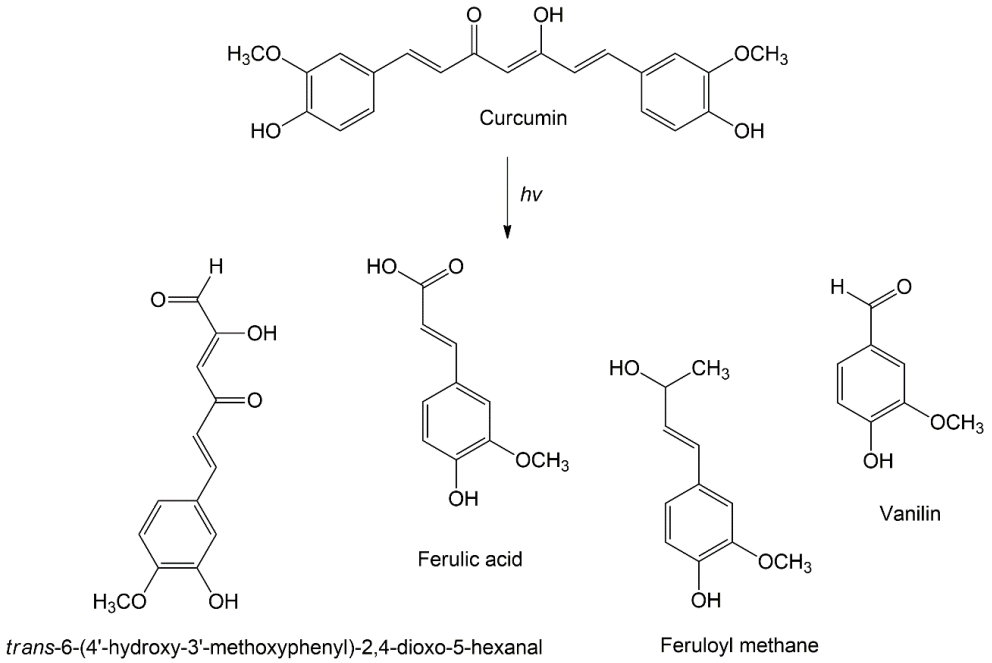

Figure 3 - Curcumin degradation products after exposure to light.

As indicated above, curcumin possesses several biological properties, namely anti-inflammatory,[37,38] antioxidant[39,40] and anticancer effects.[41,42] Therefore, curcumin is able to act as a chemopreventive agent, as well as a potential therapeutic agent for the many organ and tissue chronic disorders (Figure 4).

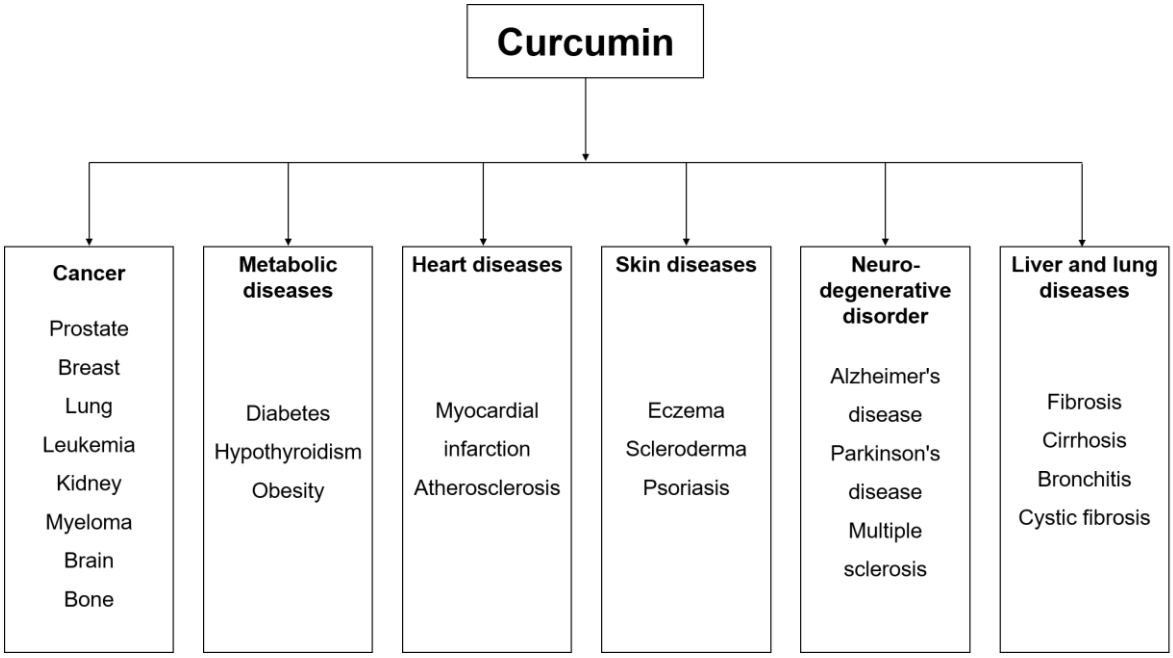

Figure 4 - Human diseases against which curcumin has exhibited activity. Adapted from He and collaborators.[43]

1.2.1. Molecular targets

The studies published in the last three decades show that the curcumin molecule is highly pleiotropic, i.e. capable of modulating the biological activity of a series of signalling molecules, affecting many signalling pathways (Table 1).[44,45]

Table 1 - Molecular targets and cell processes modulated by curcumin. Curcumin interacts directly or indirectly with various molecular targets, including transcription factors, growth factors, receptors, cytokines, anti-apoptotic proteins, pro-apoptotic proteins, enzymes, protein kinases, and adhesion molecules, altering their expression.

Family	Molecular target	Effect of curcumin in molecule activity	Reference
Transcriptional factors	NF-kB	↓	46
	AP-1	↓	47,48
	Nrf-2	↑	49
	PPAR-γ	↑	50
	STAT-3	↓	51–53
Inflammatory cytokines	TNF-α	↓	54
	IL-1,2,5,6,8,12,18	↓	55,56
Growth factors	PDGF	↓	57
	EGF	↓	58
	FGF	↓	59,60
	VEGF	↓	61–63
Receptors	AR	↓	64,65
	EGFR	↓	50,66–68
Kinases	PKA	↓	69
	MAPK	↓	69
	JNK	↓	70
Enzymes	iNOS	↓	71
	MMP	↓	72,73
	COX-2	↓	74
	Telomerase	↓	75
Anti-apoptotic proteins	Bcl-2	↓	76–79
	Bcl-XL	↓	76–78,80
Pro-apoptotic proteins	Bax	↑	76–79
	Caspase 3	↑	81,82

List of abbreviations on pages xvi-xix. Upward arrows – increased activity; downward arrows – decreased.

This curcumin feature is directly related to its ability to regulate many targets either by direct interaction with transcription factors, growth factors and their receptors, nuclear factors, hormones and hormone receptors, cytokines, or by controlling the expression of genes that regulate cell proliferation and apoptosis.[83] Curcumin may associate with serum albumin through hydrophobic interactions,[84] being transported to cells where it exerts its pharmalogical effects. Curcumin enters the cytoplasm and is able to accumulate in the plasma membrane, endoplasmic reticulum and nuclear envelope.[85] The complexity of the mechanisms associated with the action of curcumin justify its efficiency in combating various multifactorial diseases, such as cancer, metabolic diseases and others, as indicated above. Curcumin can act against three important steps in carcinogenesis, tumour promotion, angiogenesis and tumour growth by modulation of several molecular targets.

1.2.2. Bioavailability

Despite the wide range of biological activities of curcumin, some studies report limitations its use as a therapeutic agent, mainly due to its poor bioavailability. Curcumin has a relatively low absorption rate at the intestine, undergoes rapid metabolism in liver and has a short biological half-life.[86] Curcumin is metabolized by both conjugation and reduction pathways in the body resulting in formation of several metabolites. Furthermore, this low bioavailability is further enhanced by the poor solubility of curcumin in water and in physiological conditions, like many other natural polyphenols. The kinetics and availability of curcumin *in vivo* have quite distinct profiles depending on the administration routes.

Oral intake of curcumin is the most common form of contact with this compound given that it is typically incorporated into food. Nevertheless, the bioavailability of curcumin administered by this route is extremely poor.[8] Less than 1% of oral curcumin enters in the plasma and the small amount of curcumin absorbed is subjected to conjugations, like sulfation and glucuronidation in the liver. The major reasons for this are the very low solubility at physiological conditions, the poor absorption in the body, the rapid metabolism with short biological half-life and the rapid systemic elimination.[87,88] The poor absorption following oral administration

of curcumin implies that very high doses (>3.6 g per day in humans) are required to produce any medicinal effect. Studies have shown that 99% of the curcumin found in plasma is in the form of glucuronide conjugates,[89,90] and that most of these are biologically inactive. Indeed, many studies highlight the issue of having extremely low concentrations of free curcumin in booth plasma and urine after oral administration.[91] There are several published methods suggesting that low bioavailability of oral curcumin could be circumvent. These include the use of adjuvants like piperine,[92] curcumin structural analogues,[93] and development of improved delivery technologies, such as polymeric micelles[94] and nanoparticles.[95]

Additionally, parenteric forms – intraperitoneal, intravenous, intramuscular and subcutaneous - are under development. These require specific formulations to stabilize curcumin in an aqueous matrix.[89,96–102] Several formulations available, allowing repeated systemic injections of curcumin reported in preclinical studies for intraperitoneal, intravenous, intramuscular and subcutaneous administration, proved that these formulations offer platforms for this otherwise poorly soluble drug.

1.2.3. Binding to metals and effects on stability, bioavailability and cytotoxicity

The use of natural products as ligands for coordination with metal ions has been subject of intensive research, since several metal ions allow to mitigate the inherent limitations of natural compounds. The metal ions allow to increase the stability of the natural compounds under physiological conditions. Following these strategy of coordinating a metal centre with natural compounds with therapeutic properties, there are a few literature reports on coordination of metal ions with curcumin.[103–109] One of the main advantages of this coordination is the stabilisation of curcumin - an important issue when considering its potential application in medicine. The protocol used to prepare almost all of these metal complexes involves a first step of deprotonation of curcumin, thereby stabilising it in the enol form.[110] In a second step, it is made react, in appropriate molar ratio, with metal halogenates, namely of zinc(II), iron(II), nickel(II), copper(II) and ruthenium(II). Regarding coordination of the curcumin with ruthenium metal, the published reports focus mainly on ruthenium(II) organometallic complexes with curcumin (Figure 5). These

complexes were studied and their cytotoxic activity evaluated against several cell lines but without being particular light irradiation.

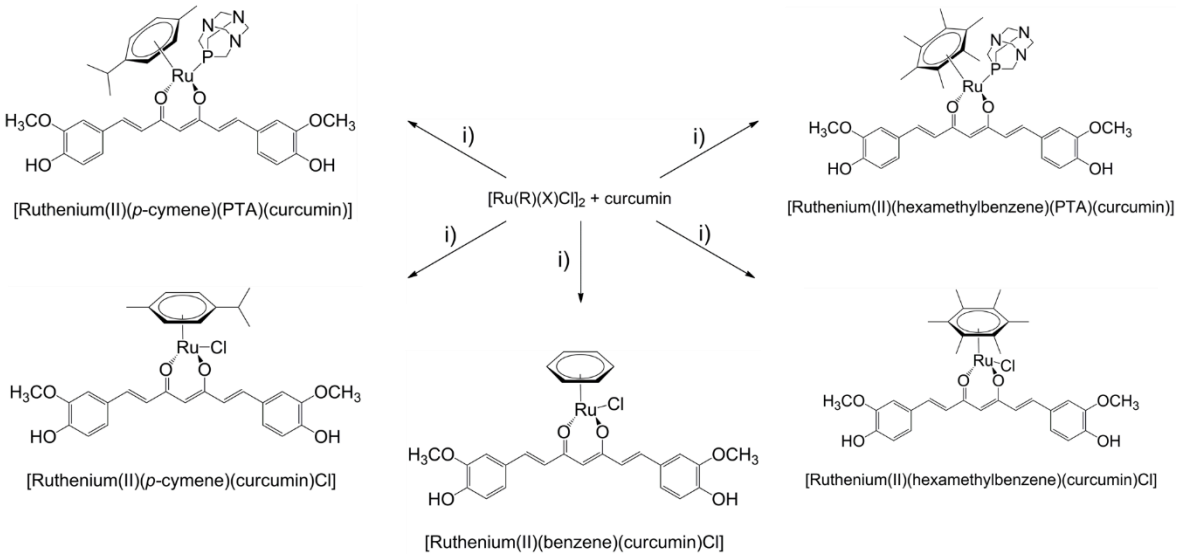

Figure 5 – Synthesis of [Ruthenium(II)(R)(curcumin)X] complexes already tested in several human tumour and non-tumour cell lines. Where, R=*p*-cymene, benzene or hexamethylbenzene and X=Cl or PTA. i) $NaOCH_3$, MeOH

The preparation of [Ru(II)(*p*-cymene)(curcumin)Cl] was described in 2012 by two different research teams in Italy.[104,105] Caruso and co-workers[104] studied the cytotoxicity of this complex, at 72 h of incubation, against the human tumour cell lines: breast (MCF7), colon-rectal (HCT116), ovarian (A2780), ovarian platinum-resistant (A2780cisR), lung (A549) and glioblastoma (U87) and compared them with that of cisplatin. Their results demonstrated that the complex has greater effect in the HCT116 cell line, with an IC_{50} of 14 mM, followed by MCF7 (20 mM), A2780 (24 mM) and A2780cisR (27 mM) cell lines; U87 (30 mM) and A549 (65 mM) were less sensitive. The effects of the complex on the four most sensitive cell lines tested (HCT116, MCF7, A2780 and CP9) were compared to those of cisplatin that were still significantly more potent against these cell lines than the [Ru(II)(*p*-cymene)(curcumin)Cl] complex as shown in Table 2.

On the other hand, the group of Bonfili and co-workers[105] studied the same curcumin complex [Ru(II)(*p*-cymene)(curcumin)Cl] along with two other ruthenium(II) complexes: [Ru(II)(benzene)(curcumin)Cl] and the [Ru(II)(hexamethylbenzene)(curcumin)Cl], against the human colorectal cancer

HCT116 cell line. The authors pointed out that after 24 h of incubation the complexes only exhibited a mild cell growth inhibition (20-30%), which was comparable or lower than the found for pure curcumin. The DNA binding ability of the complexes and their ability to regulate the activity of the proteasome were also studied. Complexes with *p*-cymene and benzene had shown greater DNA binding affinity than hexamethylbenzene complex and pure curcumin. The *p*-cymene complex also showed to be the most potent in inhibiting proteasome in comparison with other compounds and pro-apoptotic events were observed, thus representing a potentially new, nontoxic and effective compound in cancer therapy.

More recently, Pettinari and their collaborators studied the synthesis and biological activity of new ruthenium(II) complexes: the [Ru(II)(*p*-cymene)(curcumin)PTA] and the [Ru(II)(hexamethylbenzene)(curcumin)PTA].[106] The cytotoxicity of this complexes was evaluated at 72 h of incubation against ovarian cancer cell lines with and without cisplatinum resistance (A2780cisR and A2780 cell lines, respectively), as well as on a non-tumour human embryonic kidney cell line, HEK293. Cisplatin was used as reference drug, once it is used in the clinic to treat ovarian cancer. The results showed that the prepared complexes possess high anti-tumoural activity, inhibiting tumour growth at lower concentrations than the reference cisplatin. In general, the new complexes are much more selective towards the tumoural cell lines (with marginal activity towards the healthy cell line), unlike cisplatin. Besides the excellent cytotoxic results, these authors demonstrated that the solubility in water of the novel complex is exceeding cisplatin. All these findings are summarised in Table 2.

Collectively, these results demonstrate that the coordination of curcumin with various precursors of Ru(II) is the starting point for the development of new anticancer drugs. That is, the coordination of curcumin with the Ru(II) metal centre may increase in some cases their selectivity in respect to the action on tumour cells.

In general, these studies also show that metal complexes of Ru(II) further improve the stability of curcumin in solution and under light, and therefore can be suited for phototherapeutic application. Furthermore, such complexes could allow the study of cellular localization due to curcumin stabilization *in vitro.*

Table 2 – Cytotoxic activities of curcumin and [Ru(II)(R)(curcumin)X] complexes described in literature, where R= *p*-cymene, benzene or hexamethylbenzene and X= Cl or PTA. IC_{50} values of complexes in human cell lines. Cisplatin was tested as a positive control.

Complex	Cell line	IC_{50} (mM) mean ± SD	Reference
[Ru(II)(*p*-cymene)(curcumin)Cl]	MCF7	19.58 ± 2.36	[104]
	HCT116	13.98 ± 1.50	[104]
		N/A	[105]
	A2780	23.38 ± 3.33	[104]
	A2780cisR	27.00 ± 2.33	[104]
	A549	62.33 ± 8.93	[104]
	U87	29.36 ± 1.84	[104]
[Ru(II)(benzene)(Cl)(curcumin)Cl]	HCT116	N/A	[105]
[Ru(II)(hexamethylbenzene)(curcumin)Cl]	HCT116	N/A	[105]
[Ru(II)(hexamethylbenzene)(curcumin)(PTA)]	A2780	0.39 ± 0.16	[106]
	A2780cisR	0.36 ± 0.02	[106]
	HEK293	4.5 ± 0.5	[106]
[Ru(II)(*p*-cymene)(curcumin)(PTA)]	A2780	0.39 ± 0.01	[106]
	A2780cisR	0.40 ± 0.02	[106]
	HEK293	9.1 ± 1.1	[106]
Cisplatin	MCF7	1.835 ± 0.237	[104]
	HCT116	5.217 ± 0.348	[104]
	A2780	1.325 ± 0.196	[104]
		1.5 ± 0.2	[106]
	A2780cisR	25 ± 3	[106]
		9.92 ± 1.16	[104]
	HEK293	7.3 ± 0.6	[106]

N/A - not applicable. List of abbreviations on pages xvi-xix.

1.3. Metal complexes in cancer treatment

The majority of the compounds used in cancer treatment are organic molecules, mainly with origin in natural resources, such as plants, microorganisms and marine sources.[111] However, the optimisation of their large scale synthesis and their obtaining in large amount from natural resources can be problematic.[112] These factors limit their therapeutic use in chemotherapy and increase dramatically their costs.

Metal complexes, including platinum, gallium and ruthenium have properties that make them promising for the development of anticancer drugs.[113,114] These complexes offer new structural opportunities based on their wide spectrum of coordination numbers and geometries,[111,115,116] as well as accessible redox states[115,116] and thermodynamic and kinetic characteristics.[111]

1.3.1. Platinum complexes

Cisplatin is, to date, the most successful metal complex used in the treatment of cancer. After the discovery of cisplatin by Rosenberg *et al.*[117] in 1965 and its extensive application as anticancer drug, numerous platinum compounds have been synthesised. Cisplatin, carboplatin and oxaliplatin are approved platinum anticancer drugs by FDA that are used in clinic world-wide (Figure 6).

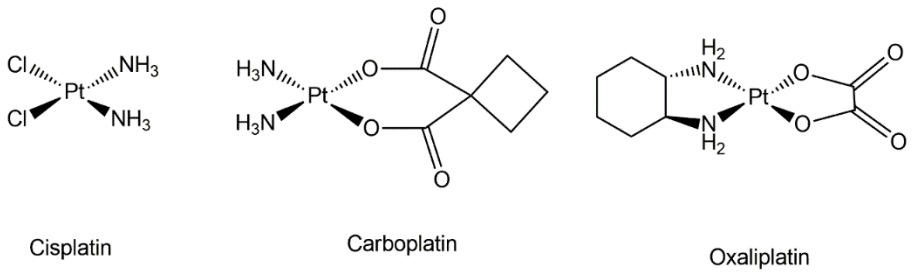

Figure 6 - Platinum complexes approved worldwide for clinical use.

The mode of action of cisplatin is well studied. Depending on the cell type and concentration, it may induce cytotoxicity by interfering with DNA transcription, replication, or both.[118–121] It is known that after entering the cell cisplatin is hydrolysed and its metal centre platinum(II) binds irreversibly to DNA, causing a significant distortion in its structure which brings replication inhibition. Currently, cisplatin is used alone or in combination with other drugs; however, it has a high toxicity leading to undesirable side effects (for instance, neurotoxicity, nausea and vomiting).[121] It is inactive against metastasis and some cancers have intrinsic resistance and others acquire resistance during treatment.[122] When cells become resistant to cisplatin, the doses have to be increased, but this can lead to severe multi-organ toxicity.[123] To minimise cisplatin resistance, alternative therapies have

been developed and have proven more effective in defeating cancer than cisplatin, namely by use of other metal complexes.[124]

1.3.2. Ruthenium complexes

During the past 20 years, ruthenium complexes have captivated a great interest as many of them were found be potential new therapeutic agents. Some of these complexes have demonstrated, in addition to *in vitro* cytotoxicity, a relevant *in vivo* anticancer action.[125–127] This interest stems mainly from a number of key features that make them excellent candidates for drugs, such as: an extensive background on the chemistry coordination of ruthenium, the kinetic stability of ruthenium in several different oxidation states, the ability of ruthenium to mimic iron in binding to human serum proteins (e.g. albumin and transferrin), the octahedral geometry which that the structural diversity and a wide range of oxidation states, which are accessible chemically and electrochemically (+2, +3 and +4) under physiological conditions, allowing their application as redox agents.[128–130] Like cisplatin, some ruthenium complexes have the ability to bind DNA but faster and with more stable bonding.[128] This is due to the octahedral geometry that, unlike the planar geometry of platinum derivatives, offers no obstacle to binding to DNA. Furthermore, it is believed that the ruthenium complex is able to induce cell death in tumour cells by either binding to proteins found on the cell surface or interacting with mitochondria.[131]

Several ruthenium complexes (II or III) have been developed and studied for their antiproliferative activity against several cancer cell lines. The **N**ew **A**ntitumour **M**etastasis **I**nhibitor **A** (NAMI-A) and the trans-[tetrachlorobis(1H-indazole)ruthenate(III)] (KP1019) were the first ruthenium complexes to enter in clinical trials (Figure 7). These complexes are structurally similar to each other, but exhibit a different cytotoxic profile and are particularly useful for the treatment of metastatic tumours or cisplatin-resistant tumours.

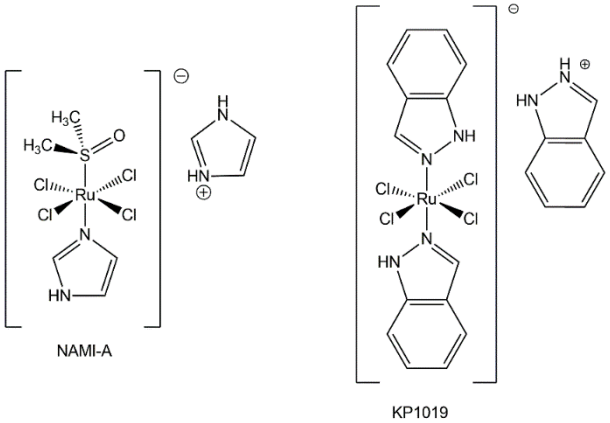

Figure 7 – Ruthenium (III) based anticancer complexes NAMI-A and KP1019 in clinical trials

1.3.2.1. Ru(II)-trithiacyclononane complexes

Recent research largely illustrates that the *in* vitro and *in vivo* properties of ruthenium compounds can be fine tuned by ligand variation. Several ligands have been studied, such as arene (the most studied), the aromatic heterocycles and others. The crown thioether 1,4,7- trithiacyclononane ([9]aneS_3) (Figure 8) forms stable octahedral complexes with several middle and late metal transition elements, namely ruthenium, coordinated in a facial manner.[132]

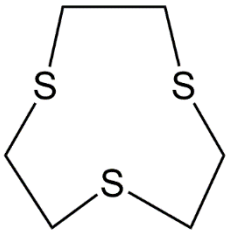

Figure 8 - Structure of macrocyclic ligand 1,4,7-trithiacyclononane ([9]aneS_3).

In 2005, it was demonstrated that the arene fragment is not essential for the activity of Ru(II) compounds and that it could be replaced by another ligand, such as [9]aneS_3.[133] These macrocyclic type ligands are very attractive due to their high polarity that increases their water solubility and gives good structural stability and strong bonding to the metal, helping to stabilise the formed complex and to make it relatively inert to the inactivating by biomolecules.[134] This typical feature is named the macrocyclic effect. They are also known to stabilise the lower oxidation states of metal ions.

In recent years, a series of new derivatives of the family Ru(II)([9]aneS$_3$) complexes have been synthesised and tested for their ability to intercalate with DNA.[135,136] An example of these precursors is [Ru(II)([9]aneS$_3$)(*S*-DMSO)Cl$_2$] , synthesized by Landgrafe and Sheldrick in 1994 (Figure 9).[137]

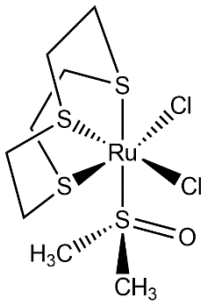

Figure 9 - Molecular structure of [Ru(II)(9aneS$_3$)(*S*-DMSO)Cl$_2$].

1.4. Cancer

Cancer is a general term used for a large number of diseases that are characterized by abnormal and uncontrolled cell growth and proliferation.[138] The initiation and progression of this disease results from the progressive accumulation of genetic and epigenetic changes.[139,140] Damages in the genetic information can be enhanced by environmental factors, including exposure to ionising radiation and/or chemical mutagenic agents.[141] The changes lead to cell cycle arrest and increased function of proteins that activate cell proliferation, in particular growth factors and their receptors, anti-apoptotic proteins and transcription factors. These proteins are thus important targets for tumour treatment.[138]

Chemotherapy, radiotherapy and surgery, either alone or in combination, are the most commonly applied techniques in cancer therapy.[142] The choice of the technique to be used depends on several factors: the location, the type and the size of the primary tumour and the presence or absence of metastasis. Chemotherapy can be neoadjuvant (before surgery to reduce the tumour size) or adjuvant (after surgery to eliminate the remaining microscopic metastases). However, chemotherapeutic compounds and radiation affect the healthy adjacent tissues, which poses restrictions to their effective use.[143] It is thus relevant to improve the existing oncological therapies or to develop new forms of treatment based on new approaches.

1.5. Prostate cancer

Prostate cancer (PCa) is a common urologic malignancy in men and the second leading cause of death from cancer in United States of America (USA) and in European countries.[144] The incidence of PCa in Asian countries is much lower compared to the USA, which may be related to the fact that Asian population consumes large amounts of fruits, vegetables and non-processed food.[145,146] Although the mechanisms involved in the development of this disease are not yet fully defined, is has been associated with the presence of some risk factors: old age, ethnicity, family history of PCa and hormonal alterations.[147] Several reports have described that more than 65% of all PCa are diagnosed in men over 65 years old[148] and that the incidence of PCa is 60% higher in black population compared to Caucasians. Besides, environmental factors, such as eating habits, exposure to chemicals and sexually transmitted infections have also been associated with the pathology.

PCa occurs as two forms: (i) localized (confined to the prostate gland) and androgen-dependent; (ii) metastatic and androgen-independent.[149] In the early stages of the disease, the growth of PCa cells are androgen-dependent and thus confined to the prostate gland. However, PCa cells often become hormone refractory (androgen-independent).[150] This progression step is followed by metastasis formation. Several molecular mechanisms are involved in PCa's propensity to metastasise. These mechanisms lead to local invasion, migration and site-specific establishment of metastases at secondary sites, such as bone, lung and liver.[151] PCa differs from other types of cancer by the late onset of the first symptoms and slow evolution. Often, the manifestation of the first symptoms, including difficulty in urinating, the presence of blood in the urine and pain or burning when urinating occurs in an advanced stage of the disease.[152]

Presently, the first approach to the diagnosis of PCa is performed by digital rectal examination (DRE), blood test for a tumour biomarker known as prostate-specific antigen (PSA), and transrectal ultrasonography (TRUS).[153,154] PSA is a serine protease extensively used for risk stratification of prostate cancer, which enables the early detection of the malignancy with possible decrease in the number of deaths.[155] Usually, a high total PSA (tPSA) value (> 4 ng/mL) in the patient's blood

indicates the presence of disease, since the tumour cells of prostate cancer tend to increase the production of PSA. However, PSA has also been found in human normal cells and its seric levels may be increased due to other conditions of the prostate, such as infection, irritation, benign prostatic hypertrophy, recent ejaculation, or medical interventions.[153,156–159] For a definitive diagnosis it is essential to conduct a biopsy on the prostate.

Treatment of prostate cancer should be selected according to the grade and stage of the tumour, the tPSA levels and the estimated lifetime of the patient.[160] Localised tumours can be efficiently treated by radical prostatectomy, radiotherapy and hormone therapy (androgen deprivation).[161] The androgen-deprivation therapy (ADT), which suppresses or reduces androgens binding to the androgen receptor (AR), is a well-known treatment strategy for early stages of PCa, since cells will not grow and survive without androgens.[162] Metastatic PCa, however, poses major therapeutic challenges: it initially responds well to androgen-deprivation therapies, but the majority of tumours evolves from an androgen-sensitive to an androgen-independent form of the disease, also known as castration-resistant prostate cancer, and often metastasise and bringing a poor prognosis.[163] Since the existing therapies for PCa are not effective for major types of cancers, chemoprevention is emerging as an attractive additional strategy for disease control.[164] Several molecular pathways of PCa could be the targets for chemoprevention (Table 3).

Naturally occurring cancer chemopreventive agents include the curcumin that modulates numerous potential targets for PCa chemoprevention. Curcumin inhibits PCa cell viability, proliferation and migration.[165] It has been reported to inhibit the NF-kB activation in PC-3 cell line.[68] Moreover, curcumin has the ability to induce apoptosis in both androgen-dependent (PC-3) and androgen-independent (LNCaP) PCa cells, downregulating apoptosis suppressor proteins, AR and co-factors,[166] and MMP (MMP-2 and MMP-9) activity, important prerequisites to tumor invasion and metastasis of PCa cells.[167]

Table 3 - Potential targets for prostate cancer chemoprevention.

Molecular events	Molecular target
Signalling pathways	AR
	EGFR
	IGFR
	STAT-3
Cell cycle	CDK-cyclin
	Telomerase
Cell survival/apoptosis	NF-kB
	Bcl-2
Angiogenesis/metastasis	VEGF
	MMP

List of abbreviations on pages xvi-xix.

1.6. Photodynamic therapy in cancer treatment

As indicated above, cancer therapy includes surgery, chemotherapy, radiotherapy and more recently, immunotherapy. However, these techniques can cause some physical damage in healthy tissues of patients.[168] Therefore, it is crucial to develop of therapeutic approaches that allow eradication of tumour with minor damages to patients. A promising strategy is photodynamic therapy (PDT) a minimally invasive and selective technique for the treatment of various cancers, and for the inactivation of bacteria, virus and other microbes.[169–172] Moreover, PDT has is approved as therapeutics for psoriasis, acne, actinic keratosis and wet age-macular degeneration.[173,174]

PDT has three key players: light, photosensitizer (PS) and oxygen. PDT is a two-step procedure: first, a drug is administered to the organism and next the target tissue is irradiated.[169] It uses a specific wavelength light laser or led that activates the PS and produces highly reactive specie of oxygen (e.g. singlet oxygen), which results in destruction of tumour cells. The same PS excited by different range of wavelengths produces different generation rates of single oxygen that can be effective against different diseases.[175] PDT relies on two different mechanisms: Type I and Type II.[176] In Type I, the PS on the triplet excited state reacts with a substrate and transfer an electron or proton. This leads to the formation of radicals

that can interact with molecular oxygen and form reactive oxygen species (ROS), such as superoxide, hydroxyl radical and peroxides. These ROS are highly reactive agents that can cause cell death. In the Type II reaction, occur an energy transference from the triplet state of the PS to molecular oxygen in its ground triplet state ($^3O_2$). In this case, singlet oxygen ($^1O_2$) is generated.

The major advantage of PDT is the fact that the select PS is non-toxic in the absence of light (although sometimes there may be a minimal toxicity). In addition, it is a localized treatment with low accumulation in non-specific tissues[177] and the non-ionizing activating light is harmless on the tissues that have no PS drug. Because of these characteristics, PDT is recognized as a highly selective form of cancer therapy.[178]

The most widely used photosensitizer in current clinical use is Photofrin®.[179] This PS is used in the treatment of early and late-stage lung cancers, oesophageal cancer, bladder cancer, early stage cervical cancer, and malignant and non-malignant skin diseases.[180,181] However, it has disadvantages including skin photosensitivity and a relative small absorbance peak at 630 nm making it somewhat inefficient in use, especially for bulky tumours where light penetration is problematic.[169]

1.6.1. Curcumin in photodynamic therapy

Some studies have proposed that the anticancer activity of curcumin may possibly be enhanced by light application and showed that curcumin with PDT is effective for inhibiting the growth of epithelial carcinoma cells (A431),[182,183] salivary gland acinar cells (SM 10-12),[184] nasopharyngeal carcinoma cells (CNE1 and CNE2),[185,186] keratinocyte cancer cells (HaCaT),[187,188] breast cancer (MCF-7)[189] and head and neck cancer cells (AMC-HN3).[190]

In 2012, the combined action of PDT and curcumin was studied on AMC-HN3, results showing 70% cell viability reduction for the combination treatment and only 50% or 10% reductions for treatments with, respectively, PDT or curcumin alone.[190] Moreover, the combination treatment enhanced the apoptotic events (e.g. nuclear fragmentation and nuclear condensation).

Other study published in 2012 evaluated the photodynamic effect of curcumin on planktonic cultures of *Streptococus mutans* and *Lactobacillus acidophilus* using a blue light emitting diode and curcumin as photosensitizer.[191] The results show that the group that used curcumin followed by blue light illumination contained a significantly lower number of bacteria than did any other group. Moreover, the photodynamic effect was dose dependent for the curcumin concentration. The authors also tested the same conditions in the dark and observed that, curcumin alone for the concentrations tested did not affect the viability of the microorganisms. More recently, a group of researchers studied the use of blue light and curcumin for elimination of *Streptococus mutans*.[192] The results showed that the combination of curcumin and light enhanced the percentage of reduction of viability of microorganisms, corroborating the results obtained previously by other authors.

In general, the results of these all studies suggest that curcumin under PDT has a better treatment efficiency *in vitro*. However, there is no information about anticancer effects of curcumin in human prostate cancer cells.

1.7. Aims of this work

The general purpose of this work is to synthesise and characterise ruthenium(II)-trithiacyclononane complexes with a biologically active ligand curcumin and evaluate its potential as anticancer agent against prostate cancer cells. This was intended to be achieved through a series of steps:

(i) the isolation and purification of curcumin from turmeric powder;

(ii) the synthesis of the novel ruthenium(II)-trithiacyclononane complexes with curcumin as a ligand;

(iii) the structural elucidation and physicochemical properties evaluation of the novel complexes using adequate characterisation techniques (elemental analysis, solution ^{1}H and ^{13}C Nuclear Magnetic Resonance spectroscopies, Mass Spectrometry (ESI-MS), UV-Visible spectroscopy solution and fluorescence spectroscopy);

(iv) the study of binding interaction of the complexes and non-complexed curcumin with salmon sperm DNA;

(v) the evaluation of the cytotoxicity of the complexes towards human prostate cells (PNT-2, non-neoplastic and PC-3, neoplastic) in comparison with that of non-complexed curcumin in dark and light conditions in order to evaluated PDT effects.

2. Experimental section

2.1. Equipment

^{1}H and ^{13}C Nuclear Magnetic Resonance (NMR) spectra were recorded on a Bruker Avance 300 spectrometer at 300.13 MHz and 75.47 MHz, respectively, at room temperature. Unequivocal ^{1}H and ^{13}C assignments were made using 2D correlation spectroscopy (COSY, ^{1}H,^{1}H), while ^{13}C assignments were made on the basis of 2D heteronuclear single quantum coherence spectroscopy (HSQC, ^{1}H,^{13}C), and heteronuclear multiple bond correlation (HMBC, delay for long-range *J* C/H couplings were optimized for 7 Hz) experiments. Deuterated chloroform ($CDCl_3$) was used as solvent (^{1}H 7.26 ppm and ^{13}C 77.29, 77.03 and 76.68 ppm) and tetramethylsilane (TMS) as internal reference. Chemical shifts are quoted in parts per million (ppm) and the coupling constants (*J*) in Hertz (Hz).

Mass spectra were recorded in a Micromass® Q-TOF 2 mass spectrometer using methanol as solvent and electrospray ionization (ESI-MS). The m/z ratios presented in the characterisation data for the sample are monoisotopic, calculated using the mass of the most abundant natural isotope of each constituent element (^{1}H, ^{12}C, ^{14}N, ^{16}O, ^{32}S, ^{35}Cl and ^{102}Ru).

Elemental analysis for CHNS was performed in a TruSpec 630-200-200 CHNS Analyser.

Ultraviolet-visible (UV-Vis) solution spectra were obtained at 25 ºC using 1 x 1 cm quartz optical cells and recorded on a Shimadzu UV-2501 PC spectrophotometer using dimethylformamide (DMF) or dimethylsulfoxide (DMSO) as solvent. Molar absorptivity of each compound were determined using Beer's law.

Fluorescence spectra were recorded on a spectrofluorimeter Fluoromax (Horiba-Jobin-Yvon) at 25 ºC in DMF using 1 x 1 cm quartz fluorescence cells under normal air conditions.

UV-Vis spectra for the DNA interaction experiments (affinity constant determination and denaturation temperature assays) were collected using 1 x 1 cm quartz cells on a GBC Cintra 500 UV-Visible spectrophotometer equipped with a temperature controller (GBC Thermocell). For the denaturation

temperature assay, the absorbance at 260 nm was measured at different temperature values using a heating rate of 0.25 ºC/min over the range 50-99 ºC.

The optical density (OD) of the microplates was then measured at 540 and 630 nm using the microplate reader Tecan Infinite® 200 PRO series.

2.2. Materials

The ruthenium complex [Ru([9]aneS$_3$)(*S*-DMSO)Cl$_2$] was kindly provided by Susana Santos Braga of the University of Aveiro. This complex was the ruthenium(II) precursor used in this work and was synthesized according to the optimization of the method of Landgrafe and Sheldrick[137] published by Madureira et al.[136] 5,10,15,20-Tetraphenylporphyrin (TPP), kindly provide by Maria do Amparo Faustino of the University of Aveiro, was used as reference in some studies of this work, such as fluorescence quantum yield and singlet oxygen measurements.

Distilled acetone was used for the extraction of curcuminoids from the turmeric powder, while distilled dichloromethane was used for the subsequent isolation of curcumin by column chromatography (CC). Hexane (≥ 99.0%), diethyl ether (≥ 99.8%), sodium methoxide (95.0%) and deoxyribonucleic acid low molecular weight from salmon sperm were supplied by Sigma-Aldrich (Sintra, Portugal) and were used without further purification. Chloroform (≥ 99.8%) was purchased from Merck (Darmstadt, Germany). Methanol, used in the synthesis of the new complex, was supplied by Fisher Scientific (Porto Salvo, Portugal). Phosphate buffered saline (PBS, 10x) Dulbecco's formula used for preparation of solutions for DNA binding studies, was purchased from Alfa Aesar (Karlsruche, Germany).

Roswell Park Memorial Institute (RPMI)-1640 medium was acquired from Gibco, Invitrogen (New York, USA). FBS, penicillin/streptomycin and trypsin-EDTA were purchased from Hyclone (Utah, USA). AlamarBlue (AB) and Trypan Blue (TB) were obtained from ThermoFisher (Massachusetts, USA).

2.3. Methods

2.3.1. Extraction and isolation of curcumin

2.3.1.1. Extraction of curcuminoids

Fifteen grams of turmeric powder were dissolved in distilled acetone and magnetically stirred for 4 h at room temperature. The mixture was decanted and concentrated in a rotary evaporator at 40 ºC. Thin layer chromatography (TLC) analysis of the crude extract using 99:1 – dichloromethane:methanol as eluent showed the presence of three major components: curcumin, desmethoxycurcumin and bisdesmethoxycurcumin.

2.3.1.2. Isolation of curcumin

The crude material obtained after extraction with acetone was dissolved in 99:1 – dichloromethane:methanol, mixed with a small amount of silica gel (60-120 mesh), introduced in the top of a glass column packed with silica and subjected to CC. The first eluent used was dichloromethane, followed by 99:1 (V/V) dichloromethane/methanol mixture to yield pure fractions of curcumin.[22] A suitable mobile phase to elute the compounds was chosen by determination of R_f values on TLC plates with UV-detection. The presence of curcumin on the major fraction collected was verified using TLC (R_f values: 0.49, 0.32, and 0.21 for curcumin, desmethoxycurcumin and bisdesmethoxycurcumin, respectively) and NMR analysis. The saffron yellow curcumin was re-dissolved in a small amount of chloroform and crystalized from a mixture of chloroform/hexane.

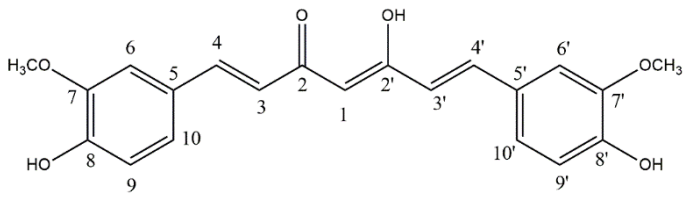

^{1}H NMR (300.13 MHz, $CDCl_3$): δ (ppm) = 16.07 (1H, s, 2'-OH), 7.60 (2H, d, *J*= 15.8 Hz, H-4,4'), 7.13 (2H, dd, *J*= 8.2 Hz, *J*= 1.9 Hz, H-10,10'), 7.06 (2H, d, *J*= 1.9 Hz, H-6,6'), 6.94 (2H, d, *J*= 8.2 Hz, H-9,9'), 6.48 (2H, d, *J*= 15.8 Hz, H-3,3'),

5.86 (2H, s, 8,8'-OH), 5.80 (1H, s, H-1), 3.95 (6H, s, 7,7'-OCH_3).

^{13}C NMR (75.47 MHz, $CDCl_3$): δ (ppm) = 183.5 (C-2,2'), 148.0 (C-8,8'), 146.8 (C-7,7'), 140.5 (C-4,4'), 127.8 (C-5,5'), 123.1 (C-3,3'), 121.9 (C-10,10'), 115.8 (C-9,9'), 114.8 (C-6,6'), 109.7 (C-1), 56.0 (7,7'-OCH_3).

UV-Vis (DMF): λ_{max} (log ε) = 430 nm ($10^{4.70}$). **UV-Vis (DMSO)**: λ_{max} (log ε) = 435 nm ($10^{4.68}$)

2.3.2. Preparation of [Ru([9]aneS_3)(curcumin)(*S*-DMSO)]Cl complex (Ru-curc complex)

A solution of curcumin (67.0 mg, 0.182 mmol) in 20 mL of methanol was treated with sodium methoxide (9.83 mg, 0.182 mmol), and it was observed the solution colour changed from saffron yellow to dark red. The mixture was stirred and heated at 68 ºC for 30 min under a nitrogen atmosphere. Then, [Ru([9]aneS_3)(*S*-DMSO)Cl_2] (62.5 mg, 0.182 mmol) dissolved in methanol (20 mL) was added and the mixture was refluxed for 24h at 68 ºC under stir. The reactional mixture was allowed to cool for 30 min, after which the methanol was evaporated on a rotary evaporator to near dryness (~2 mL methanol). It was then added diethyl ether (~5 mL) and the solution was kept in the refrigerator for three days to obtain a microcrystalline dark red precipitate. The precipitate was isolated by filtering (using Willstätter nail), washed with diethyl ether (~15 mL), and dried (49.1 mg, 37 % yield).

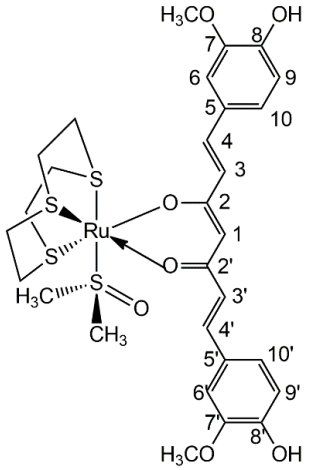

Elemental analysis for [Ru($C_6H_{12}S_3$)($C_{21}H_{19}O_6$)(C_2H_6SO)]Cl·(NaCl) (Mr = 785.01) calculated: C, 40.33; H, 4.80; S, 16.30. Found: C, 39.97; H, 4.90; S, 15.30;

ESI$^+$-MS *m/z* (relative intensity %): 727 ([Ru([9]aneS$_3$)(curc)(*S*-DMSO)]$^+$, 100); 621 ([Ru([9]aneS$_3$–CH$_2$CH$_2$)(curc)]$^+$, 56).

^{1}H NMR (300.13 MHz, $CDCl_3$): δ(ppm) = 7.30 (2H, d, *J*= 16.7 Hz, H-4,4'), 7.10 (2H, dd, *J*= 1.8 Hz, *J*= 8.3 Hz, H-10,10'), 7.01 (2H, d, *J*= 1.8 Hz, H-6,6'), 6.94 (2H, d, *J*= 8.3 Hz, H-9,9'), 6.49 (2H, d, *J*= 16.7 Hz, H-3,3'), 5.64 (1H, s, H-1) 3.96 (6H, s, 7,7'-OCH_3), 2.96 (6H, s, S-CH_3), 3.66-3.58, 3.42-3.38, 2.93-2.80, 2.72-2.65 (12H, m, CH_2-[9]aneS$_3$)

^{13}C NMR (75.47 MHz, $CDCl_3$): δ(ppm) = 178.3 (C-2,2'), 148.6 (C-8,8'), 147.5 (C-7,7'), 138.0 (C-4,4'), 129.2 (C-5,5'), 124.5 (C-3,3'), 121.9 (C-10,10'), 115.4 (C-9,9'), 110.4 (C-6,6'), 102.2 (C-1), 55.1 (7,7'-OCH_3), 42.2 (S-CH_3), 33.6, 32.1, 29.5 (CH_2-[9]aneS$_3$).

UV-Vis (DMF): λ_{max} (log ε) = 412 nm (4.51). **UV-Vis (DMSO)**: λ_{max} (log ε) = 405 nm (4.39)

2.3.3. Fluorescence quantum yield

The fluorescence quantum yields (Φ_F) of curcumin and Ru-curc complex were calculated by comparison of the area below the corrected emission spectrum with that of TPP. TPP was used as fluorescence standard (λ_{exc} = 430 nm) with Φ_F = 0.12 in DMF.[193] In all cases, the absorbance (Abs) of the sample and reference solutions was kept at 0.02 at the 430 nm (the excitation wavelength). Fluorescence quantum yield was calculated according to the equation:

$$\Phi_F^{sample} = \Phi_F^{reference} \frac{AUC^{sample}\left(1\text{-}10^{-Abs_{sample}}\right)}{AUC^{reference}\left(1\text{-}10^{-Abs_{reference}}\right)}$$

where, AUC is the integrated area under the fluorescence curves of each sample and the reference and Abs is the absorbance of the samples and the reference at the excitation wavelength (430 nm).

2.3.4. Singlet oxygen measurements

The quantum yield for singlet oxygen generation (Φ_Δ) upon excitation was evaluated in *N,N*-dimethylformamide (DMF) by a photooxidation method using

9,10-dimethylanthracene (DMA) as $^1O_2$-sensitive indicator. This process is based on the quenching of DMA by $^1O_2$, exclusively in the chemical reaction and yielding 9,10-dimethyl-9,10-dihydro-9,10-epidioxyanthracene (Figure 10).[194,195]

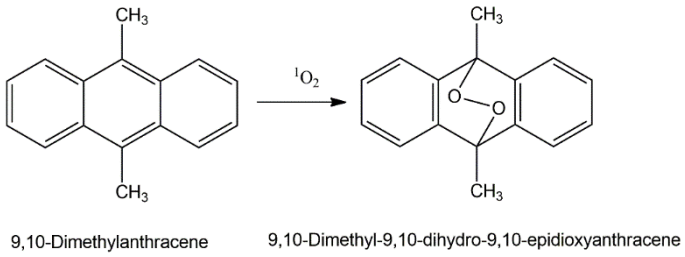

Figure 10 - Photobleaching reaction of 9,10-dimethylanthracene by $^1O_2$

The kinetics of DMA photooxidation was studied by following the decrease in its Abs at λ=378 nm. Solutions of 9,10-dimethylanthracene (DMA; 30 μM) and curcumin or Ru-curc (λ=430 nm; Abs=0.1) in DMF (2.5 mL) were irradiated in quartz cuvettes with monochromatic light at 430 nm obtained through a band-pass filter at an irradiance of 30.0 mW/cm^2. TPP was used as reference (Φ_Δ= 0.62).[196] Measurements of the samples and reference under the same conditions afforded Φ_Δ by direct comparison of the slopes in the linear region of the plots. The observed rate constants (K_{obs}) were obtained by a linear least-squares fit of semi-logarithmic plots of ln(A0/A) versus time for DMA.

2.3.5. DNA binding studies

In this work, the DNA binding studies were performed using deoxyribonucleic acid of salmon sperm (sp-DNA). The solution of sp-DNA in phosphate buffered saline (PBS) gave an absorbance ratio at 260 and 280 nm of about 1.81, indicating that the sp-DNA was free of protein. The final concentration of sp-DNA was determined spectrophotometrically by employing an extinction coefficient of 6600 M^{-1} cm^{-1} at 260 nm. Stock solutions were stored at 4ºC and used over no more than 2 days.

2.3.5.1. Determination of the DNA affinity constant

Concentrated stock solutions of free curcumin or Ru-curc complex were prepared by dissolving the compounds in 1% DMSO buffer and diluting suitably

with the buffer to the required concentrations for all the experiments. The binding propensity of the compounds to sp-DNA was evaluated using spectral methods. UV-Vis spectra of sp-DNA and tested compounds at various concentrations of sp-DNA were measured from 200 to 900 nm in PBS. The absorbance measurements were performed by keeping the free curcumin or complex solutions concentration constant (30 μM) while varying the DNA concentration from 0 to 100 μM (r_j = [DNA]/[compound] = 0-3.3). This was achieved by diluting an appropriate amount of the curcumin or complex and sp-DNA stock solutions in PBS while maintaining the total volume constant (3.0 mL).

The intrinsic binding constant (K_b) was calculated according to the following equation:

$$\frac{[DNA]}{(\varepsilon_a-\varepsilon_f)} = \frac{[DNA]}{(\varepsilon_b-\varepsilon_f)} + \frac{1}{K_b(\varepsilon_b-\varepsilon_f)}$$

where, [DNA] is the concentration of DNA. ε_a correspond to the apparent extinction coefficient of the tested compounds and is calculated by [compound tested]/$Abs_{máx}$. ε_f is the extinction coefficient for free compound in the solvent used for the preparation of solutions; ε_b is entirely DNA-bound combination. When plotting [DNA]/($\varepsilon_a - \varepsilon_f$) versus [DNA], one obtains a linear plot. The slope of the plot corresponds of 1/($\varepsilon_b - \varepsilon_f$), allowing then to obtain K_b.

2.3.5.2. DNA denaturation temperature assay

The thermal denaturation of curcumin/sp-DNA and Ru-curc/sp-DNA mixtures (1:10) was determined in a 10 mM PBS (pH 7.2) solution prepared with ultra-pure water. Melting curves were recorded by heating the mixtures in steps of 5 ºC. For each temperature point, absorbance readings were collected at the wavelength of 260 nm and the experiments occurred in triplicate. The melting temperatures (T_m) of the native and modified sp-DNA were calculated by determining the midpoints of the melting curves from the first-order derivatives. Experimental ΔT_m values were estimated to be accurate within ±1 °C.

2.3.6. Biological assays

2.3.6.1.Cell culture

In this study, two human prostate cell lines were used: PNT-2 (non-neoplastic cell line), kindly given by Dr. Ricardo Perez-Tomás (University of Barcelona, Spain) and PC-3 (neoplastic cell line androgen-independent), kindly given by Dr. Rui Medeiros (University of Porto, Portugal). Cells were cultured in RPMI-1640, supplemented with 10% FBS and 1% penicillin/streptomycin mixture, and maintained in a humidified atmosphere at 37ºC containing 5% CO_2. Cells having a narrow range of passage number were used for all experiments.

2.3.6.2. Cell viability assay

Cell viability was evaluated using the AB assay. AB, also known resasurin, is a water-soluble dye that has been used for quantifying the viability of various cells.[197,198] It allows a continuous monitoring of cultures over time due to the fact that it is extremely stable and nontoxic to cells.[198] When added to cell cultures, the oxidized form of the AB enters the cytosol and is converted to the reduced form by mitochondrial enzyme activity by accepting electrons from NADPH, FADH, FMNH, NADH, as well as from the cytochromes. This redox reaction is accompanied by a shift in color of the culture medium from indigo blue to fluorescent pink, which can be easily measured by colorimetric or fluorescence reading.[199] The number of viable cells correlates with the magnitude of the reduction of the dye and it is expressed as percentage of AB reduction.[198] The assay was developed according to the manufacturer's instructions and the percentage of AB reduction (%AB reduction) was calculated as follows:

$$\%AB\ reduction = \frac{(\varepsilon_{ox}\lambda_2)(A\lambda_1) - (\varepsilon_{ox}\lambda_1)(A\lambda_2)}{(\varepsilon_{red}\lambda_1)(A'\lambda_2) - (\varepsilon_{red}\lambda_2)(A'\lambda_1)} \times 100$$

where, $\varepsilon\lambda_1$ and $\varepsilon\lambda_2$ are constants representing the molar extinction coefficient of AB at 540 and 630 nm which represent the oxidized (ε_{ox}) and reduced (ε_{red}) forms, respectively: $A\lambda_1$ and $A\lambda_2$ represent absorbance of test wells

at 540 and 630 nm, respectively, and A'λ_1 and A'λ_2 represent absorbance of negative control at 540 and 630 nm, respectively.

Cells from confluent 100 mm plate were harvested with trypsin and counted with TB in a hemocytometer. Different cells densities (500, 1250, 2500, 5000, 10000, 20000 and 40000 cells per well) were seeded into duplicate wells of a 96-well plate (100 μL per well). Then, 10 μL AB solution were directly added to the medium. RPMI with 10% AB was used as blank. The plate was further incubated at 37 ºC. The absorbance of test and control wells was read at 1, 2, 4, 6, 8 and 24 h after adding AB at 540 and 630 nm with a plate reader.

2.3.6.3. Preparation of stock solutions of the compounds

Fresh stock solutions were prepared in DMSO and protected from light. Further dilutions of these stock solutions were made in RPMI-1640, keeping only 1% of DMSO, in order to obtain the final concentrations required for the biological assays. In all the experiments, for both control and treated samples, the highest concentration of DMSO used in each well was 1% (v/v).

2.3.6.4. Cytotoxic assay

The cytotoxicity of curcumin and Ru-curc complex was determined using the AB assay. Cells were seeded (5000 cells per well) in 96-well plates (100 μL per well) and incubated at 37 ºC for 24 h to let cells adhere. Different concentrations (80, 50 and 20 μM) of the test compounds were then added and plate was further incubated at 37 ºC. After 48 h the medium was removed and changed to fresh medium and the 96-well plates were further incubated for more 24 h. Sixteen hours before the endpoint of the experiment, 10 μL of AB solution were added to each well. RPMI with 10 % AB was used as blank, whereas cells without treatment and cells treated with 1% DMSO were used as controls. For each condition, including the control conditions, three replicates were prepared and the experiments prepared in triplicate.

2.3.6.5. Phototoxic assay

The phototoxic potential of curcumin and Ru-curc complex was determined using the AB assay. Cells were seeded (5000 cells per well) in two 96-well plates (100 µL per well) and incubated at 37 ºC for 24 h to let cells adhere. Different concentrations (80, 50 and 20 µM) of the test compounds were then added and the plate was further incubated at 37 ºC. After 48 h of incubation with compounds, plates were irradiated with white light (10 mW/cm^2) for 10 min. After illumination, the medium was removed and changed to fresh medium and the plates were incubated for 24 h. Sixteen hours before the endpoint of the experiment, 10 µL of AB solution was added to each well. RPMI with 10% AB was used as blank, whereas cells without treatment and cells treated with 1% DMSO were used as controls. For each condition, including the control conditions, three replicates were prepared and the three independent experiments were done in separate days.

2.3.7. Statistical analysis

Statistical analysis of the data from the % AB reduced by cells treated with the compounds under study, was carried out using GraphPad Prism 7.01 software for *Windows*. The results are expressed as a mean and standard deviation obtained from three independent experiments, each comprising three replicate measurements performed for each concentration of each compound tested plus the untreated control. For all the measurements, one-way ANOVA followed by the Dunnett's *post hoc* test were used to assess the statistical significance between groups. A *P*-value of <0.05 was considered significant. For intra- and inter-assay variability, data from three consecutive experiments were analysed.

3. Results and discussion

3.1. Extraction and isolation of curcumin

Curcuminoids are soluble in various organic solvents including ethanol, methanol, dichloromethane and acetone.[200] Thus, several methods and solvents systems were reported in literature for the extraction of curcuminoids from the turmeric powder, as indicated above in section 1.Introduction.[14] In this work, we used acetone as extracting solvent. An amount of 2.19 g of extracted curcuminoids were obtained from 15 g of turmeric powder. The confirmation of presence of the three curcuminoids in the extract was confirmed by TLC. All the three spots showed to be fluorescent under UV light. Several eluent systems were studied for separation of curcuminoids by chromatography, but 99:1 (v/v) dichloromethane:methanol provided the best results, being thus elected as the eluent for the separation of curcuminoids by column chromatography. With this eluent, the three main curcuminoids present in the acetone extract showed R_f values (in silica gel) of 0.49, 0.32, and 0.21 for curcumin, desmethoxycurcumin and bisdesmethoxycurcumin, respectively.

As indicated in the Introduction, several methods have been reported for the isolation of curcumin, such as TLC, CC and HPLC, using different combinations of stationary and mobile phases. In this study, we used a wet column chromatography. The stationary phase used was silica gel 60-120 mesh and for mobile phase was first dichloromethane and then a mixture of 99:1 – dichloromethane:methanol. After elution with about 1400 mL, 116 mg (5.3% yield) of pure curcumin was obtained and the other two curcuminoids were discarded on the column chromatography. The amount of curcuminoids obtained is influenced by the curcuminoids content of the turmeric powder, which varies from source to source. The solvent in the pure fractions curcumin was evaporated at reduced pressure and the residue taken into chloroform (*ca.* 1 mL) and crystallised in hexane, to obtain a saffron yellow solid powder (93 mg) comprising pure curcumin. The purity of curcumin was confirmed by ^{1}H and ^{13}C NMR and comparing the results with those of the literature and its purity was assessed using TLC.[22]

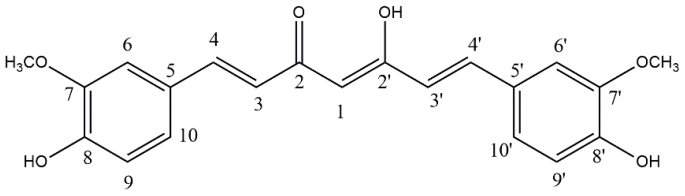

Figure 11 – Carbon labeling scheme for the curcumin

Figure 11 depicts the chemical structure of curcumin with the numbers used to identify the carbon resonances in the NMR spectrum. The ^{1}H NMR spectrum of curcumin was recorded in $CDCl_3$. This spectrum possesses resonance peaks in 3 main areas: in the aliphatic area, a singlet at δ 3.95 ppm corresponding to the resonance of 6 protons of the two methoxyl groups (-OCH_3) (Figure 12 and Table 4); in the most unprotected area at δ 16.07 ppm, a broad singlet typical of a OH in hydrogen bridge, which confirms the presence of curcumin in the enol form; and finally, in the range δ 5.7 – 7.6 ppm appear the peaks due to the resonances of the remaining protons. The values of the chemical shifts of all protons and the coupling constants are in agreement with the ones reported in the literature.[22]

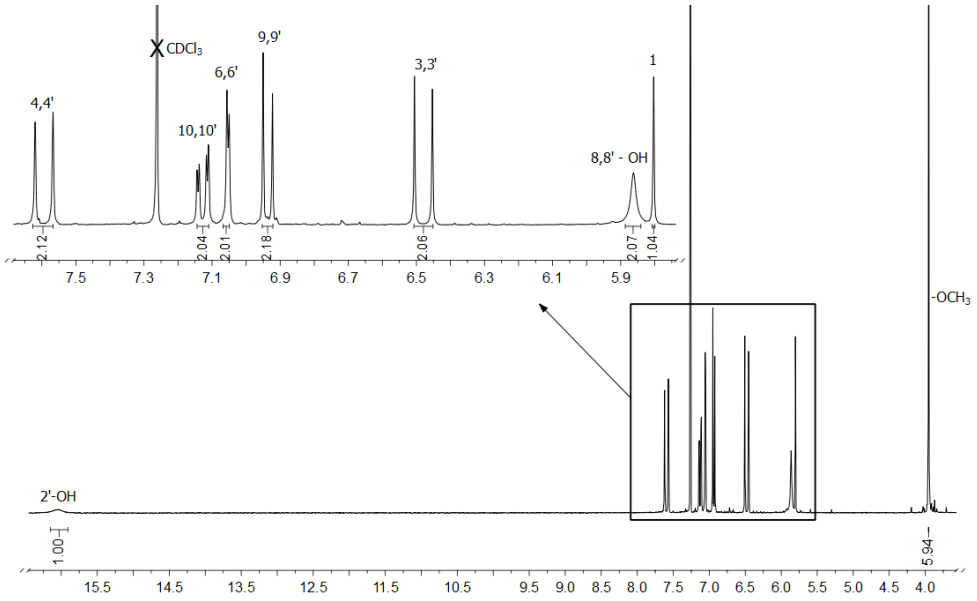

Figure 12 - ^{1}H NMR spectrum recorded in $CDCl_3$ for the curcumin

The ^{13}C NMR spectrum of curcumin was recorded in $CDCl_3$ (Figure 13 and Table 5). The 2D NMR experiments (HMBC and HSQC) allowed the identification and confirmation of the carbon resonance assignments. All the chemical shift

values obtained were in accordance with the reported resonances in the literature for curcumin.[22] Thus, we concluded that curcumin obtained from turmeric was in pure form and free of the presence of other two pigments.

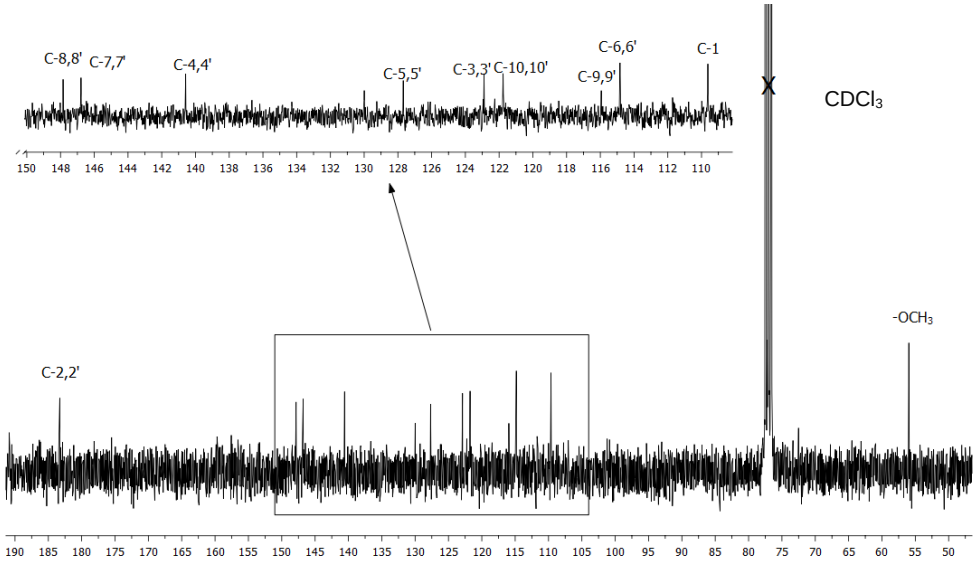

Figure 13 - ^{13}C NMR spectrum recorded in $CDCl_3$ of curcumin.

3.2. Ruthenium(II)-trithiacyclononane complex with curcumin

The scheme depicted in Figure 14 illustrate the first attempt to synthesise a Ru-curc complex. The curcumin hydroxyl group of position 2 was first deprotonated using sodium methoxide (1 equivalent), making the curcumin solution change from strong saffron yellow to red. After 30 min of reflux to ensure full deprotonation, one equivalent of the ruthenium(II) precursor [Ru([9]aneS_3)(*S*-DMSO)Cl_2 was added and the reaction was kept under reflux for another 24 h. After the reactional mixture had been cooled down, the solvent was reduced to a minimal amount under reduced pressure and the addition of diethyl ether allowed the formation of a red precipitate, which was isolated upon filtration, washed and dried (49.1 mg, 37.2 % yield). The product showed to be soluble in polar solvents as DMSO and methanol, but was insoluble in distilled water.

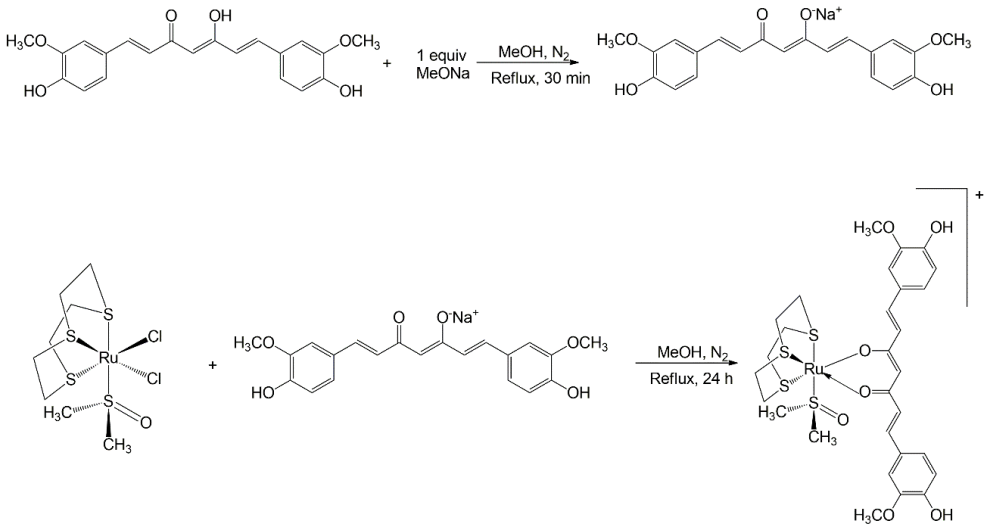

Figure 14 – Reactional scheme for the two-step synthesis of Ru-curc complex.

The structure and purity of the red product isolated was determined by ^{1}H and ^{13}C NMR, mass spectrometry and elemental analysis.

The ^{1}H NMR spectrum of the compound was recorded in $CDCl_3$ (Figure 15). In this spectrum, the resonances of methylene protons of the thioether macrocycle [9]aneS_3 appear as 4 multiplets at δ 3.66-3.58, 3.42-3.38, 2.93-2.80 and 2.72-2.65 ppm. The resonances of protons ascribed to the two equivalent methyl groups of coordinated dimethylsulfoxide appear as a singlet at δ 2.96 ppm. This feature is an evidence of a *S*-DMSO coordination. The intensities of the resonance signals in the ^{1}H NMR are in agreement with the 1:1 metal-to-curcumin stoichiometry proposed.

Upon the coordination, several changes in the signal resonances of the curcumin were observed in the ^{1}H NMR spectrum of the Ru-curc complex (Table 4). As expected, the resonances of the aromatic rings were not affected, while the signal corresponding to the resonance of 2'-OH disappeared, indicating that curcumin chelated the ruthenium ion through this group. Moreover, the resonances of the H-1 and H-4,4' were affected and appeared shielded when compared with the free curcumin. This effect was a result of the increased electronic density. This feature was an evidence of an *O,O*$^{-}$ coordination. The other signals were not significantly affected after coordination as we can see in Table 4.

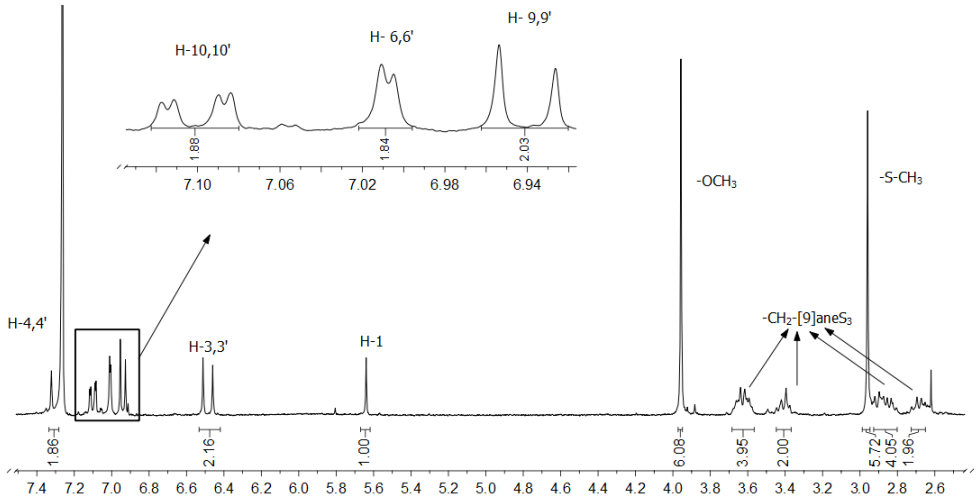

Figure 15 - ^{1}H NMR spectrum recorded in $CDCl_3$ of Ru-curc complex.

Table 4- ^{1}H NMR chemical shifts for the ligand curcumin and the Ru-curc complex in $CDCl_3$.

^{1}H	Curcumin	Ru-curc complex
2'-OH	16.07 (s)	n/a
H-4,4'	7.60 (d), J= 15.8 Hz	7.30 (d), J= 16.7 Hz
H-10,10'	7.13 (dd), J= 8.2 Hz, J= 1.9 Hz	7.10 (dd), J= 8.3 Hz, J= 1.8 Hz
H-6,6'	7.06 (d), J= 1.9 Hz	7.01 (d), J= 1.8 Hz
H-9,9'	6.94 (d), J= 8.2 Hz	6.94 (d), J= 8.3 Hz
H-3,3'	6.48 (d), J= 15.8 Hz	6.49 (d), J= 16.7 Hz
8,8'-OH	5.86 (s)	n/o
H-1	5.80 (s)	5.64 (s)
$-OCH_3$	3.95 (s)	3.96 (s)
$S-CH_3$	n/a	2.96 (s)
CH_2-[9]aneS_3	n/a	3.66-3.58 (m), 3.42-3.38 (m), 2.93-2.80 (m), 2.72-2.65 (m)

Abbreviations used are the following: s – singlet, d – doublet, dd – doublet of doublets, m – multiplet, n/a – not applicable and n/o – not observed.

The 2D NMR experiments (HSQC and HMBC) allowed the identification and confirmation of the carbon resonances. The 7,7'-OCH_3, $S-CH_3$ and CH_2-[9]aneS_3 carbons were confirmed by the ^{1}J HSQC correlations, whereas the ^{2}J and ^{3}J HMBC correlations allowed the identification of the other carbons.

In the ^{13}C NMR spectrum of Ru-curc complex (Figure 16), the resonance DMSO methyl groups appeared at 42.2 ppm, whereas the resonance of the six methylene carbons of the macrocycle (CH_2-[9]aneS_3) appeared at 33.6, 32.1 and 29.5 ppm.

Several changes in the chemical shifts of the curcumin carbon resonances were observed after coordination (Table 5). As expected, the resonances ascribed to C-1 and C-2,2' were the most affected by coordination of curcumin with ruthenium, suffering shifts of *ca.* 8 and 5 ppm, respectively. Furthermore, the C-4,4', C-5,5' and C-6,6' signals were also affected and were shielded or deshielded, depending on its position.

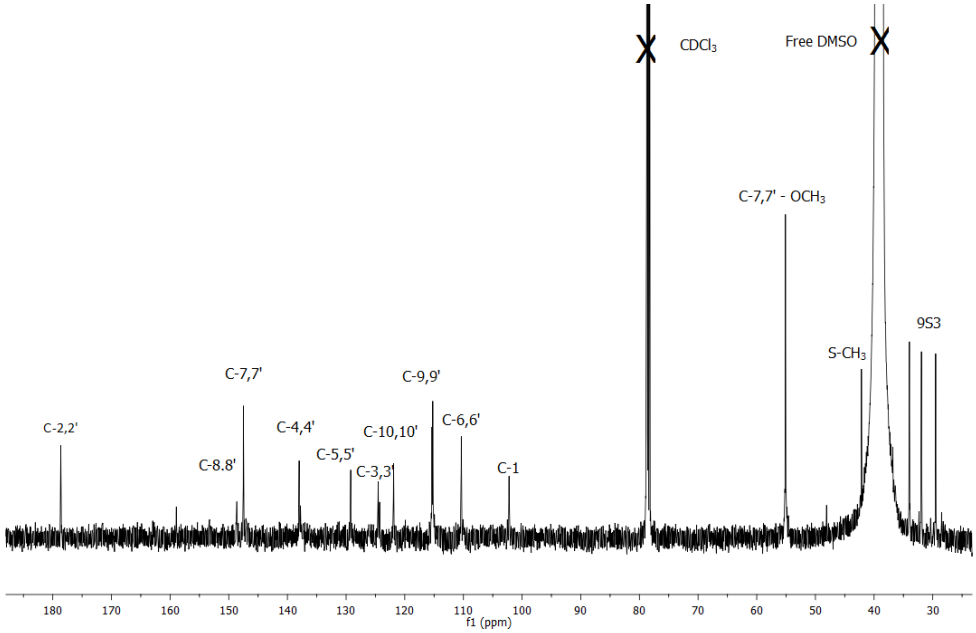

Figure 16 - ^{13}C NMR spectrum recorded in $CDCl_3$ of the Ru-curc complex.

The new complex was further analysed by ESI-MS (positive mode). The mass spectrum showed two major peaks, the most intense appearing at *m/z* = 727 corresponding to [Ru([9]aneS_3)(curcumin)(S-DMSO)]$^+$ cation, that is the molecular ion. The less intense peak appeared at *m/z* = 621 and it was attributed to the [Ru([9]aneS_3–CH_2CH_2)(curcumin)]$^+$ fragment, due to the loss of one ethylene unit of the macrocycle along with DMSO. This confirmed that the molecular structure of the synthesized was the compound depicted in the Figure 14.

Table 5 - ^{13}C NMR chemical shifts for the ligand curcumin and the Ru-curc complex.

^{13}C	Curcumin	Ru-curc complex
C-2,2’	183.5	178.3
C-8,8’	148.0	148.6
C-7,7’	146.8	147.5
C-4,4’	140.5	138.0
C-5,5’	127.8	129.2
C-3,3’	123.1	124.5
C-10,10’	121.9	121.9
C-9,9’	115.8	115.4
C-6,6’	114.8	110.4
C-1	109.7	102.2
7,7’-OCH_3	56.0	55.1
S-CH_3	n/a	42.2
CH_2-[9]aneS_3	n/a	33.6, 32.1, 29.5

n/a – not applicable

3.3. Photophysical properties

3.3.1. Absorption spectra

The absorption properties of curcumin and Ru-curc complex were studied in DMF as well as in DMSO. During the preparation of solutions in the two solvents we observed that the solvent used altered the colour of solution. The UV-Vis spectrum of curcumin and Ru-curc complex recorded in DMF and DMSO at 25 ºC are shown in Figure 17.

The spectrum of the Ru-curc complex exhibited a band in DMF at 413 nm and in DMSO at 403 nm, which shifted in comparison with the free curcumin (429 nm in DMF and 435 nm in DMSO). As shown in Figure 17, the solvent used in the preparation of the solutions influenced the maximum absorbance of both compounds ligand and complex. These results were consistent with the ones observed during the preparation of the solutions.

Molar absorptivities of curcumin and Ru-curc complex in DMF was determined using Beer-Lambert law. The results for molar absorptivity were 49638 $M^{-1}\cdot cm^{-1}$ for curcumin and 32448 $M^{-1}\cdot cm^{-1}$ for Ru-curc complex.

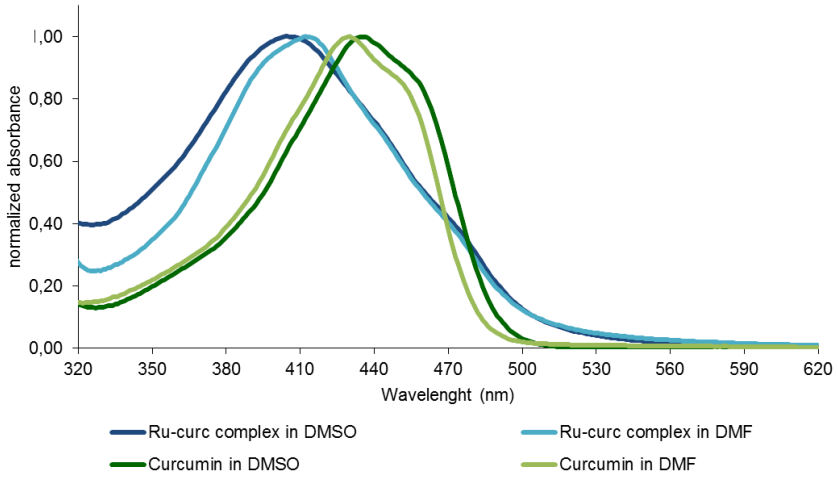

Figure 17 – Normalized UV-Vis absorption spectra of curcumin and Ru-curc complex in DMF and DMSO at 25 ºC.

The results of this study show that the absorption spectrum of curcumin is blue shifted from 429 to 413 nm in DMF after coordination with ruthenium and molar absorptivity was also affected.

3.3.2. Fluorescence spectra

The fluorescence emission spectra of curcumin and Ru-curc complex were recorded in DMF (Figure 18) using TPP as reference (Φ_F = 0.12).[193] All compounds with an OD of 0.02 were excited at 430 nm and spectra recorded in the range of 450-800 nm. The free curcumin in DMF was able to exhibit fluorescence with a quantum yield of fluorescence of 0.18, while the Ru-curc complex did not exhibit fluorescence emission after excitation under the same conditions. The emission of fluorescence in curcumin is a result of the delocalized π-conjugated electronic system and is strongly influenced by solvents, tautomerism, and structural modifications.[201] This may explain the lack of fluorescence in the new complex, since curcumin undergoes a conformational change in the keto-enol group.

Thus, the results showed that curcumin was able to show fluorescence emission after excitation, with an emission band around 530 nm, unlike the complex that showed no significant fluorescence signals (Figure 18).

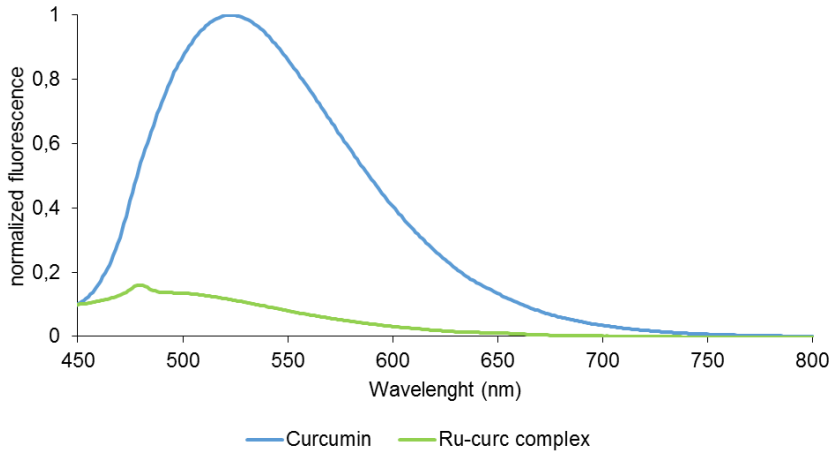

Figure 18 - Normalized fluorescence emission spectra (λ_{exc} 430 nm) of curcumin and Ru-curc complex in DMF.

3.4. Singlet oxygen studies

Photooxidation of DMA sensitized by free curcumin and Ru-curc complex was studied in DMF (Figure 19). Figure 19 shows typical semi-logarithmic plots describing the progress of the reaction of DMA. From first-order kinetic plots of the DMA absorption at 378 nm with time the values of the observed rate constant (K_{obs}) were calculated (Table 6). It was observed that no significant photodecomposition of DMA (blue circle) was detected in the absence of PS.

The quantum yield of $^1O_2$ ($^1\Delta_g$) production (Φ_Δ) by free curcumin and Ru-curc complex was calculated using TPP as reference (TPP, K_{obs} = 1.22x10^{-3} s^{-1} in DMF, Φ_Δ = 0.62). The values of Φ_Δ for free curcumin (K_{obs} = 1.18x10^{-4} s^{-1} in DMF) and Ru-curc complex (K_{obs} = 8.00x10^{-5} s^{-1} in DMF) found were 0.07 and 0.04, respectively. As can be observed, curcumin and Ru-curc complex sensitised the decomposition of DMA in similar rates, indicating no major differences in their photoactivities. However, the decomposition rates were quite lower than the reference. The results of the photooxidation of DMA in the presence of the curcumin or Ru-curc complex showed that they were not good singlet oxygen generators, once curcumin has both antioxidant and pro-oxidant properties.

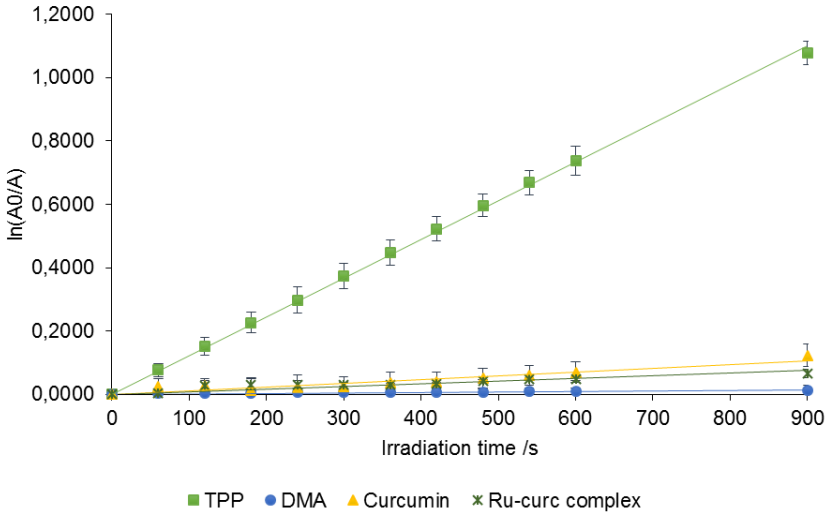

Figure 19 - First-order plots for the photooxidation of DMA (30 μM) photosensitized by TPP (green squares), curcumin (yellow triangles) and Ru-curc complex (grey crosses) in DMF, under irradiation at 430 nm at the irradiance of 30 mW/cm^2. Values represent mean ± standard deviation of three independent experiments.

Table 6 - Kinetic parameters, K_{obs} (s^{-1}) of the photooxidation reaction of DMA by TPP, curcumin and Ru-curc complex after exposure to light of 430 nm at the irradiance of 30 mW/cm^2 and $^1O_2$ quantum yield in DMF.

Photosensitiser	K_{obs} x 10^4 (s^{-1})	Φ_Δ
TPP	12.2	0.68
Curcumin	1.18	0.07
Ru-curc complex	0.80	0.04

3.5. DNA binding studies

Small molecules or ligands can interact with DNA double-helix structures by three different modes: intercalation, groove binding, or external electrostatic binding. However, while groove binding determines only little deviations in the B-form of DNA double helix, the intercalation mode induces the most dramatic changes in the DNA structure.[202] Thus, intercalative binding is the most effective mode binding for drugs targeted to DNA. The interaction between free curcumin or Ru-curc complex and sp-DNA was investigated by UV-Vis absorption spectroscopy and DNA melting method. The results of these experiments are discussed in the following sub-sections.

3.5.1. Absorption spectral studies

Absorption spectroscopy is an effective method and one of the most useful techniques for studying the binding mode of compounds to DNA.[203,204] Some spectral properties, such as hyperchromism and hypochromism or bathochromic and hypsochromic (red or blue shift, respectively) are regarded as characteristic of DNA double-helix structural variation during DNA-ligand/complex interactions. The hyperchromism on compounds tested means the breakage of the secondary structure of DNA; the hypochromism originates from the stabilization of the DNA duplex by either the intercalation binding mode or the electrostatic effect of small molecules.[205] As a rule, complexes that bind to DNA through intercalation result in hypochromism along with a bathochromic shift, due to the intercalative mode involving a strong stacking interaction between a chromophore and the base pairs of DNA.

The UV-Vis absorption spectra of sp-DNA/curcumin and sp-DNA/ Ru-curc complex with various concentrations of sp-DNA in PBS (pH 7.2) at room temperature are shown in Figure 20 and Figure 21, respectively. As shown, the maximum absorption band of sp-DNA in PBS was around 260 nm. Furthermore, the maximum absorption bands of curcumin and Ru-curc complex appeared at 428 and 403 nm, respectively. These values are in agreement with those obtained previously for us in a preliminary study in PBS (data not showed).

The absorption spectra of the free curcumin upon addition of DNA are shown in Figure 20. As shown in this figure, the maximum absorption band of curcumin demonstrated a gradual reduction (hypochromism effect) with increasing concentration of DNA and a blue shift (hypochromism) was observed from 428 to 423 nm. Those spectral modifications can be attributed to the sp-DNA interaction with the drug, which subsequently affect both the absorbance intensity and the absorption band position of curcumin.

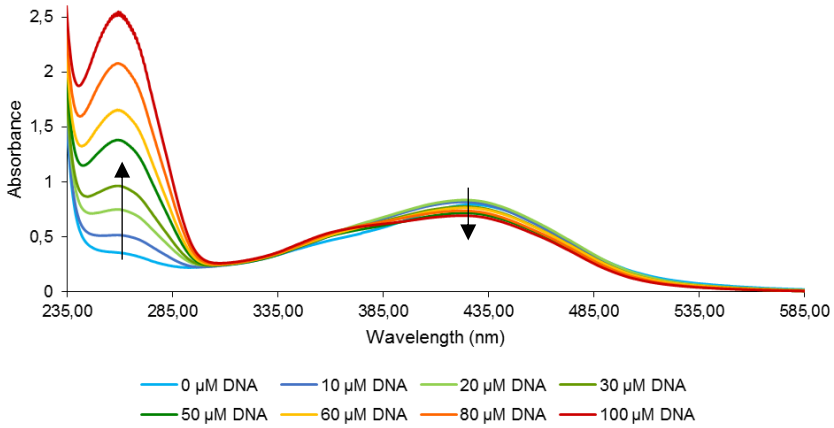

Figure 20 – UV-Vis absorption spectra of curcumin (30 µM) with increasing concentrations of sp-DNA in PBS.

The absorption spectra of the Ru-curc complex upon addition of DNA are shown in Figure 21. As shown in Figure 21, the maximum absorption band of Ru-curc complex in the presence of sp-DNA demonstrated a gradual reduction with increasing concentration of DNA and a very weak red shift (bathochromism) was observed from 402 to 403 nm. These observations are consistent with the intercalation of the complex into the double helix of DNA and provide the evidence of the formation of a new complex-DNA adduct. Moreover, this suggests that sp-DNA might interact with the Ru-curc complex and subsequently affect both the absorbance and the absorption band position of the complex. The hypochromic effect was observed on the interaction between sp-DNA and Ru-curc complex, which constitutes concrete proof of DNA binding to ruthenium metal ion complex.

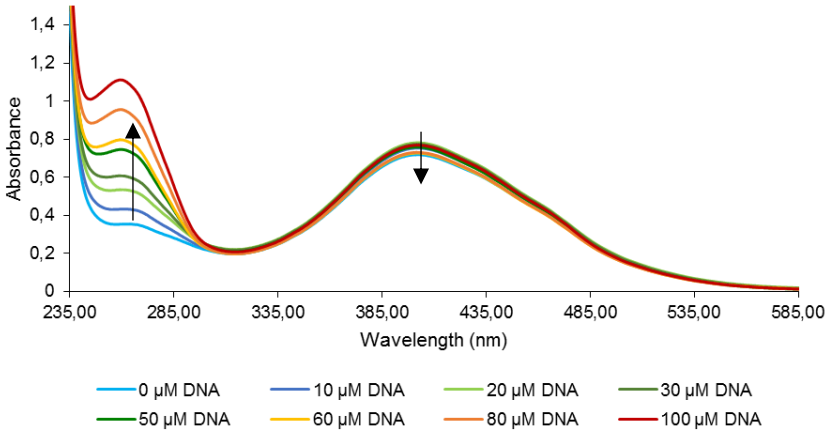

Figure 21 – UV-Vis absorption spectra of Ru-curc complex (30 µM) with increasing concentrations of sp-DNA in PBS.

The intrinsic binding constant was calculated according to the equation indicated in the section 2.3.5. DNA binding studies. The binding constant (K_b) for curcumin was 6.75 x 10^4 M^{-1} and for Ru-curc complex was 4.00 x 10^5 M^{-1}. Spectroscopic evidence showed that curcumin binds to the major and minor grooves of DNA duplex with a binding constant of 5.2 x 10^4 M^{-1}.[206] This value is consistent with the one calculated by us. The K_b value obtained for Ru-curc complex is similar to those reported for typical classical intercalators.

Table 7 Ligand-based absorption spectral properties and binding constant of compounds to sp-DNA.

Compound	λ_{max} (nm)		Binding constant (K_b) (M^{-1})
	Before titration	After titration	
Curcumin	428	423	6.75 x 10^4
Ru-curc complex	402	403	4.00 x 10^5

3.5.2. Thermal denaturation of DNA

The thermal denaturation experiment is a further evidence for the intercalation, or not of compounds into the DNA helix. The DNA melting temperature (*Tm*) is the temperature at which half of the double-stranded DNA is dissociated into single strands.[207] The intercalation of a drug with DNA can stabilize the natural structure of DNA and thus increase the *Tm* value, whereas electrostatic attraction and groove binding lead to no distinct variation in *Tm*. Thermal denaturation studies for sp-DNA should provide a means of gauging the efficacy of the compounds intercalation.

In this work, the thermal denaturation curves of sp-DNA/curcumin and sp-DNA/Ru-curc complex (10:1) mixtures were recorded in 10 mM PBS at pH 7.2. Figure 22 depicts the thermal denaturation curves for pure sp-DNA and for the mixtures sp-DNA/curcumin and sp-DNA/Ru-curc complex. The *Tm* values calculated for sp-DNA, sp-DNA/curcumin and sp-DNA/Ru-curc complex were 84.8 ºC, 85.2 ºC and 92.2 ºC, respectively, as shown in Table 8. The variation on DNA melting temperature (ΔT_m) values are also listed in Table 8. These ΔTm values were obtained from the midpoint of the melting curves of sp-DNA in the absence or presence of curcumin or Ru-curc complex.

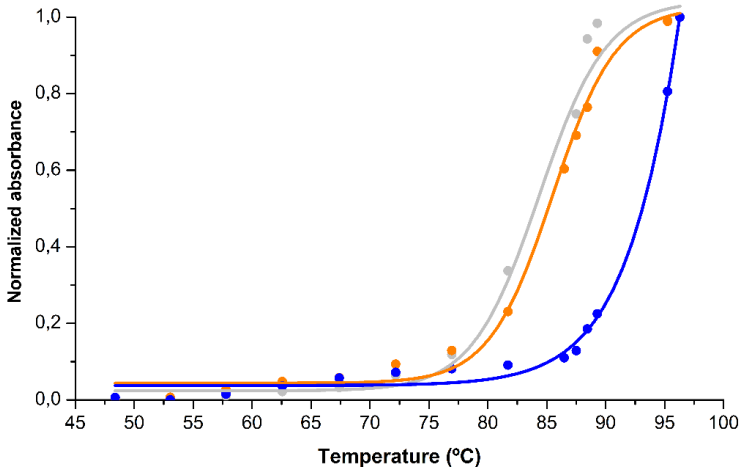

Figure 22 - Comparison of the thermal denaturation curves for pure sp-DNA (grey), sp-DNA/curcumin (orange) and sp-DNA/Ru-curc complex (blue) mixtures in 10:1 molar ratio. Curves were recorded under equilibrium conditions in 10 mM PBS at pH 7.2.

As shown by the data of the Figure 22 and the Table 8, curcumin did not cause significant changes in the melting temperate of sp-DNA. Contrariwise, the mixture of sp-DNA with Ru-curc complex exhibits a dramatically higher melting temperature. The ΔTm value of 7.4 ºC in sp-DNA/Ru-curc complex mixture is indicative of an intercalative agent (ΔTm > 2 ºC) and reveals enhanced stabilization of the sp-DNA double-helix structure after intercalative binding.

Table 8 – Comparison of thermal denaturation for pure sp-DNA, sp-DNA/curcumin or sp-DNA/Ru-curc complex mixtures. The values for *Tm* were obtained from the midpoint of melting curves for pure sp-DNA, sp-DNA/curcumin and sp-DNA/Ru-curc complex mixtures (10:1).

Mixture	T_m (°C)	ΔT_m (°C)
sp-DNA	84.8	—
sp-DNA/Curcumin	85.2	0.4
sp-DNA/Ru-curc complex	92.2	7.4

The results of this section with those of section 3.5.1. (Absorption spectral studies) show that although curcumin binds to sp-DNA it does not form intercalative adducts with it and thus do not induce changes in denaturation temperature. On the other hand, the ruthenium complex has a binding constant similar to classical intercalators and, moreover, causes an increase in the denaturation temperature of sp-DNA. Thus, these results supported the fact that the Ru-curc complex can bind to sp-DNA by the mode of intercalation. This feature, makes this complex a potential anticancer agent.

3.6. Biological evaluation

In order to assess the biological potential of the synthesized Ru-curc complex, its cytotoxic and photocytotoxic activities were evaluated using two human prostate cell lines: PNT-2 (non-neoplastic cell line) and PC-3 (neoplastic cell line, androgen-independent). Curcumin was used as a positive control, since it is a compound with confirmed cytotoxicity against several tumour cell lines.[208]

3.6.1. Cellular Viability

To determine the optimal working cell density for PNT-2 and PC-3 cell lines, the % AB reduction was followed in different cell densities up to 24 h in culture. The % AB reduction increased over culture time, starting from 1 h after addition of AB (Figure 23 for PNT-2 cell line and Figure 24 for PC-3 cell line).

Based on these results, we decided to conduct further experiments using a cell density of 5000 cells per well, once cells were in the logarithmic phase at 24 h. The incubation time was set at 72 h with base on literature reports on the cytotoxic evaluation of curcumin and structural analogues. Studies on prostate cancer cell lines (PC-3 and LNCaP) indicated that the cytotoxicity of curcumin is concentration dependent (higher concentrations of curcumin were more potent than the minor ones) and the cytotoxicity increase with the time of exposure of cells to curcumin (a longer duration of treatment was more potent than a short duration).[209,210]

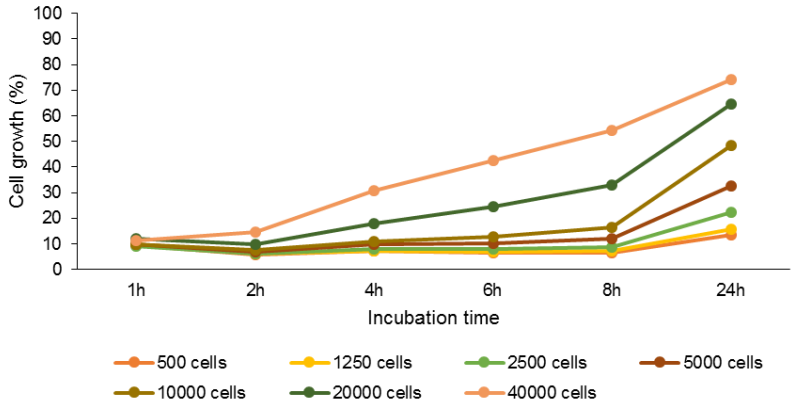

Figure 23 - Alamar Blue (AB) assay for PNT-2 cell viability. PNT-2 cells were seeded at varying densities in a 96-well plate. The AB solution (10% of cell culture volume) was added to the plate and relative absorbance units at 540 and 630 nm were measured at 1, 2, 4, 6, 8 and 24 h.

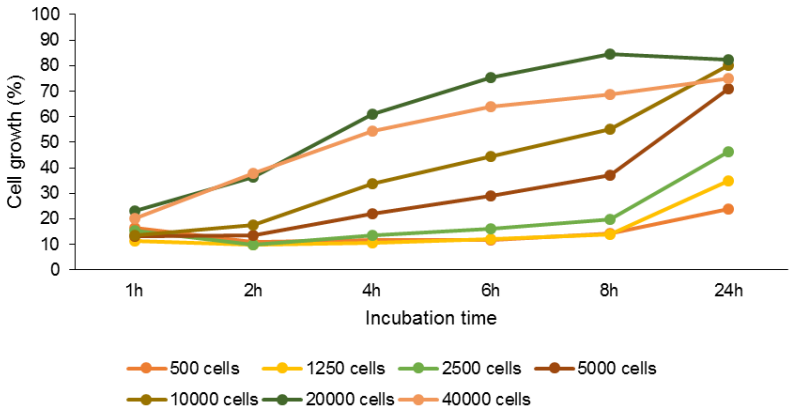

Figure 24 - Alamar Blue (AB) assay for PC-3 cell viability. PC-3 cells were seeded at varying densities in a 96-well plate. The AB solution (10% of cell culture volume) was added to the plate and relative absorbance units at 540 and 630 nm were measured at 1, 2, 4, 6, 8 and 24 h.

The inhibitory effects of curcumin and Ru-curc complex on the growth of cultured PNT-2 and PC-3 cells were determined by using the AB assay. Initially, PNT-2 and PC-3 cells were treated with various concentrations of curcumin and Ru-curc complex (20, 50 and 80 μM) for 72 h in the absence of light. The concentrations to test in this study were chosen based on both literature data[209,210] and Ru-curc complex solubility which limited the maximum concentration to 80 μM.

The inhibitory effects of different concentrations of curcumin and Ru-curc complex in cultured PNT-2 cells are presented in Figure 25. As shown in this figure, PNT-2 cell viability of cells treated with curcumin at 50 and 80 μM was significantly reduced compared with control (P-value<0.05 and P-value<0.001, respectively). On the other hand, Ru-curc complex has no cytotoxic effect on PNT-2 cells. Thus, curcumin has stronger inhibitory effect than Ru-curc complex as determined by AB assay.

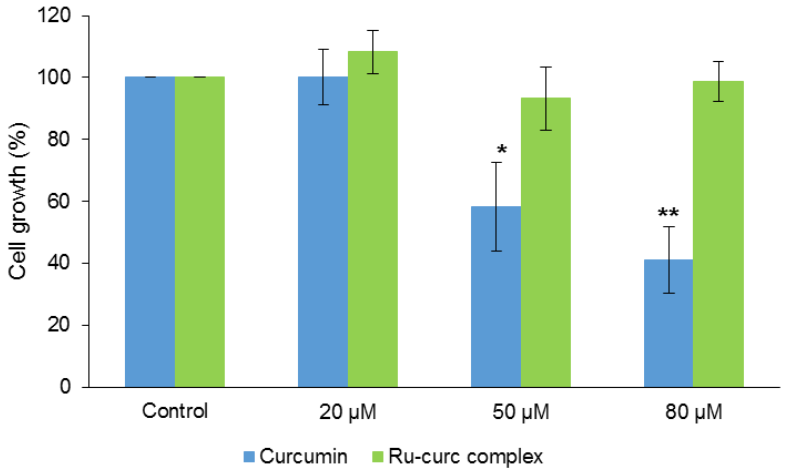

Figure 25 - Effect of curcumin and Ru-curc complex on cell viability of PNT-2 cell line. PNT-2 cells were treated with different concentrations of curcumin, Ru-curc complex or vehicle control DMSO at 1% for 72 h at 37 ºC in dark. The AB assay was used to determine cell viability. Data are representative of three independent trials and are expressed as the mean ± SD. **P*-value<0.05 and ***P*-value<0.001, compared to the group control.

The inhibitory effects of different concentrations of curcumin and Ru-curc complex in cultured PC-3 cells are presented in Figure 26. As shown in figure, PC-3 cell viability of cells treated with curcumin at 50 and 80 µM was once again significantly reduced compared to control (*P*-value<0.001 and *P*-value<0.0001, respectively). Similarly to the results obtained for PNT-2 cells, the Ru-curc complex has no cytotoxic effect on PC-3 cells. Curcumin has stronger inhibitory effect than Ru-curc complex.

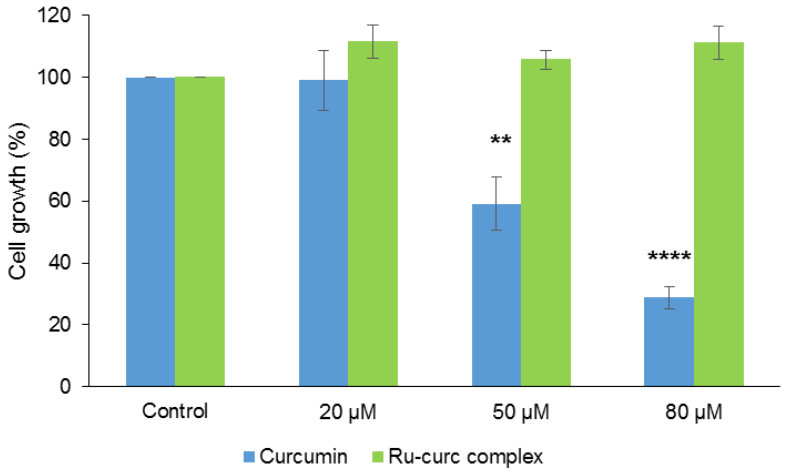

Figure 26 - Effect of curcumin and Ru-curc complex on cell viability of PC-3 cell line. PC-3 cells were treated with different concentrations of curcumin and Ru-curc complex or vehicle control DMSO at 1% for 72 h at 37 ºC in Dark. The AB assay was used to determine cell viability. Data are representative of three independent trials and are expressed as the mean ± SD. ***P*-value<0.001 and *****P*-value<0.0001, compared to the group control.

In the Figure 27 the effect of the curcumin on non tumoral PNT-2 cells is compared with that on PC-3 cells for evaluate the specificity of curcumin. Results show that curcumin is not specific, inhibiting the growth of tumoral and non-tumoral cell lines in a similar fashion. Moreover, the statistical analysis corroborates these observations. As expected, this comparison was not made for the Ru-curc complex, once it showed no inhibitory effect on any of the two cell lines.

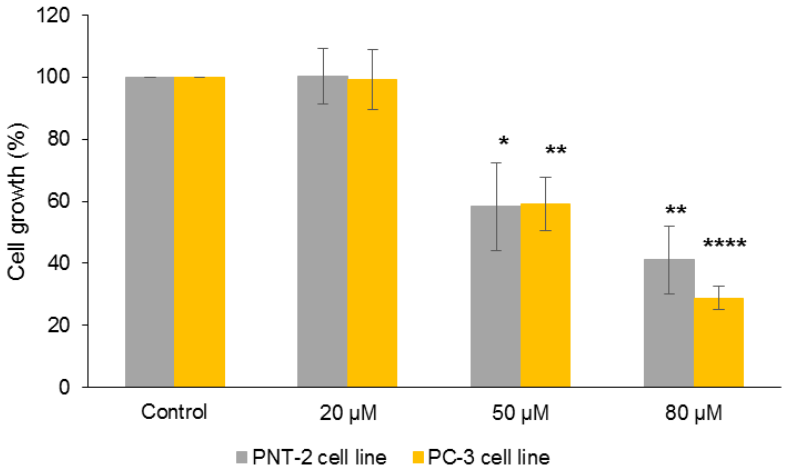

Figure 27 - Effect of curcumin on cell viability of PNT-2 and PC-3 cell lines in dark conditions. PNT-2 and PC-3 cells were treated with different concentrations of curcumin or vehicle control DMSO at 1% for 72 h at 37 ºC in dark conditions. The AB assay was used to determine cell viability. Data are representative of three independent trials and are expressed as the mean ± SD. **P*-value<0.05, ***P*-value<0.001 and ****P*-value<0.0001, compared to the group control.

Knowing that curcumin is a photosensitive compound, we decided to take advantage of this fact and assess their phototoxic potential in the cell lines used. Thus, were performed further studies comprising evaluation of the effects of curcumin and Ru-curc complex under exposure to white light (400-700 nm). PNT-2 and PC-3 cells were treated with curcumin or Ru-curc complex, in the same concentrations of the experiment performed in absence of light, for 48 h, followed by illumination with white light at an irradiance of 10 mW/cm^2 with a total light dose of 6 J/cm^2. After 24 h, cells were examined for viability using AB assay.

Figure 28 shows the experiment that evaluated the effect of combination of curcumin and light in PNT-2 cell viability. As shown, at curcumin concentrations at 50 and 80 µM in combination to light supressed PNT-2 cell viability but no growth effect was observed for the concentration of 20 µM, similarly to the results

obtained for the experiment in the absence of light. Indeed, these two results (light and dark) for 20 µM have no significant differences. In turn, for curcumin concentrations of 50 and 80 µM, statistical analysis indicated significante differences from light experiment (*P*-value<0.001 and *P*-value<0.0001) compared to the group control. Moreover, when comparing PNT-2 inhibition under dark and light conditions, statistical differences were found for the concentrations of 50 and 80 µM (*P*-value<0.05).

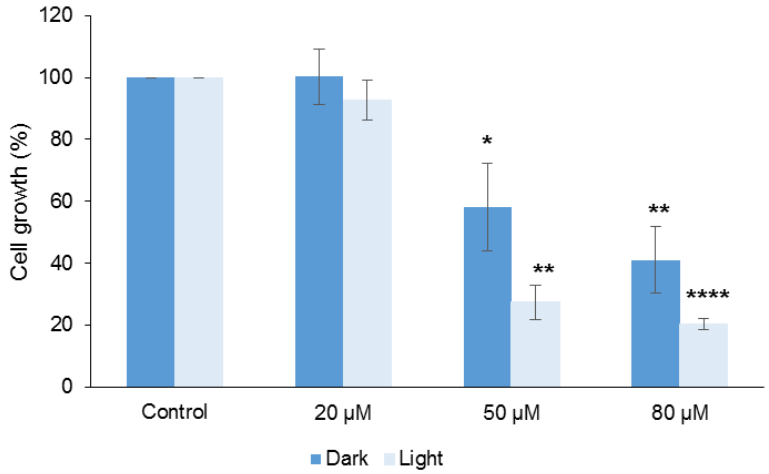

Figure 28 - Effect of curcumin on cell viability of PNT-2 cell line in dark and with irradiation. PNT-2 cells were treated with different concentrations of curcumin or vehicle control DMSO at 1% for 72 h at 37 ºC in dark or with irradiation. The AB assay was used to determine cell viability. Data are representative of three independent trials and are expressed as the mean ± SD. **P*-value<0.05, ***P*-value<0.001 and ****P*-value<0.0001, compared to the group control.

Figure 29 shows the inhibitory effect of curcumin on PC-3 cell viability in the dark and light conditions. The results show that only at concentrations of 50 and 80 µM of curcumin the PC-3 cell viability were significantly different when compared to the non-treated cells, both dark and light experiments. When comparing PC-3 inhibition under light and dark conditions, statistical differences were found only for the concentration up 50 µM (*P*-value<0.05).

Overall, the results indicated that curcumin suppressed PNT-2 and PC-3 cell proliferation in both dose- and light-dependent manner. We observed that curcumin in combination with white light displays a phototoxicity increased and can be consider as potential photosensitizer to treat prostate cancer. However, this study did not investigate which type of ROS were generated in curcumin-PDT

treatment and has been involved in cell death. Our results may provide a rationale for the potential use of curcumin in combination with white light as a chemopreventive agent for prostate cancer.

All these results are in agreement with previously published ones for curcumin in combination with absence or presence of light for other human cell lines. Several reports demonstrated that curcumin is able to induce several cell death pathways and significantly inhibit cell growth, migration and invasion on several cell lines.[211–213] Thus, the curcumin-mediated cell growth inhibition, in this study, could be due to the induced of the apoptosis or inhibition of cell proliferation.

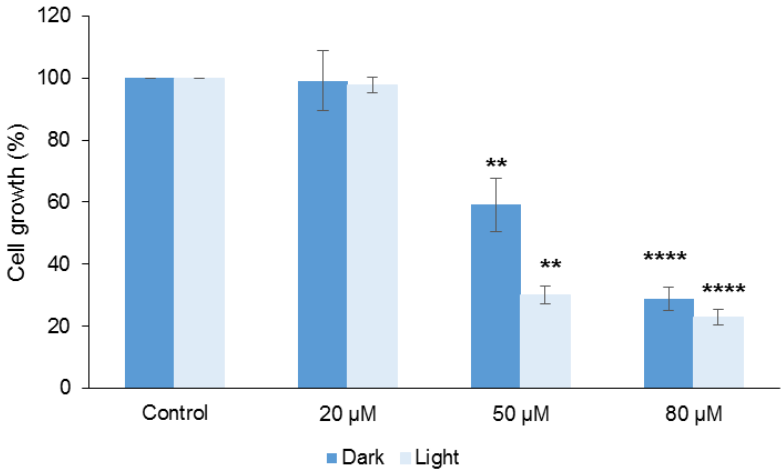

Figure 29 – Effect of curcumin on cell viability of PC-3 cell line in dark and with irradition. PC-3 cells were treated with different concentrations of curcumin or vehicle control DMSO at 1% for 72 h at 37 ºC in Dark or with irradiation whit white light at an irradiance of 10 mW/cm^2 and a total light dose of 6 J/cm^2. The AB assay was used to determine cell proliferation. Data are representative of three independent trials and are expressed as the mean ± SD. *P-value<0.05, **P-value<0.001 and ****P-value<0.0001, compared to the group control.

Figure 30 shows a comparison of the effect of curcumin on PNT-2 and PC-3 cells under light condition, to assess whether the light confers some specificity of the curcumin. Same as the results under dark conditions, the action with light shows that curcumin is not selective, inhibiting growth of the PNT-2 and PC-3 cells in a similar percentage. These evidences were corroborated by statistical analysis.

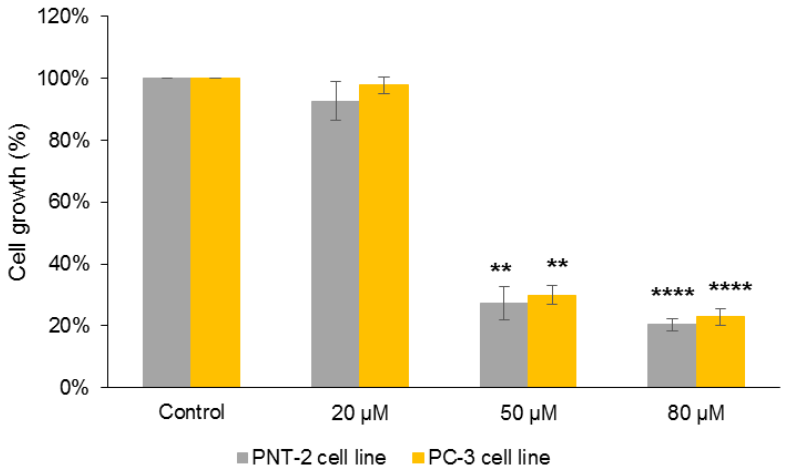

Figure 30 - Effect of curcumin on cell viability of PNT-2 and PC-3 cell lines in light conditions. PNT-2 and PC-3 cells were treated with different concentrations of curcumin or vehicle control DMSO at 1% for 72 h at 37 ºC in light conditions. The AB assay was used to determine cell viability. Data are representative of three independent trials and are expressed as the mean ± SD. ***P*-value<0.001 and ****P-value<0.0001, compared to the group control.

On the other hand, we evaluated phototoxic potential of the Ru-curc complex against PNT-2 and PC-3 cell lines and results are shown in Figure 31 and Figure 32, respectively. Cells (PNT-2 and PC-3) were treated with complex and after 48 h of treatment were exposure to light. The results obtained point out that the Ru-curc complex was not toxic for PNT-2 as well as for PC-3 cell lines (up to 80 µM) either in dark or after exposure to light.

These results were not expected since the complex is able to intercalate with the DNA and thus would be expected to have a cytotoxic effect. Moreover, several studies that used metal complexes of curcumin for anticancer activity demonstrated that curcumin in the metal-bound form retains its therapeutic potential.[214,215] Further, these last authors found that various metals also have increased the stability of curcumin and their solubility under physiological conditions. A possible hypothesis to explain our results is that the compound does not enter into cells and thus, does not reach the nucleus. The non-entry of the Ru-curc complex into cells may be occurring due to their poor solubility under physiological conditions or because it cannot cross the cell membrane. However, we could not evaluate the uptake of the compound by the cells since this complex does not show fluorescence.

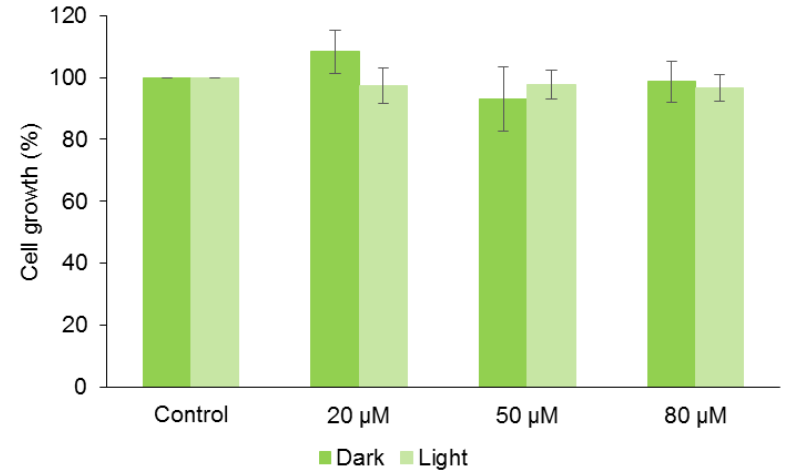

Figure 31 - Effect of Ru-curc complex on cell viability of PNT-2 cell line. PNT-2 cells were treated with different concentrations of Ru-curc complex or vehicle control 1% DMSO for 72 h in dark or exposure to white light at an irradiance of 10 mW/cm^2 and a total light dose of 6 J/cm^2 light dose. The AB assay was used to determine cell proliferation. Data are representative of three independent trials and are expressed as the mean ± SD.

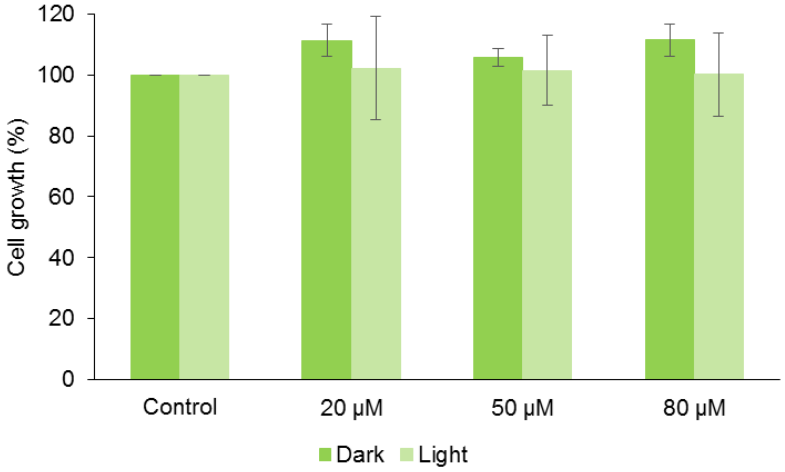

Figure 32 - Effect of Ru-curc complex on cell viability of PC-3 cell line. PC-3 cells were treated with different concentrations of Ru-curc complex or vehicle control 1% DMSO for 72 h in dark or exposure to white light at an irradiance of 10 mW/cm^2 and a total light dose of 6 J/cm^2 light dose. The AB assay was used to determine cell viability. Data are representative of three independent trials and are expressed as the mean ± SD.

The IC_{50} values for curcumin are represented in Table 9. The activity of curcumin on the prostate cancer cell lines yields an IC_{50} value similar to that reported for other cell lines treated with curcumin in absence or presence of light.[208] The IC_{50} values obtained from the curcumin in our two cell lines do not significantly differ. However, promising IC_{50} values were obtained in curcumin treatment under light conditions. Statistical analysis, confirm that the IC_{50} values

in dark and light conditions are significantly different but, the differences between two cell lines are not significant. For Ru-curc complex the IC_{50} could not be determined because the compound was not effective at any of the concentrations tested.

Table 9 - The IC_{50} values (μM) of curcumin and Ru-curc complex towards PNT-2 and PC-3 cell lines with and without light exposure.

Condition tested		PNT-2	PC-3
Curcumin	Dark	64.7	59.3
	Light	44.6*	45.8*
Ru-curc complex	Dark	n.d.	n.d.
	Light	n.d.	n.d.

n.d. – not determined; the IC_{50} could not be determined because the Ru-curc complex Cl complex was not effective at any of the concentrations tested. * Extrapolated value since the minimum concentration tested was 50 μM.

4.Conclusions and future prospects

4.1. Conclusions

In this work, curcumin was successfully isolated from *Curcuma longa* dry powder using column chromatography and its purity was confirmed by ^{1}H and ^{13}C NMR. The pure curcumin was used to prepare a new complex, identified as [Ru([9]aneS_3)(curcumin)(*S*-DMSO)]Cl by elemental analysis, solution NMR and mass spectrometry. The complex was obtained in a 37% yield, which is somewhat low but still comparable with those of other ruthenium complexes with *O*-coordinated ligands, such as 7,3',4'-trihydroxyflavone (38% yield), 3-methoxy-5,7-dihydroxyflavone (23% yield) and 5,7-dihydroxyflavone (43% yield).[216]

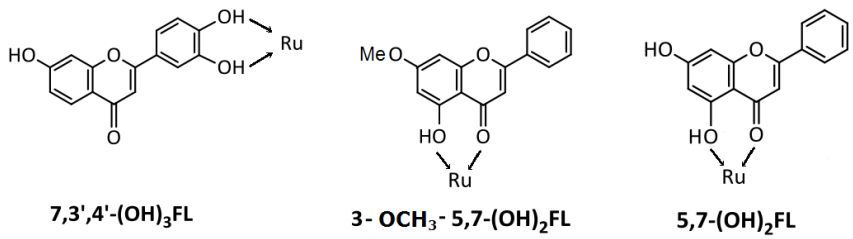

Figure 33 – Examples of *O*-coordinated ligands with ruthenium(II) metal centers. FL=flavonate.

The present study reports that the new curcumin-ruthenium(II) binds to sp-DNA by the mode of intercalation, supported by evidence from two assays. First, the new complex exhibits high binding affinity to sp-DNA with an intrinsic binding constant comparable to intercalative complexes. Moreover, the complex causes a dramatic increase in the sp-DNA melting temperature, a typical feature of intercalative complexes.

Then, the *in vitro* cytotoxic action of Ru-curc complex was studied in the absence and presence of light using both healthy and tumoural prostate cell lines, respectively PNT-2 and PC-3, and using curcumin as a positive control. Surprisingly, the results of the assays show that the growth of both cell line was not influenced by treatment with Ru-curc complex even under light irradiation. Thus, it is necessary to evaluate the uptake of this complex in cells using, for instance, fluorescence probes (the herein reported studies did not evaluate cell

uptake of the compounds). Moreover, it is important to improve the solubility of the complex in physiological conditions which will allow to increase the concentrations to be tested. But, on the other hand, promising results were obtained for the phototoxic assay with curcumin. The results show that the growth of PNT-2 and PC-3 cells line was inhibited by curcumin in a concentration- and light dose-dependent manner.

To conclude, it is our belief that this work focuses in a current subject and proposes the exploration of curcumin as a potential agent for treatment of prostate cancer in photodynamic therapy. Moreover, the most of the studies that evaluated the effect of curcumin on human tumour cells, used the mixture of curcuminoids commercially available but, in this study, all tests were made using pure curcumin obtained in the first part of the work.

4.2. Future prospects

The obvious follow-up of this work will be to test the cytotoxic activity of the new complex in different human cell lines (tumoural and non-tumoural), and try higher concentrations of the compound (after achieving the increase of the solubility of the compound in a physiological medium) and other dose and time of irradiation. Further, it will be important to explore other biological properties of the complex, namely its antibacterial activity and to evaluate the effect of light conditions in this activity, once several reports indicate that some metal complexes of curcumin have antibacterial properties and that this effect can be potentiated by irradiation.[110]

Moreover, it is known from literature that the ruthenium(II)-curcumin derivatives with best anticancer activity are those with arene and 1,3,5-triaza-7-phosphaadamantane (PTA). However, even though to confer greater solubility to derivatives, arene moiety is responsible for the poor solubility of the compound in a physiological medium. Thus, it would be interesting to synthesize other novel derivatives of ruthenium(II)-curcumin having as substituents the 9aneS_3 and PTA. Thus, remain promising properties of macrocyclic effect and is still possible to increase the solubility of the complex.

For the promising properties of curcumin as an agent for photodynamic therapy, is essential to study the application of lower concentrations, that are not

toxic in the dark, other times and light doses of the irradiation and also explore the application of the treatment of other cell lines. Moreover, is important making studies of the cellular localization of curcumin and evaluate the effect of curcumin in the cell death pathways.

References

(1) Chattopadhyay, I.; Biswas, K.; Bandyopadhyay, U.; Banerjee, R. K. Turmeric and Curcumin: Biological Actions and Medicinal Applications. *Curr. Sci.* **2004**, *87* (1), 44–53.

(2) Akram, M.; Uddin, S.; Ahmed, A.; Khan, U.; Hannan, A.; Mohihuddin, E.; Asif, M. Curcuma Longa and Curcumin. *Rom. J. Biol. Plant Biol.* **2010**, *55*, 65–70.

(3) Scartezzini, P.; Speroni, E. Review on Some Plants of Indian Traditional Medicine with Antioxidant Activity. *J. Ethnopharmacol.* **2000**, *71* (1-2), 23–43.

(4) Mukherjee, P. K.; Wahile, A. Integrated Approaches towards Drug Development from Ayurveda and Other Indian System of Medicines. *J. Ethnopharmacol.* **2006**, *103* (1), 25–35.

(5) Toda, S.; Miyase, T.; Arichi, H.; Tanizawa, H.; Takino, Y. Natural Antioxidants. III. Antioxidative Components Isolated from Rhizome of Curcuma Longa L. *Chem. Pharm. Bull.* **1985**, *33* (4), 1725–1728.

(6) Osawa, T.; Sugiyama, Y.; Inayoshi, M.; Kawakishi, S. Antioxidative Activity of Tetrahydrocurcuminoids. *Biosci. Biotechnol. Biochem.* **1995**, *59* (9), 1609–1612.

(7) Govindarajan, V. S. Turmeric - Chemistry, Technology, and Quality. *Crit. Rev. Food Sci. Nutr.* **1980**, *12* (3), 199–301.

(8) Shehzad, A.; Wahid, F.; Lee, Y. S. Curcumin in Cancer Chemoprevention: Molecular Targets, Pharmacokinetics, Bioavailability, and Clinical Trials. *Arch. Pharm.* **2010**, *343* (9), 489–499.

(9) Grynkiewicz, G.; Ślifirski, P. Curcumin and Curcuminoids in Quest for Medicinal Status. *Acta Biochim. Pol.* **2012**, *59* (2), 201–212.

(10) Jayaprakasha, G. K.; Jagan Mohan Rao, L.; Sakariah, K. K. Improved HPLC Method for the Determination of Curcumin, Demethoxycurcumin, and Bisdemethoxycurcumin. *J. Agric. Food Chem.* **2002**, *50* (13), 3668–3672.

(11) Choudhary, N.; Sekhon, B. S. Potential Therapeutic Effect of Curcumin – An Update. *J Pharm Educ Res* **2012**, *3* (2), 64–71.

(12) Antony, S.; Elumalai, S.; Benny, M. Isolation, Purification and Identification of Curcuminoids from Turmeric (Curcuma Longa L.) by Column Chromatography. *J. Exp. Sci.* **2011**, *2* (7), 21–25.

(13) Schieffer, G. W. Pressurized Liquid Extraction of Curcuminoids and Curcuminoid Degradation Products from Turmeric (Curcuma Longa) with Subsequent HPLC Assays. *J. Liq. Chromatogr. Relat. Technol.* **2002**, *25* (19), 3033–3044.

(14) Manzan, A. C. C. M.; Toniolo, F. S.; Bredow, E.; Povh, N. P. Extraction of Essential Oil and Pigments from Curcuma Longa [L] by Steam Distillation and Extraction with Volatile Solvents. *J. Agric. Food Chem.* **2003**, *51* (23), 6802–6807.

(15) Braga, M. E. M.; Leal, P. F.; Carvalho, J. E.; Meireles, M. A. A. Comparison of Yield, Composition, and Antioxidant Activity of Turmeric (Curcuma Longa L.) Extracts Obtained Using Various Techniques. *J. Agric. Food Chem.* **2003**, *51* (22), 6604–6611.

(16) Green, C. E.; Hibbert, S. L.; Bailey-Shaw, Y. A.; Williams, L. A. D.; Mitchell, S.; Garraway, E. Extraction, Processing, and Storage Effects on Curcuminoids and Oleoresin Yields from Curcuma Longa L. Grown in Jamaica. *J. Agric. Food Chem.* **2008**, *56* (10), 3664–3670.

(17) Mandal, V.; Mohan, Y.; Hemalatha, S. Microwave Assisted Extraction of Curcumin by Sample-Solvent Dual Heating Mechanism Using Taguchi L9 Orthogonal Design. *J. Pharm. Biomed. Anal.* **2008**, *46* (2), 322–327.

(18) Mandal, V.; Dewanjee, S.; Sahu, R.; Mandal, S. C. Design and Optimization of Ultrasound Assisted Extraction of Curcumin as an Effective Alternative for Conventional Solid Liquid Extraction of Natural Products. *Nat. Prod. Commun.* **2009**, *4* (1), 95–100.

(19) Revathy, S.; Elumalai, S.; Benny, M.; Antony, B. Isolation, Purification and Identification of Curcuminoids from Turmeric (Curcuma Longa L.) by Column Chromatography. *J. Exp. Sci.* **2011**, *2* (7), 21–25.

(20) Dandekar, D. V.; Gaikar, V. G. Microwave Assisted Extraction of Curcuminoids from Curcuma Longa. *Sep. Sci. Technol.* **2002**, *37* (11), 2669–2690.

(21) Rasmussen, H. B.; Christensen, S. B.; Kvist, L. P.; Karazmi, A. A Simple and Efficient Separation of the Curcumins, the Antiprotozoal Constituents of Curcuma Longa. *Planta Med.* **2000**, *66* (4), 396–398.

(22) Péret-Almeida, L.; Cherubino, A. P. F.; Alves, R. J.; Dufossé, L.; Glória, M. B. A. Separation and Determination of the Physico-Chemical Characteristics of Curcumin, Demethoxycurcumin and Bisdemethoxycurcumin. *Food Res. Int.* **2005**, *38* (8-9), 1039–1044.

(23) Zhang, J.; Jinnai, S.; Ikeda, R.; Wada, M.; Hayashida, S.; Nakashima, K. A Simple HPLC-Fluorescence Method for Quantitation of Curcuminoids and Its Application to Turmeric Products. *Anal. Sci.* **2009**, *25* (3), 385–388.

(24) Paramasivam, M.; Poi, R.; Banerjee, H.; Bandyopadhyay, A. High-Performance Thin Layer Chromatographic Method for Quantitative Determination of Curcuminoids in Curcuma Longa Germplasm. *Food Chem.* **2009**, *113* (2), 640–644.

(25) Ali, I.; Haque, A.; Saleem, K. Separation and Identification of Curcuminoids in Turmeric Powder by HPLC Using Phenyl Column. *Anal. Methods* **2014**, *6* (8), 2526.
(26) Pelletier, J.; Vogel, A. Examen Chimique de La Racine de Curcuma. *J. Pharm.* **1815**, *i*, 289–300.
(27) Daube, F. W. Ueber Curcumin, Den Farbstoff Der Curcumawurzel. *Berichte der Dtsch. Chem. Gesellschaft* **1870**, *3* (1), 609–613.
(28) Miłobedzka, J.; v. Kostanecki, S.; Lampe, V. Zur Kenntnis Des Curcumins. *Berichte der Dtsch. Chem. Gesellschaft* **1910**, *43* (2), 2163–2170.
(29) Lampe, V.; Milobedzka, J. Studien Über Curcumin. *Berichte der Dtsch. Chem. Gesellschaft* **1913**, *46* (2), 2235–2240.
(30) Kuttan, R.; Sudheeran, P. C.; Josph, C. D. Turmeric and Curcumin as Topical Agents in Cancer Therapy. *Tumori* **1987**, *73* (1), 29–31.
(31) Priyadarsini, K. I. The Chemistry of Curcumin: From Extraction to Therapeutic Agent. *Molecules* **2014**, *19* (12), 20091–20112.
(32) Aggarwal, B. B.; Sung, B. Pharmacological Basis for the Role of Curcumin in Chronic Diseases: An Age-Old Spice with Modern Targets. *Trends Pharmacol. Sci.* **2009**, *30* (2), 85–94.
(33) Priyadarsini, K. I. Chemical and Structural Features Influencing the Biological Activity of Curcumin. *Curr. Pharm. Des.* **2013**, *19* (11), 2093–2100.
(34) Tønnesen, H. H.; Karlsen, J.; van Henegouwen, G. B. Studies on Curcumin and Curcuminoids. VIII. Photochemical Stability of Curcumin. *Zeitschrift für Leb. und -forsch.* **1986**, *183* (2), 116–122.
(35) Wang, Y. J.; Pan, M. H.; Cheng, A. L.; Lin, L. I.; Ho, Y. S.; Hsieh, C. Y.; Lin, J. K. Stability of Curcumin in Buffer Solutions and Characterization of Its Degradation Products. *J. Pharm. Biomed. Anal.* **1997**, *15* (12), 1867–1876.
(36) Tønnesen, H. H.; Karlsen, J. Studies on Curcumin and Curcuminoids. VI. Kinetics of Curcumin Degradation in Aqueous Solution. *Zeitschrift für Leb. und -forsch.* **1985**, *180* (5), 402–404.
(37) Holt, P. R.; Katz, S.; Kirshoff, R. Curcumin Therapy in Inflammatory Bowel Disease: A Pilot Study. *Dig. Dis. Sci.* **2005**, *50* (11), 2191–2193.
(38) Shishodia, S.; Sethi, G.; Aggarwal, B. B. Curcumin: Getting back to the Roots. *Ann. N. Y. Acad. Sci.* **2005**, *1056*, 206–217.
(39) Subramanian, M.; Sreejayan; Rao, M. N.; Devasagayam, T. P.; Singh, B. B. Diminution of Singlet Oxygen-Induced DNA Damage by Curcumin and Related Antioxidants. *Mutat. Res.* **1994**, *311* (2), 249–255.

(40) Iqbal, M.; Sharma, S. D.; Okazaki, Y.; Fujisawa, M.; Okada, S. Dietary Supplementation of Curcumin Enhances Antioxidant and Phase II Metabolizing Enzymes in ddY Male Mice: Possible Role in Protection against Chemical Carcinogenesis and Toxicity. *Pharmacol. Toxicol.* **2003**, *92* (1), 33–38.

(41) Busquets, S.; Carbó, N.; Almendro, V.; Quiles, M. T.; López-Soriano, F. J.; Argilés, J. M. Curcumin, a Natural Product Present in Turmeric, Decreases Tumor Growth but Does Not Behave as an Anticachectic Compound in a Rat Model. *Cancer Lett.* **2001**, *167* (1), 33–38.

(42) Duvoix, A.; Blasius, R.; Delhalle, S.; Schnekenburger, M.; Morceau, F.; Henry, E.; Dicato, M.; Diederich, M. Chemopreventive and Therapeutic Effects of Curcumin. *Cancer Lett.* **2005**, *223* (2), 181–190.

(43) He, Y.; Yue, Y.; Zheng, X.; Zhang, K.; Chen, S.; Du, Z. Curcumin, Inflammation, and Chronic Diseases: How Are They Linked? *Molecules* **2015**, *20* (5), 9183–9213.

(44) Gupta, S. C.; Prasad, S.; Kim, J. H.; Patchva, S.; Webb, L. J.; Priyadarsini, I. K.; Aggarwal, B. B. Multitargeting by Curcumin as Revealed by Molecular Interaction Studies. *Nat. Prod. Rep.* **2011**, *28* (12), 1937–1955.

(45) Ravindran, J.; Prasad, S.; Aggarwal, B. B. Curcumin and Cancer Cells: How Many Ways Can Curry Kill Tumor Cells Selectively? *AAPS J.* **2009**, *11* (3), 495–510.

(46) Singh, S.; Aggarwal, B. B. Activation of Transcription Factor NF-kB Is Suppressed by Curcumin (Diferuloylmethane). *J. Biol. Chem.* **1995**, *270* (42), 24995–25000.

(47) Chen, Y. R.; Zhou, G.; Tan, T. H. C-Jun N-Terminal Kinase Mediates Apoptotic Signaling Induced by N-(4-Hydroxyphenyl)retinamide. *Mol. Pharmacol.* **1999**, *56* (6), 1271–1279.

(48) Bierhaus, A.; Zhang, Y.; Quehenberger, P.; Luther, T.; Haase, M.; Müller, M.; Mackman, N.; Ziegler, R.; Nawroth, P. P. The Dietary Pigment Curcumin Reduces Endothelial Tissue Factor Gene Expression by Inhibiting Binding of AP-1 to the DNA and Activation of NF-Kappa B. *Thromb. Haemost.* **1997**, *77* (4), 772–782.

(49) Kang, E. S.; Woo, I. S.; Kim, H. J.; Eun, S. Y.; Paek, K. S.; Kim, H. J.; Chang, K. C.; Lee, J. H.; Lee, H. T.; Kim, J.-H.; Nishinaka, T.; Yabe-Nishimura, C.; Seo, H. G. Up-Regulation of Aldose Reductase Expression Mediated by Phosphatidylinositol 3-kinase/Akt and Nrf2 Is Involved in the Protective Effect of Curcumin against Oxidative Damage. *Free Radic. Biol. Med.* **2007**, *43* (4), 535–545.

(50) Chen, A.; Xu, J. Activation of PPAR(gamma) by Curcumin Inhibits Moser Cell Growth and Mediates Suppression of Gene Expression of Cyclin D1 and EGFR. *Am. J. Physiol. Gastrointest. Liver Physiol.* **2005**, *288* (3), 447–456.

(51) Bharti, A. C.; Donato, N.; Aggarwal, B. B. Curcumin (diferuloylmethane) Inhibits Constitutive and IL-6-Inducible STAT3 Phosphorylation in Human Multiple Myeloma Cells. *J. Immunol.* **2003**, *171* (7), 3863–3871.

(52) Uddin, S.; Hussain, A. R.; Manogaran, P. S.; Al-Hussein, K.; Platanias, L. C.; Gutierrez, M. I.; Bhatia, K. G. Curcumin Suppresses Growth and Induces Apoptosis in Primary Effusion Lymphoma. *Oncogene* **2005**, *24* (47), 7022–7030.

(53) Rajasingh, J.; Raikwar, H. P.; Muthian, G.; Johnson, C.; Bright, J. J. Curcumin Induces Growth-Arrest and Apoptosis in Association with the Inhibition of Constitutively Active JAK-STAT Pathway in T Cell Leukemia. *Biochem. Biophys. Res. Commun.* **2006**, *340* (2), 359–368.

(54) Fu, Y.; Zheng, S.; Lin, J.; Ryerse, J.; Chen, A. Curcumin Protects the Rat Liver from CCl4-Caused Injury and Fibrogenesis by Attenuating Oxidative Stress and Suppressing Inflammation. *Mol. Pharmacol.* **2008**, *73* (2), 399–409.

(55) Hidaka, H.; Ishiko, T.; Furuhashi, T.; Kamohara, H.; Suzuki, S.; Miyazaki, M.; Ikeda, O.; Mita, S.; Setoguchi, T.; Ogawa, M. Curcumin Inhibits Interleukin 8 Production and Enhances Interleukin 8 Receptor Expression on the Cell Surface. *Cancer* **2002**, *95* (6), 1206–1214.

(56) Gulcubuk, A.; Altunatmaz, K.; Sonmez, K.; Haktanir-Yatkin, D.; Uzun, H.; Gurel, A.; Aydin, S. Effects of Curcumin on Tumour Necrosis Factor-Alpha and Interleukin-6 in the Late Phase of Experimental Acute Pancreatitis. *J. Vet. Med. Ser. A* **2006**, *53* (1), 49–54.

(57) Yang, X.; Thomas, D. P.; Zhang, X.; Culver, B. W.; Alexander, B. M.; Murdoch, W. J.; Rao, M. N. A.; Tulis, D. A.; Ren, J.; Sreejayan, N. Curcumin Inhibits Platelet-Derived Growth Factor-Stimulated Vascular Smooth Muscle Cell Function and Injury-Induced Neointima Formation. *Arterioscler. Thromb. Vasc. Biol.* **2006**, *26* (1), 85–90.

(58) Zhou, Y.; Zheng, S.; Lin, J.; Zhang, Q.-J.; Chen, A. The Interruption of the PDGF and EGF Signaling Pathways by Curcumin Stimulates Gene Expression of PPARγ in Rat Activated Hepatic Stellate Cell in Vitro. *Lab. Investig.* **2007**, *87* (5), 488–498.

(59) Mohan, R.; Sivak, J.; Ashton, P.; Russo, L. A.; Pham, B. Q.; Kasahara, N.; Raizman, M. B.; Fini, M. E. Curcuminoids Inhibit the Angiogenic Response Stimulated by Fibroblast Growth Factor-2, Including Expression of Matrix Metalloproteinase Gelatinase B. *J. Biol. Chem.* **2000**, *275* (14), 10405–10412.

(60) Shao, Z.-M.; Shen, Z.-Z.; Liu, C.-H.; Sartippour, M. R.; Go, V. L.; Heber, D.; Nguyen, M. Curcumin Exerts Multiple Suppressive Effects on Human Breast Carcinoma Cells. *Int. J. Cancer* **2002**, *98* (2), 234–240.

(61) Arbiser, J. L.; Klauber, N.; Rohan, R.; Van Leeuwen, R.; Huang, M. T.; Fisher, C.; Flynn, E.; Byers, H. R. Curcumin Is an in Vivo Inhibitor of Angiogenesis. *Mol. Med.* **1998**, *4* (6), 376–383.

(62) Gururaj, A. E.; Belakavadi, M.; Venkatesh, D. A.; Marmé, D.; Salimath, B. P. Molecular Mechanisms of Anti-Angiogenic Effect of Curcumin. *Biochem. Biophys. Res. Commun.* **2002**, *297* (4), 934–942.

(63) Lin, Y. G.; Kunnumakkara, A. B.; Nair, A.; Merritt, W. M.; Han, L. Y.; Armaiz-Pena, G. N.; Kamat, A. A.; Spannuth, W. A.; Gershenson, D. M.; Lutgendorf, S. K.; Aggarwal, B. B.; Sood, A. K. Curcumin Inhibits Tumor Growth and Angiogenesis in Ovarian Carcinoma by Targeting the Nuclear Factor-kappaB Pathway. *Clin. Cancer Res.* **2007**, *13* (11), 3423–3430.

(64) Guo, H.; Xu, Y.-M.; Ye, Z.-Q.; Yu, J.-H.; Hu, X.-Y. Curcumin Induces Cell Cycle Arrest and Apoptosis of Prostate Cancer Cells by Regulating the Expression of IkappaBalpha, c-Jun and Androgen Receptor. *Pharmazie* **2013**, *68* (6), 431–434.

(65) Nakamura, K.; Yasunaga, Y.; Segawa, T.; Ko, D.; Moul, J. W.; Srivastava, S.; Rhim, J. S. Curcumin down-Regulates AR Gene Expression and Activation in Prostate Cancer Cell Lines. *Int. J. Oncol.* **2002**, *21* (4), 825–830.

(66) Dorai, T.; Gehani, N.; Katz, A. Therapeutic Potential of Curcumin in Human Prostate Cancer. II. Curcumin Inhibits Tyrosine Kinase Activity of Epidermal Growth Factor Receptor and Depletes the Protein. *Mol. Urol.* **2000**, *4* (1), 1–6.

(67) Dorai, T.; Cao, Y. C.; Dorai, B.; Buttyan, R.; Katz, A. E. Therapeutic Potential of Curcumin in Human Prostate Cancer. III. Curcumin Inhibits Proliferation, Induces Apoptosis, and Inhibits Angiogenesis of LNCaP Prostate Cancer Cells in Vivo. *Prostate* **2001**, *47* (4), 293–303.

(68) Khor, T. O.; Keum, Y.-S.; Lin, W.; Kim, J.-H.; Hu, R.; Shen, G.; Xu, C.; Gopalakrishnan, A.; Reddy, B.; Zheng, X.; Conney, A. H.; Kong, A.-N. T. Combined Inhibitory Effects of Curcumin and Phenethyl Isothiocyanate on the Growth of Human PC-3 Prostate Xenografts in Immunodeficient Mice. *Cancer Res.* **2006**, *66* (2), 613–621.

(69) Woo, M.-S.; Jung, S.-H.; Kim, S.-Y.; Hyun, J.-W.; Ko, K.-H.; Kim, W.-K.; Kim, H.-S. Curcumin Suppresses Phorbol Ester-Induced Matrix Metalloproteinase-9 Expression by Inhibiting the PKC to MAPK Signaling Pathways in Human Astroglioma Cells. *Biochem. Biophys. Res. Commun.* **2005**, *335* (4), 1017–1025.

(70) Chen, Y. R.; Tan, T. H. Inhibition of the c-Jun N-Terminal Kinase (JNK) Signaling Pathway by Curcumin. *Oncogene* **1998**, *17* (2), 173–178.

(71) Chan, M. M.; Huang, H. I.; Fenton, M. R.; Fong, D. In Vivo Inhibition of Nitric Oxide Synthase Gene Expression by Curcumin, a Cancer Preventive Natural Product with Anti-Inflammatory Properties. *Biochem. Pharmacol.* **1998**, *55* (12), 1955–1962.
(72) Menon, L. G.; Kuttan, R.; Kuttan, G. Inhibition of Lung Metastasis in Mice Induced by B16F10 Melanoma Cells by Polyphenolic Compounds. *Cancer Lett.* **1995**, *95* (1-2), 221–225.
(73) Menon, L. G.; Kuttan, R.; Kuttan, G. Anti-Metastatic Activity of Curcumin and Catechin. *Cancer Lett.* **1999**, *141* (1-2), 159–165.
(74) Chen, H.; Zhang, Z. S.; Zhang, Y. L.; Zhou, D. Y. Curcumin Inhibits Cell Proliferation by Interfering with the Cell Cycle and Inducing Apoptosis in Colon Carcinoma Cells. *Anticancer Res.* **1999**, *19* (5A), 3675–2680.
(75) Cui, S.-X.; Qu, X.-J.; Xie, Y.-Y.; Zhou, L.; Nakata, M.; Makuuchi, M.; Tang, W. Curcumin Inhibits Telomerase Activity in Human Cancer Cell Lines. *Int. J. Mol. Med.* **2006**, *18* (2), 227–231.
(76) Bush, J. A.; Cheung, K. J.; Li, G. Curcumin Induces Apoptosis in Human Melanoma Cells through a Fas Receptor/caspase-8 Pathway Independent of p53. *Exp. Cell Res.* **2001**, *271* (2), 305–314.
(77) Anto, R. J.; Mukhopadhyay, A.; Denning, K.; Aggarwal, B. B. Curcumin (diferuloylmethane) Induces Apoptosis through Activation of Caspase-8, BID Cleavage and Cytochrome c Release: Its Suppression by Ectopic Expression of Bcl-2 and Bcl-Xl. *Carcinogenesis* **2002**, *23* (1), 143–150.
(78) Lin, S.-S.; Huang, H.-P.; Yang, J.-S.; Wu, J.-Y.; Hsia, T.-C.; Hsai, T.-C.; Lin, C.-C.; Lin, C.-W.; Kuo, C.-L.; Gibson Wood, W.; Chung, J.-G. DNA Damage and Endoplasmic Reticulum Stress Mediated Curcumin-Induced Cell Cycle Arrest and Apoptosis in Human Lung Carcinoma A-549 Cells through the Activation Caspases Cascade- and Mitochondrial-Dependent Pathway. *Cancer Lett.* **2008**, *272* (1), 77–90.
(79) Jiang, A.-J.; Jiang, G.; Li, L.-T.; Zheng, J.-N. Curcumin Induces Apoptosis through Mitochondrial Pathway and Caspases Activation in Human Melanoma Cells. *Mol. Biol. Rep.* **2015**, *42* (1), 267–275.
(80) Shishodia, S.; Amin, H. M.; Lai, R.; Aggarwal, B. B. Curcumin (diferuloylmethane) Inhibits Constitutive NF-kappaB Activation, Induces G1/S Arrest, Suppresses Proliferation, and Induces Apoptosis in Mantle Cell Lymphoma. *Biochem. Pharmacol.* **2005**, *70* (5), 700–713.
(81) Bae, J. H.; Park, J.-W.; Kwon, T. K. Ruthenium Red, Inhibitor of Mitochondrial Ca^{2+} Uniporter, Inhibits Curcumin-Induced Apoptosis via the Prevention of Intracellular Ca^{2+}

Depletion and Cytochrome c Release. *Biochem. Biophys. Res. Commun.* **2003**, *303* (4), 1073–1079.

(82) Ibrahim, A.; El-Meligy, A.; Lungu, G.; Fetaih, H.; Dessouki, A.; Stoica, G.; Barhoumi, R. Curcumin Induces Apoptosis in a Murine Mammary Gland Adenocarcinoma Cell Line through the Mitochondrial Pathway. *Eur. J. Pharmacol.* **2011**, *668* (1-2), 127–132.

(83) Gupta, S. C.; Patchva, S.; Koh, W.; Aggarwal, B. B. Discovery of Curcumin, a Component of Golden Spice, and Its Miraculous Biological Activities. *Clin. Exp. Pharmacol. Physiol.* **2012**, *39* (3), 283–299.

(84) Pulla Reddy, A. C.; Sudharshan, E.; Appu Rao, A. G.; Lokesh, B. R. Interaction of Curcumin with Human Serum Albumin--a Spectroscopic Study. *Lipids* **1999**, *34* (10), 1025–1029.

(85) Jaruga, E.; Salvioli, S.; Dobrucki, J.; Chrul, S.; Bandorowicz-Pikuła, J.; Sikora, E.; Franceschi, C.; Cossarizza, A.; Bartosz, G. Apoptosis-Like, Reversible Changes in Plasma Membrane Asymmetry and Permeability, and Transient Modifications in Mitochondrial Membrane Potential Induced by Curcumin in Rat Thymocytes. *FEBS Lett.* **1998**, *433* (3), 287–293.

(86) Lin, H.-Y.; Lin, J.-N.; Ma, J.-W.; Yang, N.-S.; Ho, C.-T.; Kuo, S.-C.; Way, T.-D. Demethoxycurcumin Induces Autophagic and Apoptotic Responses on Breast Cancer Cells in Photodynamic Therapy. *J. Funct. Foods* **2015**, *12*, 439–449.

(87) Anand, P.; Kunnumakkara, A. B.; Newman, R. A.; Aggarwal, B. B. Bioavailability of Curcumin: Problems and Promises. *Mol. Pharm.* **2007**, *4*, 807–818.

(88) Sharma, R. A.; Steward, W. P.; Gescher, A. J. Pharmacokinetics and Pharmacodynamics of Curcumin. *Adv. Exp. Med. Biol.* **2007**, *595*, 453–470.

(89) Pan, M. H.; Huang, T. M.; Lin, J. K. Biotransformation of Curcumin through Reduction and Glucuronidation in Mice. *Drug Metab. Dispos.* **1999**, *27* (4), 486–494.

(90) Ireson, C.; Orr, S.; Jones, D. J.; Verschoyle, R.; Lim, C. K.; Luo, J. L.; Howells, L.; Plummer, S.; Jukes, R.; Williams, M.; Steward, W. P.; Gescher, A. Characterization of Metabolites of the Chemopreventive Agent Curcumin in Human and Rat Hepatocytes and in the Rat *in Vivo*, and Evaluation of Their Ability to Inhibit Phorbol Ester-Induced Prostaglandin E2 Production. *Cancer Res.* **2001**, *61* (3), 1058–1064.

(91) Asai, A.; Miyazawa, T. Occurrence of Orally Administered Curcuminoid as Glucuronide and Glucuronide/sulfate Conjugates in Rat Plasma. *Life Sci.* **2000**, *67* (23), 2785–2793.

(92) Sehgal, A.; Kumar, M.; Jain, M.; Dhawan, D. K. Combined Effects of Curcumin and Piperine in Ameliorating Benzo(a)pyrene Induced DNA Damage. *Food Chem. Toxicol.* **2011**, *49* (11), 3002–3006.

(93) Youssef, K. M.; El-Sherbeny, M. A. Synthesis and Antitumor Activity of Some Curcumin Analogs. *Arch. Pharm.* **2005**, *338* (4), 181–189.

(94) Song, L.; Shen, Y.; Hou, J.; Lei, L.; Guo, S.; Qian, C. Polymeric Micelles for Parenteral Delivery of Curcumin: Preparation, Characterization and *in Vitro* Evaluation. *Colloids Surfaces A Physicochem. Eng. Asp.* **2011**, *390* (1), 25–32.

(95) Mulik, R. S.; Mönkkönen, J.; Juvonen, R. O.; Mahadik, K. R.; Paradkar, A. R. Transferrin Mediated Solid Lipid Nanoparticles Containing Curcumin: Enhanced *in Vitro* Anticancer Activity by Induction of Apoptosis. *Int. J. Pharm.* **2010**, *398* (1-2), 190–203.

(96) Singletary, K.; MacDonald, C.; Wallig, M.; Fisher, C. Inhibition of 7,12-Dimethylbenz[a]anthracene (DMBA)-Induced Mammary Tumorigenesis and DMBA-DNA Adduct Formation by Curcumin. *Cancer Lett.* **1996**, *103* (2), 137–141.

(97) Li, L.; Braiteh, F. S.; Kurzrock, R. Liposome-Encapsulated Curcumin: *In Vitro* and *in Vivo* Effects on Proliferation, Apoptosis, Signaling, and Angiogenesis. *Cancer* **2005**, *104* (6), 1322–1331.

(98) Yang, K.-Y.; Lin, L.-C.; Tseng, T.-Y.; Wang, S.-C.; Tsai, T.-H. Oral Bioavailability of Curcumin in Rat and the Herbal Analysis from Curcuma Longa by LC-MS/MS. *J. Chromatogr. B. Analyt. Technol. Biomed. Life Sci.* **2007**, *853* (1-2), 183–189.

(99) Bisht, S.; Feldmann, G.; Soni, S.; Ravi, R.; Karikar, C.; Maitra, A.; Maitra, A. Polymeric Nanoparticle-Encapsulated Curcumin ("nanocurcumin"): A Novel Strategy for Human Cancer Therapy. *J. Nanobiotechnology* **2007**, *5* (1), 3.

(100) Begum, A. N.; Jones, M. R.; Lim, G. P.; Morihara, T.; Kim, P.; Heath, D. D.; Rock, C. L.; Pruitt, M. A.; Yang, F.; Hudspeth, B.; Hu, S.; Faull, K. F.; Teter, B.; Cole, G. M.; Frautschy, S. A. Curcumin Structure-Function, Bioavailability, and Efficacy in Models of Neuroinflammation and Alzheimer's Disease. *J. Pharmacol. Exp. Ther.* **2008**, *326* (1), 196–208.

(101) Parveen, S.; Sahoo, S. K. Polymeric Nanoparticles for Cancer Therapy. *J. Drug Target.* **2008**, *16* (2), 108–123.

(102) Shahani, K.; Panyam, J. Highly Loaded, Sustained-Release Microparticles of Curcumin for Chemoprevention. *J. Pharm. Sci.* **2011**, *100* (7), 2599–2609.

(103) Zhao, X.-Z.; Jiang, T.; Wang, L.; Yang, H.; Zhang, S.; Zhou, P. Interaction of Curcumin with Zn(II) and Cu(II) Ions Based on Experiment and Theoretical Calculation. *J. Mol. Struct.* **2010**, *984* (1), 316–325.

(104) Caruso, F.; Rossi, M.; Benson, A.; Opazo, C.; Freedman, D.; Monti, E.; Gariboldi, M. B.; Shaulky, J.; Marchetti, F.; Pettinari, R.; Pettinari, C. Ruthenium-Arene Complexes of Curcumin: X-Ray and Density Functional Theory Structure, Synthesis, and Spectroscopic

Characterization, *in Vitro* Antitumor Activity, and DNA Docking Studies of (p-cymene)Ru(curcuminato)chloro. *J. Med. Chem.* **2012**, *55* (3), 1072–1081.

(105) Bonfili, L.; Pettinari, R.; Cuccioloni, M.; Cecarini, V.; Mozzicafreddo, M.; Angeletti, M.; Lupidi, G.; Marchetti, F.; Pettinari, C.; Eleuteri, A. M. Arene-Ru(II) Complexes of Curcumin Exert Antitumor Activity via Proteasome Inhibition and Apoptosis Induction. *ChemMedChem* **2012**, *7* (11), 2010–2020.

(106) Pettinari, R.; Marchetti, F.; Condello, F.; Pettinari, C.; Lupidi, G.; Scopelliti, R.; Mukhopadhyay, S.; Riedel, T.; Dyson, P. J. Ruthenium(II)–Arene RAPTA Type Complexes Containing Curcumin and Bisdemethoxycurcumin Display Potent and Selective Anticancer Activity. *Organometallics* **2014**, *33* (14), 3709–3715.

(107) Antonyan, A.; De, A.; Vitali, L. A.; Pettinari, R.; Marchetti, F.; Gigliobianco, M. R.; Pettinari, C.; Camaioni, E.; Lupidi, G. Evaluation of (arene)Ru(II) Complexes of Curcumin as Inhibitors of Dipeptidyl Peptidase IV. *Biochimie* **2014**, *99*, 146–152.

(108) Lei, X.; Su, W.; Li, P.; Xiao, Q.; Huang, S.; Qian, Q.; Huang, C.; Qin, D.; Lan, H. Ruthenium(II) Arene Complexes of Curcuminoids: Synthesis, X-Ray Diffraction Structure and Cytotoxicity. *Polyhedron* **2014**, *81*, 614–618.

(109) Sareen, R.; Jain, N.; Dhar, K. L. Curcumin-Zn(II) Complex for Enhanced Solubility and Stability: An Approach for Improved Delivery and Pharmacodynamic Effects. *Pharm. Dev. Technol.* **2015**, *20* (1), 1–6.

(110) Wanninger, S.; Lorenz, V.; Subhan, A.; Edelmann, F. T. Metal Complexes of Curcumin-Synthetic Strategies, Structures and Medicinal Applications. *Chem. Soc. Rev.* **2015**, *44* (15), 4986–5002.

(111) Ott, I.; Gust, R. Non Platinum Metal Complexes as Anti-Cancer Drugs. *Arch. Pharm.* **2007**, *340* (3), 117–126.

(112) Clardy, J.; Walsh, C. Lessons from Natural Molecules. *Nature* **2004**, *432* (7019), 829–837.

(113) Tripathi, L.; Kumar, P.; Singhai, A. Role of Chelates in Treatment of Cancer. *Indian J. Cancer* **2007**, *44* (2), 62–71.

(114) Frezza, M.; Dou, Q. P.; Xiao, Y.; Samouei, H.; Rashidi, M.; Samari, F.; Hemmateenejad, B. *In Vitro* and *in Vivo* Antitumor Activities and DNA Binding Mode of Five Coordinated Cyclometalated organoplatinum(II) Complexes Containing Biphosphine Ligands. *J. Med. Chem.* **2011**, *54* (18), 6166–6176.

(115) Bruijnincx, P. C. A.; Sadler, P. J. New Trends for Metal Complexes with Anticancer Activity. *Curr. Opin. Chem. Biol.* **2008**, *12* (2), 197–206.

(116) Alama, A.; Tasso, B.; Novelli, F.; Sparatore, F. Organometallic Compounds in Oncology: Implications of Novel Organotins as Antitumor Agents. *Drug Discov. Today* **2009**, *14* (9-10), 500–508.
(117) Rosenberg, B.; Van Camp, L.; Krigas, T. Inhibition of Cell Division in Escherichia Coli by Electrolysis Products from a Platinum Electrode. *Nature* **1965**, *205* (4972), 698–699.
(118) Zhang, C. X.; Lippard, S. J. New Metal Complexes as Potential Therapeutics. *Curr. Opin. Chem. Biol.* **2003**, *7* (4), 481–489.
(119) Wang, D.; Lippard, S. J. Cellular Processing of Platinum Anticancer Drugs. *Nat. Rev. Drug Discov.* **2005**, *4* (4), 307–320.
(120) Kelland, L. The Resurgence of Platinum-Based Cancer Chemotherapy. *Nat. Rev. Cancer* **2007**, *7* (8), 573–584.
(121) Florea, A.-M.; Büsselberg, D. Cisplatin as an Anti-Tumor Drug: Cellular Mechanisms of Activity, Drug Resistance and Induced Side Effects. *Cancer* **2011**, *3* (1), 1351–1371.
(122) Kostova, I. Platinum Complexes as Anticancer Agents. *Recent Pat. Anticancer. Drug Discov.* **2006**, *1* (1), 1–22.
(123) Brabec, V.; Kasparkova, J. Modifications of DNA by Platinum Complexes. Relation to Resistance of Tumors to Platinum Antitumor Drugs. *Drug Resist. Update* **2005**, *8* (3), 131–146.
(124) Ozben, T. Mechanisms and Strategies to Overcome Multiple Drug Resistance in Cancer. *FEBS Lett.* **2006**, *580* (12), 2903–2909.
(125) Bratsos, I.; Jedner, S.; Gianferrara, T.; Alessio, E. Ruthenium Anticancer Compounds: Challenges and Expectations. *Chim. Int. J. Chem.* **2007**, *61* (11), 692–697.
(126) Antonarakis, E. S.; Emadi, A. Ruthenium-Based Chemotherapeutics: Are They Ready for Prime Time? *Cancer Chemother. Pharmacol.* **2010**, *66* (1), 1–9.
(127) Bergamo, A.; Sava, G. Ruthenium Anticancer Compounds: Myths and Realities of the Emerging Metal-Based Drugs. *Dalton Trans.* **2011**, *40* (31), 7817–7823.
(128) Brabec, V.; Nováková, O. DNA Binding Mode of Ruthenium Complexes and Relationship to Tumor Cell Toxicity. *Drug Resist. Update* **2006**, *9* (3), 111–122.
(129) Jakupec, M. A.; Galanski, M.; Arion, V. B.; Hartinger, C. G.; Keppler, B. K. Antitumour Metal Compounds: More than Theme and Variations. *Dalton Trans.* **2008**, *14* (2), 183–194.
(130) Reedijk, J. Metal-Ligand Exchange Kinetics in Platinum and Ruthenium Complexes. *Platin. Met. Rev.* **2008**, *52* (1), 2–11.
(131) Kapitza, S.; Pongratz, M.; Jakupec, M. A.; Heffeter, P.; Berger, W.; Lackinger, L.; Keppler, B. K.; Marian, B. Heterocyclic Complexes of ruthenium(III) Induce Apoptosis in Colorectal Carcinoma Cells. *J. Cancer Res. Clin. Oncol.* **2005**, *131* (2), 101–110.

(132) Beech, J.; Cragg, P. J.; Drew, M. G. B. Conformational Study of the Macrocycle 1,4,7-Trithiacyclononane in Metal Complexes. *Dalton Trans.* **1994**, *23* (5), 719.

(133) Serli, B.; Zangrando, E.; Gianferrara, T.; Scolaro, C.; Dyson, P. J.; Bergamo, A.; Alessio, E. Is the Aromatic Fragment of Piano-Stool Ruthenium Compounds an Essential Feature for Anticancer Activity? The Development of New Ru(II)-[9]aneS_3 Analogues. *Eur. J. Inorg. Chem.* **2005**, *2005* (17), 3423–3434.

(134) Haymore, B. L.; Lamb, J. D.; Izatt, R. M.; Christensen, J. J. Thermodynamic Origin of the Macrocyclic Effect in Crown Ether Complexes of sodium(1+), potassium(1+), and barium(2+). *Inorg. Chem.* **1982**, *21* (4), 1598–1602.

(135) Goodfellow, B. J.; Félix, V.; Pacheco, S. M. D.; de Jesus, J. P.; Drew, M. G. B. Structural Characterisation of Ru(II)[9]aneS_3 Polypyridyl Complexes by NMR Spectroscopy and Single Crystal X-Ray Diffraction. *Polyhedron* **1997**, *16* (3), 393–401.

(136) Madureira, J.; Santos, T. M.; Goodfellow, B. J.; Lucena, M.; Pedrosa de Jesus, J.; Santana-Marques, M. G.; Drew, M. G. B.; Félix, V. Structural Characterisation of New Ru(II)[9]aneS_3 Polypyridylic Complexes. *Dalton Trans.* **2000**, 23, 4422–4431.

(137) Landgrafe, C.; Sheldrick, W. S. Structure and Reactions of the Thioether Half-Sandwich ruthenium(II) Complexes $[Ru(MeCN)_3([9]aneS_3)][CF_3SO_3]_2$ and $[Ru(MeCN)_2(PPh_3)([9]aneS_3)][CF_3SO_3]_2$([9]ane$S_3$= 1,4,7-Trithiacyclononane). *Dalton Trans.* **1994**, No. 13, 1885–1893.

(138) Crosby, M. E. Cell Cycle: Principles of Control. *Yale J. Biol. Med.* **2007**, *80* (3), 141–142.

(139) Vogelstein, B.; Kinzler, K. W. Cancer Genes and the Pathways They Control. *Nat. Med.* **2004**, *10* (8), 789–799.

(140) Millimouno, F. M.; Dong, J.; Yang, L.; Li, J.; Li, X. Targeting Apoptosis Pathways in Cancer and Perspectives with Natural Compounds from Mother Nature. *Cancer Prev. Res.* **2014**, *7* (11), 1081–1107.

(141) Lobo, I. Multifactorial Inheritance and Genetic Disease. *Nat. Educ.* **2008**, *1* (1), 1–5.

(142) Hambley, T. W. Developing New Metal-Based Therapeutics: Challenges and Opportunities. *Dalton Trans.* **2007**, *21* (43), 4929–4937.

(143) *World Cancer Report 2014*; Stewart, B., Wild, C., Eds.; International Agency for Research on Cancer: Lyon, 2014.

(144) Siegel, R. L.; Miller, K. D.; Jemal, A. Cancer Statistics, 2016. *Cancer J. Clin.* **2015**, *66* (1), 7–30.

(145) Kolonel, L. N.; Hankin, J. H.; Whittemore, A. S.; Wu, A. H.; Gallagher, R. P.; Wilkens, L. R.; John, E. M.; Howe, G. R.; Dreon, D. M.; West, D. W.; Paffenbarger, R. S. Vegetables,

Fruits, Legumes and Prostate Cancer: A Multiethnic Case-Control Study. *Cancer Epidemiol. Biomarkers Prev.* **2000**, *9* (8), 795–804.

(146) Namiki, M.; Akaza, H.; Lee, S. E.; Song, J.-M.; Umbas, R.; Zhou, L.; Lee, B. C.; Cheng, C.; Chung, M. K.; Fukagai, T.; Hinotsu, S.; Horie, S. Prostate Cancer Working Group Report. *Jpn. J. Clin. Oncol.* **2010**, *40 Suppl 1*, 70–75.

(147) Nelson, W. G.; De Marzo, A. M.; Isaacs, W. B. Prostate Cancer. *N. Engl. J. Med.* **2003**, *349* (4), 366–381.

(148) Madu, C. O.; Lu, Y. Novel Diagnostic Biomarkers for Prostate Cancer. *J. Cancer* **2010**, *1*, 150–177.

(149) Matos, C. S.; de Carvalho, A. L. M. B.; Lopes, R. P.; Marques, M. P. M. New Strategies against Prostate Cancer--Pt(II)-Based Chemotherapy. *Curr. Med. Chem.* **2012**, *19* (27), 4678–4687.

(150) Heinlein, C. A.; Chang, C. Androgen Receptor in Prostate Cancer. *Endocr. Rev.* **2004**, *25* (2), 276–308.

(151) Bubendorf, L.; Schöpfer, A.; Wagner, U.; Sauter, G.; Moch, H.; Willi, N.; Gasser, T. C.; Mihatsch, M. J. Metastatic Patterns of Prostate Cancer: An Autopsy Study of 1,589 Patients. *Hum. Pathol.* **2000**, *31* (5), 578–583.

(152) Society, A. C. Cancer Facts and Figures 2015. *Am. Cancer Soc.* **2015**, 1–51.

(153) Rhea, J. M.; Molinaro, R. J. Cancer Biomarkers: Surviving the Journey from Bench to Bedside. *MLO. Med. Lab. Obs.* **2011**, *43* (3), 10–12.

(154) Heidenreich, A.; Bellmunt, J.; Bolla, M.; Joniau, S.; Mason, M.; Matveev, V.; Mottet, N.; Schmid, H.-P.; van der Kwast, T.; Wiegel, T.; Zattoni, F. EAU Guidelines on Prostate Cancer. Part 1: Screening, Diagnosis, and Treatment of Clinically Localised Disease. *Eur. Urol.* **2011**, *59* (1), 61–71.

(155) Kohli, M.; Tindall, D. J. New Developments in the Medical Management of Prostate Cancer. *Mayo Clin. Proc.* **2010**, *85* (1), 77–86.

(156) Chu, T. M. Prostate-Specific Antigen and Early Detection of Prostate Cancer. *Tumour Biol.* **1997**, *18* (2), 123–134.

(157) Polascik, T. J.; Oesterling, J. E.; Partin, A. W. Prostate Specific Antigen: A Decade of Discovery-What We Have Learned and Where We Are Going. *J. Urol.* **1999**, *162* (2), 293–306.

(158) Rao, A. R.; Motiwala, H. G.; Karim, O. M. A. The Discovery of Prostate-Specific Antigen. *BJU Int.* **2008**, *101* (1), 5–10.

(159) Makarov, D. V.; Loeb, S.; Getzenberg, R. H.; Partin, A. W. Biomarkers for Prostate Cancer. *Annu Rev Med.* **2009**, 60, 139-151.

(160) Heidenreich, A.; Bastian, P. J.; Bellmunt, J.; Bolla, M.; Joniau, S.; Mason, M. D.; Matveev, V.; Mottet, N.; Zattoni, F. Guidelines on Prostate Cancer. *Eur. Assoc. Urol.* **2015**, 35–42.

(161) Duchesne, G. Localised Prostate Cancer - Current Treatment Options. *Aust. Fam. Physician* **2011**, *40* (10), 768–771.

(162) Crawford, E. D.; Moul, J. W. ADT Risks and Side Effects in Advanced Prostate Cancer: Cardiovascular and Acute Renal Injury. *Oncology* **2015**, *29* (1), 55–58, 65–66.

(163) Parray, A.; Siddique, H. R.; Nanda, S.; Konety, B. R.; Saleem, M. Castration-Resistant Prostate Cancer: Potential Targets and Therapies. *Biologics* **2012**, *6*, 267–276.

(164) Singh, R. P.; Agarwal, R. Mechanisms of Action of Novel Agents for Prostate Cancer Chemoprevention. *Endocr. Relat. Cancer* **2006**, *13* (3), 751–778.

(165) Lall, R. K.; Syed, D. N.; Adhami, V. M.; Khan, M. I.; Mukhtar, H. Dietary Polyphenols in Prevention and Treatment of Prostate Cancer. *Int. J. Mol. Sci.* **2015**, *16* (2), 3350–3376.

(166) Dorai, T.; Gehani, N.; Katz, A. Therapeutic Potential of Curcumin in Human Prostate Cancer-I. Curcumin Induces Apoptosis in Both Androgen-Dependent and Androgen-Independent Prostate Cancer Cells. *Prostate Cancer Prostatic Dis.* **2000**, *3* (2), 84–93.

(167) Hong, J. H.; Ahn, K. S.; Bae, E.; Jeon, S. S.; Choi, H. Y. The Effects of Curcumin on the Invasiveness of Prostate Cancer *in Vitro* and *in Vivo*. *Prostate Cancer Prostatic Dis.* **2006**, *9* (2), 147–152.

(168) Master, A.; Livingston, M.; Sen Gupta, A. Photodynamic Nanomedicine in the Treatment of Solid Tumors: Perspectives and Challenges. *J. Control. Release* **2013**, *168* (1), 88–102.

(169) Agostinis, P.; Berg, K.; Cengel, K. A.; Foster, T. H.; Girotti, A. W.; Gollnick, S. O.; Hahn, S. M.; Hamblin, M. R.; Juzeniene, A.; Kessel, D.; Korbelik, M.; Moan, J.; Mroz, P.; Nowis, D.; Piette, J.; Wilson, B. C.; Golab, J. Photodynamic Therapy of Cancer: An Update. *CA. Cancer J. Clin.* **2011**, *61* (4), 250–281.

(170) Yoo, J.-O.; Ha, K.-S. New Insights into the Mechanisms for Photodynamic Therapy-Induced Cancer Cell Death. *Int. Rev. Cell Mol. Biol.* **2012**, *295*, 139–274.

(171) Allison, R. R.; Moghissi, K. Oncologic Photodynamic Therapy: Clinical Strategies That Modulate Mechanisms of Action. *Photodiagnosis Photodynamic Therapy* **2013**, *10* (4), 331–341.

(172) Allison, R. R. Photodynamic Therapy: Oncologic Horizons. *Future Oncol.* **2014**, *10* (1), 123–124.

(173) Dolmans, D. E. J. G. J.; Fukumura, D.; Jain, R. K. Photodynamic Therapy for Cancer. *Nat. Rev. Cancer* **2003**, *3* (5), 380–387.

(174) Lane, N. New Light on Medicine. *Sci. Am.* **2008**, *18* (3), 80–87.
(175) Zorlu, Y.; Dumoulin, F.; Durmuş, M.; Ahsen, V. Comparative Studies of Photophysical and Photochemical Properties of Solketal Substituted platinum(II) and zinc(II) Phthalocyanine sets. *Tetrahedron* **2010**, *66* (17), 3248–3258.
(176) Juarranz, Á.; Jaén, P.; Sanz-Rodríguez, F.; Cuevas, J.; González, S. Photodynamic Therapy of Cancer. Basic Principles and Applications. *Clin. Transl. Oncol.* **2008**, *10* (3), 148–154.
(177) Miller, J. D.; Baron, E. D.; Scull, H.; Hsia, A.; Berlin, J. C.; McCormick, T.; Colussi, V.; Kenney, M. E.; Cooper, K. D.; Oleinick, N. L. Photodynamic Therapy with the Phthalocyanine Photosensitizer Pc 4: The Case Experience with Preclinical Mechanistic and Early Clinical-Translational Studies. *Toxicol. Appl. Pharmacol.* **2007**, *224* (3), 290–299.
(178) O'Connor, A. E.; Gallagher, W. M.; Byrne, A. T. Porphyrin and Nonporphyrin Photosensitizers in Oncology: Preclinical and Clinical Advances in Photodynamic Therapy. *Photochem. Photobiol.* **2009**, *85* (5), 1053–1074.
(179) Josefsen, L. B.; Boyle, R. W. Photodynamic Therapy and the Development of Metal-Based Photosensitisers. *Met. Based Drugs* **2008**, *2008*, 1–24.
(180) Pushpan, S. K.; Venkatraman, S.; Anand, V. G.; Sankar, J.; Parmeswaran, D.; Ganesan, S.; Chandrashekar, T. K. Porphyrins in Photodynamic Therapy - a Search for Ideal Photosensitizers. *Curr. Med. Chem. Anticancer. Agents* **2002**, *2* (2), 187–207.
(181) Usuda, J.; Kato, H.; Okunaka, T.; Furukawa, K.; Tsutsui, H.; Yamada, K.; Suga, Y.; Honda, H.; Nagatsuka, Y.; Ohira, T.; Tsuboi, M.; Hirano, T. Photodynamic Therapy (PDT) for Lung Cancers. *J. Thorac. Oncol.* **2006**, *1* (5), 489–493.
(182) Chan, W.-H.; Wu, H.-J. Anti-Apoptotic Effects of Curcumin on Photosensitized Human Epidermal Carcinoma A431 Cells. *J. Cell. Biochem.* **2004**, *92* (1), 200–212.
(183) Dujic, J.; Kippenberger, S.; Ramirez-Bosca, A.; Diaz-Alperi, J.; Bereiter-Hahn, J.; Kaufmann, R.; Bernd, A.; Hofmann, M. Curcumin in Combination with Visible Light Inhibits Tumor Growth in a Xenograft Tumor Model. *Int. J. Cancer* **2009**, *124* (6), 1422–1428.
(184) Bruzell, E. M.; Morisbak, E.; Tønnesen, H. H. Studies on Curcumin and Curcuminoids. XXIX. Photoinduced Cytotoxicity of Curcumin in Selected Aqueous Preparations. *Photochem. Photobiol. Sci.* **2005**, *4* (7), 523–530.
(185) Koon, H.; Leung, A. W. N.; Yue, K. K. M.; Mak, N. K. Photodynamic Effect of Curcumin on NPC/CNE2 Cells. *J. Environ. Pathol. Toxicol. Oncol.* **2006**, *25* (1-2), 205–215.
(186) Wang, D.; Hu, J.; Lv, L.; Xia, X.; Liu, J.; Li, X. Enhanced Inhibitory Effect of Curcumin via Reactive Oxygen Species Generation in Human Nasopharyngeal Carcinoma Cells Following Purple-Light Irradiation. *Oncol. Lett.* **2013**, *6* (1), 81–85.

(187) Dujic, J.; Kippenberger, S.; Hoffmann, S.; Ramirez-Bosca, A.; Miquel, J.; Diaz-Alperi, J.; Bereiter-Hahn, J.; Kaufmann, R.; Bernd, A. Low Concentrations of Curcumin Induce Growth Arrest and Apoptosis in Skin Keratinocytes Only in Combination with UVA or Visible Light. *J. Invest. Dermatol.* **2007**, *127* (8), 1992–2000.

(188) Park, K.; Lee, J.-H. Photosensitizer Effect of Curcumin on UVB-Irradiated HaCaT Cells through Activation of Caspase Pathways. *Oncol. Rep.* **2007**, *17* (3), 537–540.

(189) Zeng, X. B.; Leung, A. W. N.; Xia, X. S.; Yu, H. P.; Bai, D. Q.; Xiang, J. Y.; Jiang, Y.; Xu, C. S. Effect of Blue Light Radiation on Curcumin-Induced Cell Death of Breast Cancer Cells. *Laser Phys.* **2010**, *20* (6), 1500–1503.

(190) Ahn, J.-C.; Kang, J.-W.; Shin, J.-I.; Chung, P.-S. Combination Treatment with Photodynamic Therapy and Curcumin Induces Mitochondria-Dependent Apoptosis in AMC-HN3 Cells. *Int. J. Oncol.* **2012**, *41* (6), 2184–2190.

(191) Araújo, N. C.; Fontana, C. R.; Bagnato, V. S.; Gerbi, M. E. M. Photodynamic Effects of Curcumin against Cariogenic Pathogens. *Photomed. Laser Surg.* **2012**, *30* (7), 393–399.

(192) Paschoal, M. A.; Tonon, C. C.; Spolidório, D. M. P.; Bagnato, V. S.; Giusti, J. S. M.; Santos-Pinto, L. Photodynamic Potential of Curcumin and Blue LED against Streptococcus Mutans in a Planktonic Culture. *Photodiagnosis Photodynamic Therapy* **2013**, *10* (3), 313–319.

(193) Milanesio, M. E.; Alvarez, M. G.; Silber, J. J.; Rivarola, V.; Durantini, E. N. Photodynamic Activity of Monocationic and Non-Charged Methoxyphenylporphyrin Derivatives in Homogeneous and Biological Media. *Photochem. Photobiol. Sci.* **2003**, *2* (9), 926–933.

(194) Stevens, B.; Algar, B. E. Photoperoxidation of Unsaturated Organic Molecules. I. Relaxation and Oxygen-Quenching Parameters of the Sensitizer Singlet State. *J. Phys. Chem.* **1968**, *72* (7), 2582–2587.

(195) Stevens, B.; Algar, B. E. Photoperoxidation of Unsaturated Organic Molecules. II. Autoperoxidation of Aromatic Hydrocarbons. *J. Phys. Chem.* **1968**, *72* (10), 3468–3474.

(196) Dzhagarov, B. M.; Salokhiddinov, K. I.; Egorova, G. D.; Gurinovich, G. P. Efficiency of Singlet Oxygen Formation, Photosensitized by Water-Soluble Porphyrins. *Russ. J. Phys. Chem.* **1987**, *61* (9), 2450–2454.

(197) Fields, R. D.; Lancaster, M. V. Dual-Attribute Continuous Monitoring of Cell Proliferation/cytotoxicity. *Am. Biotechnol. Lab.* **1993**, *11* (4), 48–50.

(198) Ahmed, S. A.; Gogal, R. M.; Walsh, J. E. A New Rapid and Simple Non-Radioactive Assay to Monitor and Determine the Proliferation of Lymphocytes: An Alternative to [3H]thymidine Incorporation Assay. *J. Immunol. Methods* **1994**, *170* (2), 211–224.

(199) Al-Nasiry, S.; Geusens, N.; Hanssens, M.; Luyten, C.; Pijnenborg, R. The Use of Alamar Blue Assay for Quantitative Analysis of Viability, Migration and Invasion of Choriocarcinoma Cells. *Hum. Reprod.* **2007**, *22* (5), 1304–1309.

(200) Itokawa, H.; Shi, Q.; Akiyama, T.; Morris-Natschke, S. L.; Lee, K.-H. Recent Advances in the Investigation of Curcuminoids. *Chin. Med.* **2008**, *3* (11), 1–13.

(201) Lee, W.-H.; Loo, C.-Y.; Bebawy, M.; Luk, F.; Mason, R.; Rohanizadeh, R. Curcumin and Its Derivatives: Their Application in Neuropharmacology and Neuroscience in the 21st Century. *Curr. Neuropharmacol.* **2013**, *11* (4), 338–378.

(202) Pucci, D.; Bellini, T.; Crispini, A.; D'Agnano, I.; Liguori, P. F.; Garcia-Orduña, P.; Pirillo, S.; Valentini, A.; Zanchetta, G. DNA Binding and Cytotoxicity of Fluorescent Curcumin-Based Zn(II) Complexes. *MedChemComm* **2012**, *3* (4), 462-468.

(203) Ramakrishnan, S.; Palaniandavar, M. Mixed-Ligand copper(II) Complexes of Dipicolylamine and 1,10-Phenanthrolines: The Role of Diimines in the Interaction of the Complexes with DNA. *J. Chem. Sci.* **2005**, *117* (2), 179–186.

(204) Liu, Z.-C.; Wang, B.-D.; Yang, Z.-Y.; Li, Y.; Qin, D.-D.; Li, T.-R. Synthesis, Crystal Structure, DNA Interaction and Antioxidant Activities of Two Novel Water-Soluble Cu^{2+} Complexes Derivated from 2-Oxo-Quinoline-3-Carbaldehyde Schiff-Bases. *Eur. J. Med. Chem.* **2009**, *44* (11), 4477–4484.

(205) Shi, Y.; Guo, C.; Sun, Y.; Liu, Z.; Xu, F.; Zhang, Y.; Wen, Z.; Li, Z. Interaction between DNA and Microcystin-LR Studied by Spectra Analysis and Atomic Force Microscopy. *Biomacromolecules* **2011**, *12* (3), 797–803.

(206) Rajesh, J.; Rajasekaran, M.; Rajagopal, G.; Athappan, P. Analytical Methods to Determine the Comparative DNA Binding Studies of curcumin–Cu(II) Complexes. *Spectrochim. Acta Part A Mol. Biomol. Spectrosc.* **2012**, *97*, 223–230.

(207) Kumar, C. V.; Turner, R. S.; Asuncion, E. H. Groove Binding of a Styrylcyanine Dye to the DNA Double Helix: The Salt Effect. *J. Photochem. Photobiol. A Chem.* **1993**, *74* (2-3), 231–238.

(208) Shehzad, A.; Lee, J.; Lee, Y. S. Curcumin in Various Cancers. *Biofactors* **2013**, *39* (1), 56–68.

(209) Li, W.; Wang, Y.; Song, Y.; Xu, L.; Zhao, J.; Fang, B. A Preliminary Study of the Effect of Curcumin on the Expression of p53 Protein in a Human Multiple Myeloma Cell Line. *Oncol. Lett.* **2015**, *9* (4), 1719–1724.

(210) Ni, X.; Zhang, A.; Zhao, Z.; Shen, Y.; Wang, S. Demethoxycurcumin Inhibits Cell Proliferation, Migration and Invasion in Prostate Cancer Cells. *Oncol. Rep.* **2012**, *28* (1), 85–90.

(211) Mohankumar, K.; Pajaniradje, S.; Sridharan, S.; Singh, V. K.; Ronsard, L.; Banerjea, A. C.; Benson, C. S.; Coumar, M. S.; Rajagopalan, R. Mechanism of Apoptotic Induction in Human Breast Cancer Cell, MCF-7, by an Analog of Curcumin in Comparison with Curcumin – An *in Vitro* and *in Silico* Approach. *Chem. Biol. Interact.* **2014**, *210*, 51–63.

(212) Notarbartolo, M.; Poma, P.; Perri, D.; Dusonchet, L.; Cervello, M.; D'Alessandro, N. *Antitumor Effects of Curcumin, Alone or in Combination with Cisplatin or Doxorubicin, on Human Hepatic Cancer Cells. Analysis of Their Possible Relationship to Changes in NF-kB Activation Levels and in IAP. Gene Expression*; **2005**; 224, 53-65.

(213) Wang, L.; Ye, X.; Cai, X.; Su, J.; Ma, R.; Yin, X.; Zhou, X.; Li, H.; Wang, Z.; Wang, L.; Ye, X.; Cai, X.; Su, J.; Ma, R.; Yin, X.; Zhou, X.; Li, H.; Wang, Z. Curcumin Suppresses Cell Growth and Invasion and Induces Apoptosis by down-Regulation of Skp2 Pathway in Glioma Cells. *Oncotarget* **2015**, *6* (20), 18027–18037.

(214) Banerjee, S.; Chakravarty, A. R. Metal Complexes of Curcumin for Cellular Imaging, Targeting, and Photoinduced Anticancer Activity. *Acc. Chem. Res.* **2015**, *48* (7), 2075–2083.

(215) Pröhl, M.; Schubert, U. S.; Weigand, W.; Gottschaldt, M. Metal Complexes of Curcumin and Curcumin Derivatives for Molecular Imaging and Anticancer Therapy. *Coord. Chem. Rev.* **2016**, *307*, 32–41.

(216) Marques, J. T. Ruthenium(II)-Trithiacyclononane Complexes as Potential Antitumourals, Tese de Doutoramento, Departamento de Química, Universidade de Aveiro, **2013**.

Appendix

Appendix 1: Calibration curves

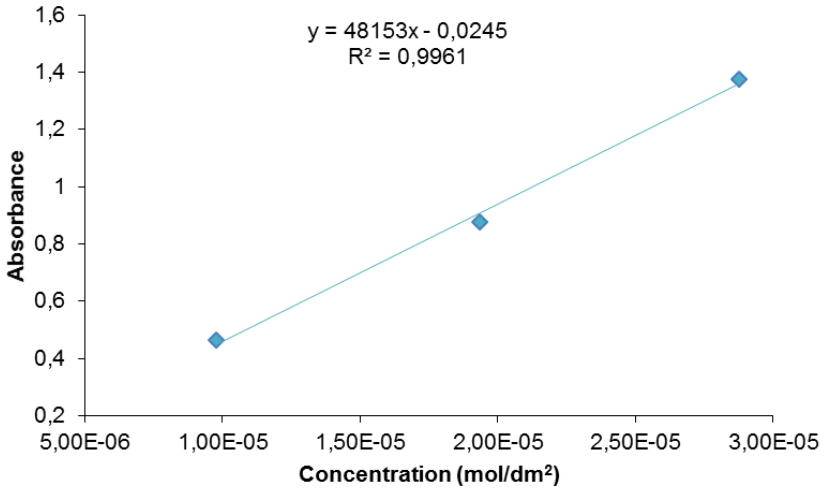

Figure A 1 – Calibration curve for determination of the molar absorptivity of the curcumin in DMSO.

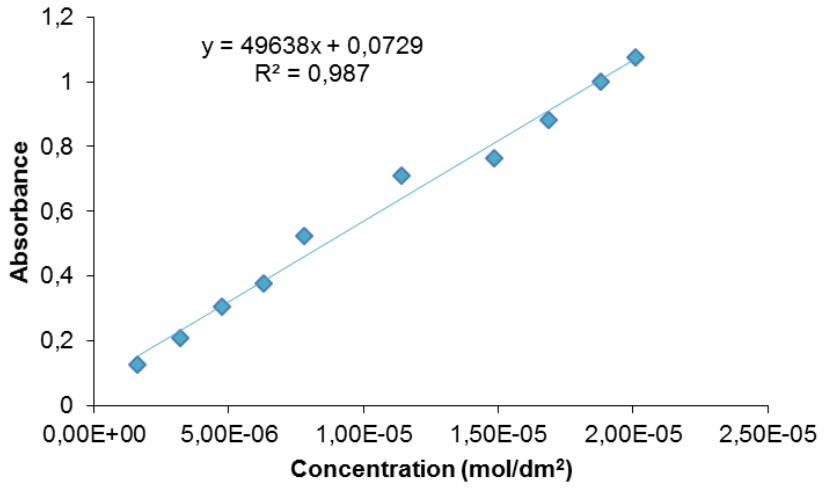

Figure A 2 – Calibration curve for determination of the molar absorptivity of the curcumin in DMF.

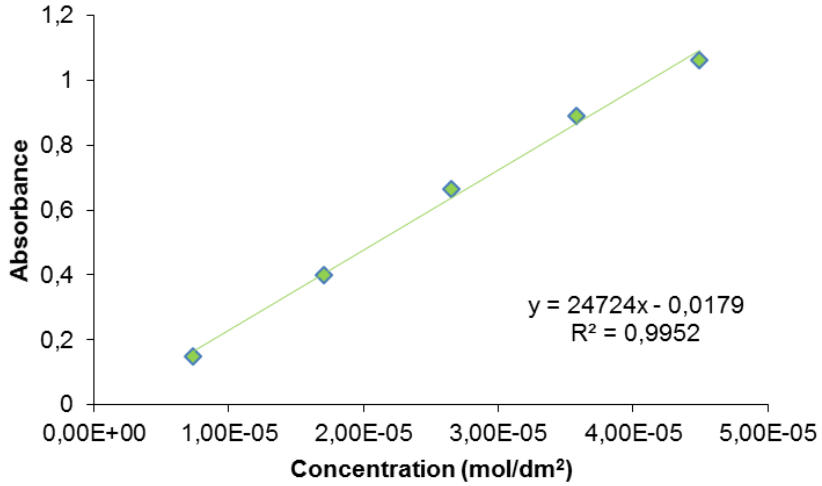

Figure A 3 – Calibration curve for determination of the molar absorptivity of the Ru-curc complex in DMSO.

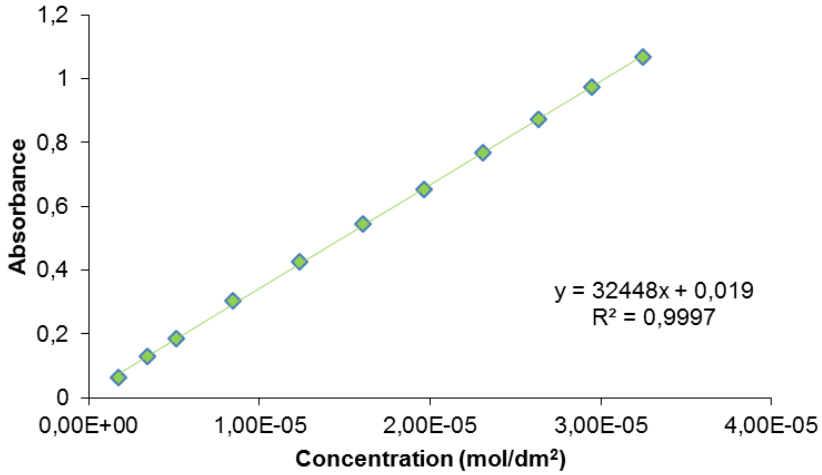

Figure A 4 - Calibration curve for determination of the molar absorptivity of the Ru-curc complex in DMF.